A Virtual Engineering Framework for Simulating Advanced Power Systems

Final Technical Report

Reporting Period Start Date: September 19, 2005
Reporting Period End Date: June 18, 2008

Mike Bockelie, REI
Dave Swensen, REI
Martin Denison, REI
Stanislav Borodai, REI

December 12, 2008

DOE Cooperative Agreement No: DE-FC26-05NT42444

Reaction Engineering International
77 West 200 South, Suite 210
Salt Lake City, UT 84101

Disclaimer

Abstract

In this report is described the work effort performed to provide NETL with VE-Suite based Virtual Engineering software and enhanced equipment models to support NETL's Advanced Process Engineering Co-simulation (APECS) framework for advanced power generation systems. Enhancements to the software framework facilitated an important link between APECS and the virtual engineering capabilities provided by VE-Suite (e.g., equipment and process visualization, information assimilation). Model enhancements focused on improving predictions for the performance of entrained flow coal gasifiers and important auxiliary equipment (e.g., Air Separation Units) used in coal gasification systems. In addition, a Reduced Order Model generation tool and software to provide a coupling between APECS/AspenPlus and the GE GateCycle simulation system were developed. CAPE-Open model interfaces were employed where needed. The improved simulation capability is demonstrated on selected test problems.

As part of the project an Advisory Panel was formed to provide guidance on the issues on which to focus the work effort. The Advisory Panel included experts from industry and academics in gasification, CO2 capture issues, process simulation and representatives from technology developers and the electric utility industry. To optimize the benefit to NETL, REI coordinated its efforts with NETL and NETL funded projects at Iowa State University, Carnegie Mellon University and ANSYS/Fluent, Inc.

The improved simulation capabilities incorporated into APECS will enable researchers and engineers to better understand the interactions of different equipment components, identify weaknesses and processes needing improvement and thereby allow more efficient, less expensive plants to be developed and brought on-line faster and in a more cost-effective manner. These enhancements to APECS represent an important step toward having a fully integrated environment for performing plant simulation and engineering. Furthermore, with little effort the modeling capabilities described in this report can be extended to support other DOE programs, such as ultra super critical boiler development, oxy-combustion boiler development or modifications to existing plants to include CO2 capture and sequestration.

Table of Contents

1

Executive Summary

The US DOE National Energy Technology Laboratory (NETL) is facilitating the development of future zero-emission, high-efficiency energy plants which could include co-production, from fossil fuels and opportunity fuels, a broad mix of power, heat, transportation fuels, and chemical products, using a wide range of plant sizes and configurations. Many of the proposed plant concepts are based on coal – an abundant, secure, stably priced fuel – and will use Integrated Coal Gasification Combined Cycle (IGCC) technology. Some plants, such as FutureGen, will include carbon capture. Computer simulation will play an important role in developing and deploying these advanced power generation systems. To reduce the time, cost and technical risk of evaluating the different possible plant configurations will require assessment tools with modeling capabilities that go far beyond the tools traditionally used.

In this project, Reaction Engineering International (REI) has provided NETL with VE-Suite based Virtual Engineering software and enhanced equipment models to support NETL's Advanced Process Engineering Co-simulation (APECS) framework for advanced power generation systems. Enhancements to the software framework facilitated a critical link between APECS and the virtual engineering capabilities provided by VE-Suite (e.g., equipment and process visualization, information assimilation). Model enhancements focused on improving predictions for the performance of entrained flow coal gasifiers – a key component to the advanced plant concepts – and important auxiliary equipment (e.g., Air Separation Units) used in coal gasification systems. In addition, a Reduced Order Model generation tool and software to provide a coupling between APECS/AspenPlus and the GE GateCycle simulation system have been provided. CAPE-Open model interfaces have been employed where needed. The improved simulation capability has been demonstrated on selected test problems.

REI performed the bulk of the technical work for the project. An Advisory Panel was formed to provide guidance on which issues to focus the work effort. The Advisory Panel included experts from industry and academics in gasification (N.Holt, Electric Power Research Institute), CO2 capture issues (H.Herzog), process simulation (Enginomix) and representatives from technology developers (Praxair) and the electric utility industry (American Electric Power, AmerenUE). In addition to participating on the Advisory Panel, Enginomix and Praxair contributed to portions of the technical work effort performed for the project. AspenTech, Inc. and GE Energy provided process simulation software used for the project. To optimize the benefit to NETL, REI coordinated its efforts with NETL and NETL funded projects at Iowa State University (ISU), Carnegie Mellon University (CMU) and ANSYS/Fluent, Inc.

Overall, the project was quite successful. The improved simulation capabilities contained in APECS will enable researchers and engineers to better understand the interactions of different equipment components, identify weaknesses and processes needing improvement and thereby allow more efficient, less expensive plants to be developed and brought on-line faster and in a more cost-effective manner. These enhancements, as well as model validation results, have been highlighted through participation at NETL-sponsored technical conferences focused on coal utilization and gasification, NETL program workshops, NETL program reviews and project-specific meetings held between REI and NETL personnel. The software and component models developed in this project have been provided to NETL. Results from the simulations performed

during this project have been used in discussions with personnel from the gasification industry to provide guidance and suggestions on equipment design and operational improvements. Likewise, the results of this project have been used in discussions with electric utility personnel and fuel suppliers to the utility industry in discussions on IGCC issues. In addition to advanced power systems, REI has successfully reused software elements and lessons learned from this project to develop modeling tools for addressing problems in other industries and other applications.

NETL will benefit in several ways from the power plant performance modeling capability developed in this project. APECS represents an important step toward the ultimate goal for simulation for the NETL Advanced Research program - a fully integrated environment for performing dynamic plant simulation and engineering. APECS also provides DOE with a mechanism to enable and foster collaborations amongst a broad range of power plant researchers from universities, industry, and DOE, whether US or internationally based, to assist in the development and deployment of advanced power generation plants. Last, other DOE programs focused on advanced power generation systems can benefit from the developed software and models. With little effort, APECS can be extended to support Ultra Super Critical (USC) boiler development, Oxy-combustion boiler development, and existing plants with CO_2 capture and sequestration in addition to gasification.

As per the DOE reporting instructions, the remainder of this report is organized as follows:

- Chapter 1 - Experimental Methods, which includes sections describing software enhancements to couple VE-Suite and APECS and component model development and enhancement efforts;
- Chapter 2 - Results and Discussion, which highlights usage of the framework and models to perform simulations; and
- Chapter 3 - Conclusions.

These are followed by sections containing the List of Figures and List of Tables contained in the report, literature References cited in the report, a Bibliography of relevant background material and Acronyms and Abbreviations used in the report.

Chapter 1 – Experimental Methods

In this chapter is provided a description of the work performed in the four tasks for the project. These are:

Task 1: APECS Framework Enhancement – Software;
Task 2: APECS Framework Enhancement – Models;
Task 3: Demonstration; and
Task 4: Program Management, Reporting and Technology Transfer.

REI staff members performed the bulk of the technical work for the project, which involved software development, component model enhancement and demonstration of the improved modeling capabilities included in APECS for selected test problems. An Advisory Panel was formed to provide guidance on which issues to focus our efforts. The Advisory Panel included experts from industry and academics in gasification (N.Holt, Electric Power Research Institute), CO2 capture issues (H.Herzog), process simulation (Enginomix) and representatives from technology developers (Praxair) and the electric utility industry (American Electric Power, AmerenUE). In addition to participating on the Advisory Panel, Enginomix and Praxair contributed to portions of the technical work effort performed for the project. AspenTech, Inc. and GE Energy provided process simulation software used for the project. To optimize the benefit to NETL, REI coordinated its efforts with NETL and NETL funded projects at Iowa State University (ISU), Carnegie Mellon University (CMU) and ANSYS/Fluent, Inc..

Presented below are descriptions of the technical work effort for each Task. For simplicity, the discussion items are presented in the order of the Tasks as outlined above.

1.1 Task 1 – APECS Framework Enhancements - Software

The objective of this task was to enhance the APECS software infrastructure to include 3D visualization capabilities. Some items within this task were on-going throughout the course of the project. To ensure high quality software was produced, the software design for the APECS enhancements was performed according to accepted industry standard procedures. The development team followed the standard practice of creating functional specifications, and conducting design reviews to ensure interoperability among the various software elements.

1.1.1 Task 1.1 Couple VE-Suite 3D, Immersive Capabilities with APECS

Within this task, REI in coordination with ISU, NETL and ANSYS/Fluent, performed the following:

1. Connected APECS simulation framework to VE-Suite (VE-Conductor) to support: automatic and manual mapping of pre-configured flowsheet interconnectivity to VE-Suite (VE-Conductor), automatic and manual configuration of APECS parameters for access in VE-Suite (VE-Conductor), and basic run-time control of APECS co-simulation from VE-Suite (VE-Conductor);
2. Enhanced communication between VE-Suite (VE-Explorer) graphical plug-ins and APECS computational units, including process models and CFD models; and
3. Added support for pre-configured, immersive, 3D visualizations for APECS-based plant models.

REI's primary involvement in this task was to develop the capabilities necessary for VE-Suite to communicate and interact with AspenPlus/APECS. This work included two major subtasks: 1) development of a C++ interfacing library for AspenPlus (CASI) and 2) modifications to VE-Suite to support the VE-Suite-to-AspenPlus coupling. The following sections describe REI's efforts on these subtasks.

Development of a Prototype VE-Suite-to-APECS Coupling

Early in the project a basic software design for a prototype VE-Suite-to-APECS coupling was developed. The goal of this design was to decide how the prototype coupling would be accomplished and what the level of functionality would be. The conceptual design was developed through close interaction with NETL and ISU. Additional details of the software design are given below.

> ***Flowsheet Mapping***: For proof-of-concept purposes, it was decided (in coordination with NETL) that a one-to-one mapping would be used between AspenPlus blocks and VE-Suite modules. Thus, each AspenPlus block and stream had a corresponding VE-Suite representation where AspenPlus input/output options can be chosen.
>
> ***VE-Suite User Interface Modifications***: The software design requires C++ user interface development in VE-Suite to allow the user to define, manipulate and view AspenPlus

input and output parameters. By selecting a stream or component in the VE-Suite User Interface (UI), the user is presented with a dialog that shows the corresponding AspenPlus variable explorer nodes. From this list of variables, the user is able to choose which variables are made available in VE-Suite as input and output parameters. The choices made by the user on this dialog are stored as xml configuration data along with the VE-Suite network file for easy retrieval.

AspenPlus Interface Engine: As part of the design, REI developed an interface engine, which provided the necessary functionality for VE-Suite and AspenPlus interaction. This interface was implemented as a C++ class to provide seamless integration with the C++-based user interface code. The interface class, at a low-level, utilized a C++ library to actually perform the AspenPlus automation tasks. The C++ library functions by making use of the component object model (COM) interface. This interface engine was the initial version of the CASI library.

Virtual Engineering (Immersive 3D) Modifications: ISU utilized a combination of new and existing capabilities of the VE-Suite software to interface with the REI-developed AspenPlus Interface Engine described above. ISU developed custom immersive 3D visualization capabilities for the data. These customizations were added to the graphical engine of VE-Suite.

This prototype software for coupling VE-Suite to APECS was implemented and demonstrated to NETL. The intention of the prototype was to provide a stepping-stone to the implementation of a fully-capable, generalized coupling between VE-Suite and APECS.

At a high level, the integration of the VE-suite and APECS frameworks was accomplished by creating an APECS plugin component to VE-Suite. Development of a VE-Suite plugin involves creating two separate software components that integrate with VE-Suite.

- The first is the GUI plugin, which is loaded by the VE-Conductor application.
- The second is the back-end Common Object Request Broker Architecture (CORBA) server (unit) plugin, which is coupled to the computational engine (see Figure 1.1.1 for a schematic diagram of the VE-Suite software architecture).

The GUI plugin provides all component-specific GUI functionality required by the plugin, including the ability to specify model inputs and view model results. The back-end CORBA server wraps the core computational model, which in this case will be the entire AspenPlus application. The back-end server provides all execution control and interaction with AspenPlus via a wrapper class. Development of these subcomponents is discussed in additional detail in the following sections.

The prototype Graphical User Interface (GUI) plugin for the APECS component is shown in Figure 1.1.2. The GUI was designed to display all the queried data from the current AspenPlus flowsheet. As the project progressed, the team assumed these capabilities would be enhanced to allow selecting input and output parameters of interest and thus limit the amount of information that is transferred through the interface to AspenPlus. However, it was eventually found that providing access to the full AspenPlus flowsheet dataset was the most reasonable approach.

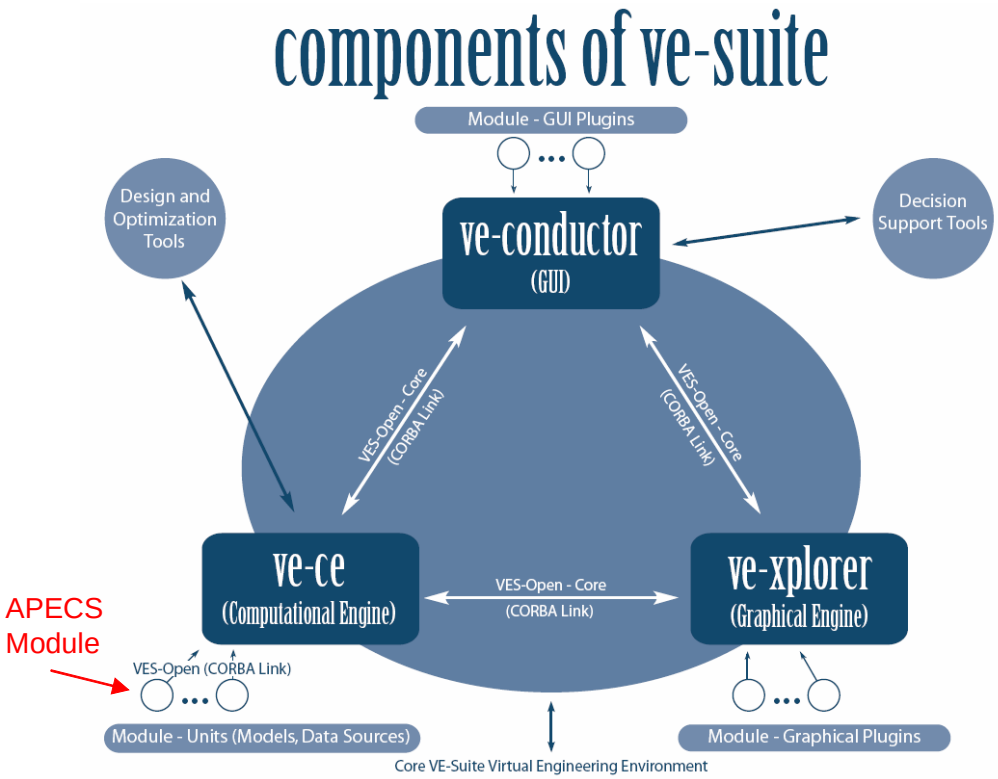

Figure 1.1.1. The Schematic diagram of the VE-Suite Software Architecture and the point of integration for the APECS plugin.

Hyper Aspen Plus Inputs/Outputs in VE-Conductor

Hyper Aspen Plus Flowsheet in VE-Conductor

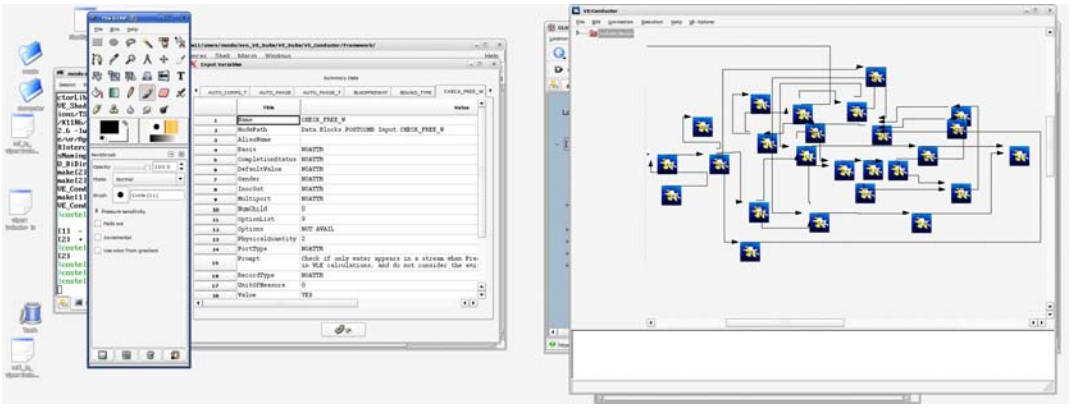

Figure 1.1.2. The VE-Conductor user interface showing the network diagram for the NETL Hyper facility (NETL test case) flowsheet.

The prototype back-end server that wraps AspenPlus utilized a sophisticated approach for interfacing between the VE-Suite computational engine and AspenPlus. Figure 1.1.3 is a schematic diagram of the architecture of the component. As seen in this figure, AspenPlus lives at the lowest-level of functionality. Wrapping AspenPlus at the next layer up is a C++ interface library developed by REI (CASI). This interface library was created to help abstract AspenPlus from software being developed for this project.

The final layer in the hierarchy is the VE-Suite back-end CORBA server, which wraps all the aforementioned levels. This server interacts with the VE-Suite computational engine and moves data and operational requests to and from AspenPlus through the various software layers. This server also contains code to read and parse the AspenPlus .bkp file to determine the network layout and connectivity for the target flowsheet (this code was provided by NETL and ISU).

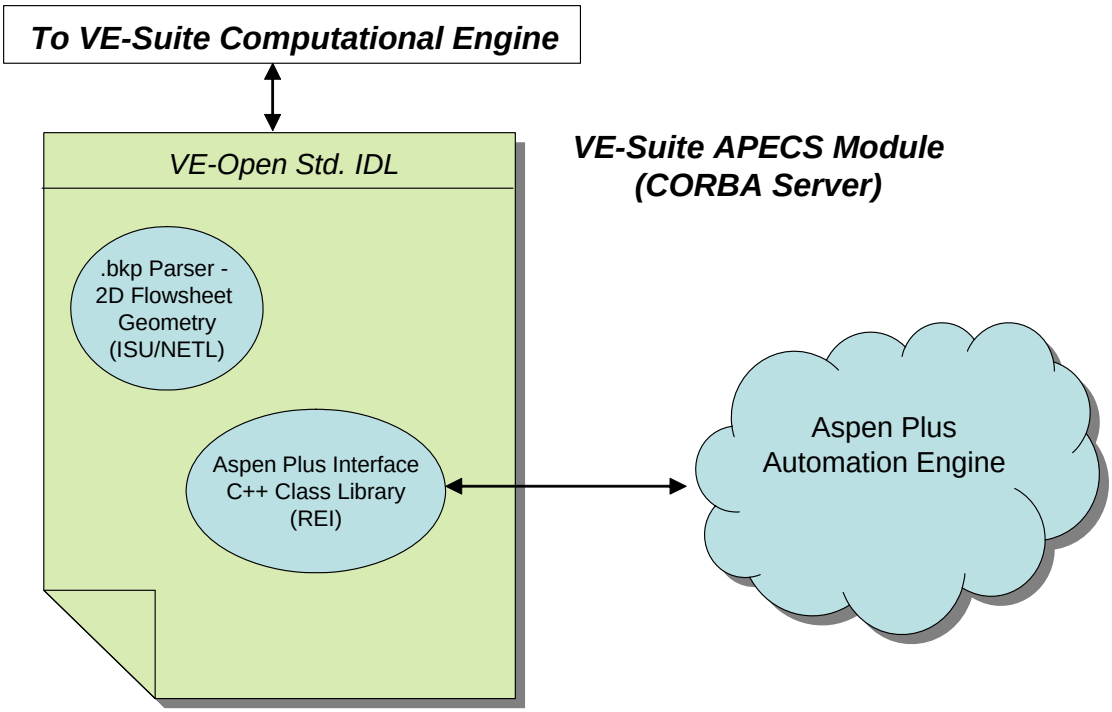

Figure 1.1.3. Schematic diagram of the VE-Suite APECS Module.

VE-Suite-to-APECS Coupling – Prototype Demonstration

Using the prototype implementation of the VE-Suite-to-APECS coupling software described above, REI and ISU performed a demonstration to illustrate the basic functionality.

The physical layout of the computational resources used in the demonstration is illustrated in Figure 1.1.4. VE-Conductor (the user interface component) and the Computational Engine were run on computers located at the ISU campus. The APECS VE-Suite component, which encapsulates AspenPlus, the AspenPlus C++ interface and CORBA wrapper, were run at the REI offices in Salt Lake City.

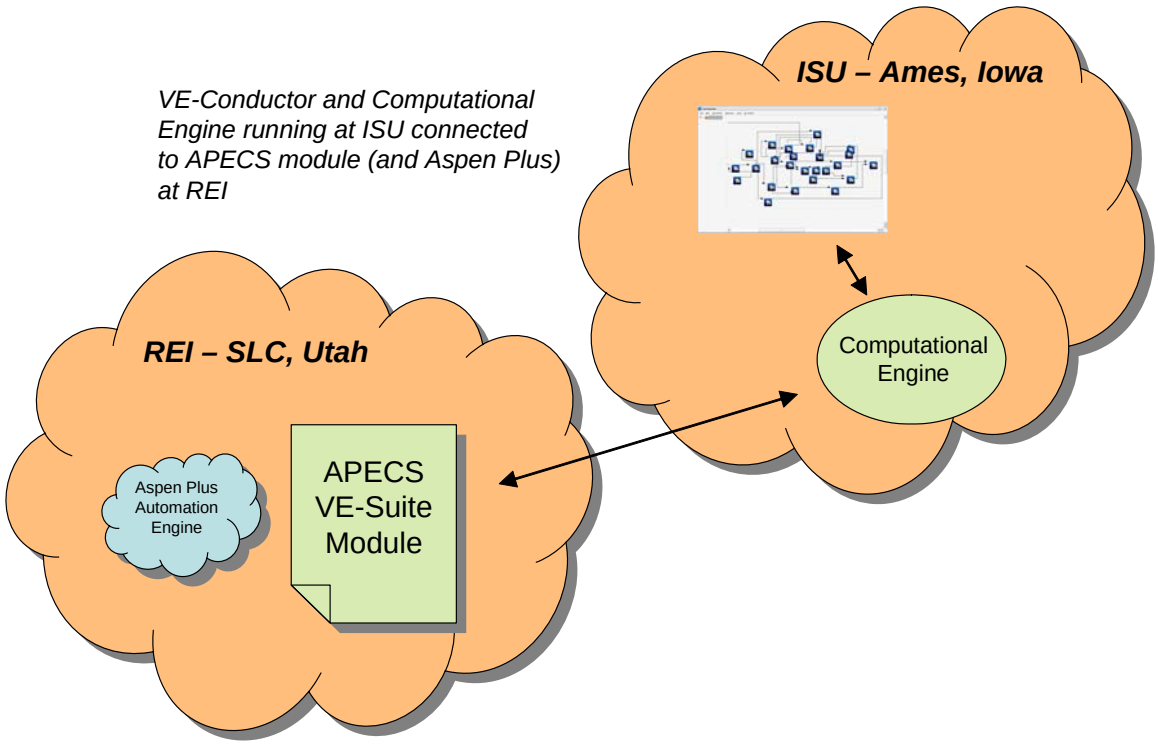

Figure 1.1.4. Schematic diagram of VE-Suite-to-APECS coupling demonstration scenario.

By using VE-Conductor, the team at ISU was able to load an AspenPlus flowsheet file that had been provided by NETL (i.e., the Hyper facility flowsheet). The resulting module network was then recreated within the Conductor application using information extracted from the AspenPlus .bkp file (see Figure 1.1.1 for details). In addition, the Conductor application was able to receive a complete data set for the flowsheet via the computational engine and the APECS VE-Suite module. This data set included all the information contained within AspenPlus itself.

While convenient from a programming perspective, moving the entire AspenPlus Data Explorer tree for even a simple flowsheet (like the Hyper facility) was intractable. The queries for data into AspenPlus through the COM interface took approximately 20 minutes to complete and the resulting data set to be transferred through the CORBA interface calls was approximately 20 MB in size. It was clear from this demonstration that the fully-functional, general purpose interface software must perform intelligent queries of AspenPlus flowsheets and move correspondingly smaller data sets.

The prototype software demonstration provided insight into a number of issues that needed to be addressed for the fully-functional coupled software. These included:

- the raw data associated with each calculation block in AspenPlus is large;
- transferring the complete information for an entire flowsheet (even at the level of the Hyper facility) is not practical (~20MB for Hyper);

- querying information from AspenPlus via the COM interface is very time consuming (~20min for Hyper sheet) – as with the raw data, queries must be limited to only what is required; and
- integration of APECS with VE-Suite requires modification of the original VE-Suite component methodology.

As a result, additional redesign of the VE-Suite-to-APECS interface was performed. These enhancements are discussed in the following section.

VE-Suite-to-APECS Coupling – Redesign

The following material provides an overview of the redesign of the coupling software that was performed as a result of the findings from the prototype demonstration discussed in the previous section. In addition, a discussion of how these changes affect the various software components that comprise VE-Suite is given. The major components of the VE-Suite software are:

- VE-Conductor (GUI),
- Computational Engine (CE), and
- Computational Units (Backend CORBA servers).

The following sections provide a brief summary of the changes made to these components as part of the redesign effort.

VE-Conductor

- The Conductor GUI was modified to support two modes of operation: 1) Offline and 2) Online. Offline mode supports traditional VE-Suite plugins that do not require interaction with the computational unit until model execution. Online mode supports plugins that do require communication during model configuration. The AspenPlus computational unit requires the Online mode of operation.
- A data-browser-like default plugin was developed to handle display and editing of model parameter data for query-enabled (Online-enabled) units. This plugin serves as a template C++ class for all Online units.
- Using the template C++ class for Online units, an interactive GUI plugin was developed to support selecting and specifying model parameters for AspenPlus.

Computational Engine

- The Computational Engine's functionality was reduced to that of a data proxy and execution scheduling only. It no longer stores computational unit input parameters or results.
- The CORBA interface was modified to support a new query-based design. Command queries from VE-Conductor are redirected to the appropriate computational unit.
- The Computational Engine interface was modified with additional functions to support VE-Conductor's Online operating mode.

Computational Units

- A command-based Query interface was added to the computational unit CORBA IDL.
- The Query interface for the AspenPlus computational unit was modified to support AspenPlus-specific functionality (calls into the AspenPlus interface wrapper).
- The core computational unit template was modified to allow units to store their own data (model input parameters and model outputs).

The on-demand data model provided by the new VE-Suite design significantly reduced the overhead of communicating with AspenPlus. While the required changes to the VE-Suite architecture were non-trivial, the team believes the efforts paid off with a significantly improved capability for a hybrid VE-Suite / AspenPlus application.

VE-Suite-to-APECS Coupling – Implementation of Redesign

The efforts required to implement the changes for the redesign were conducted as a collaborative effort between REI, ISU and NETL software engineers.

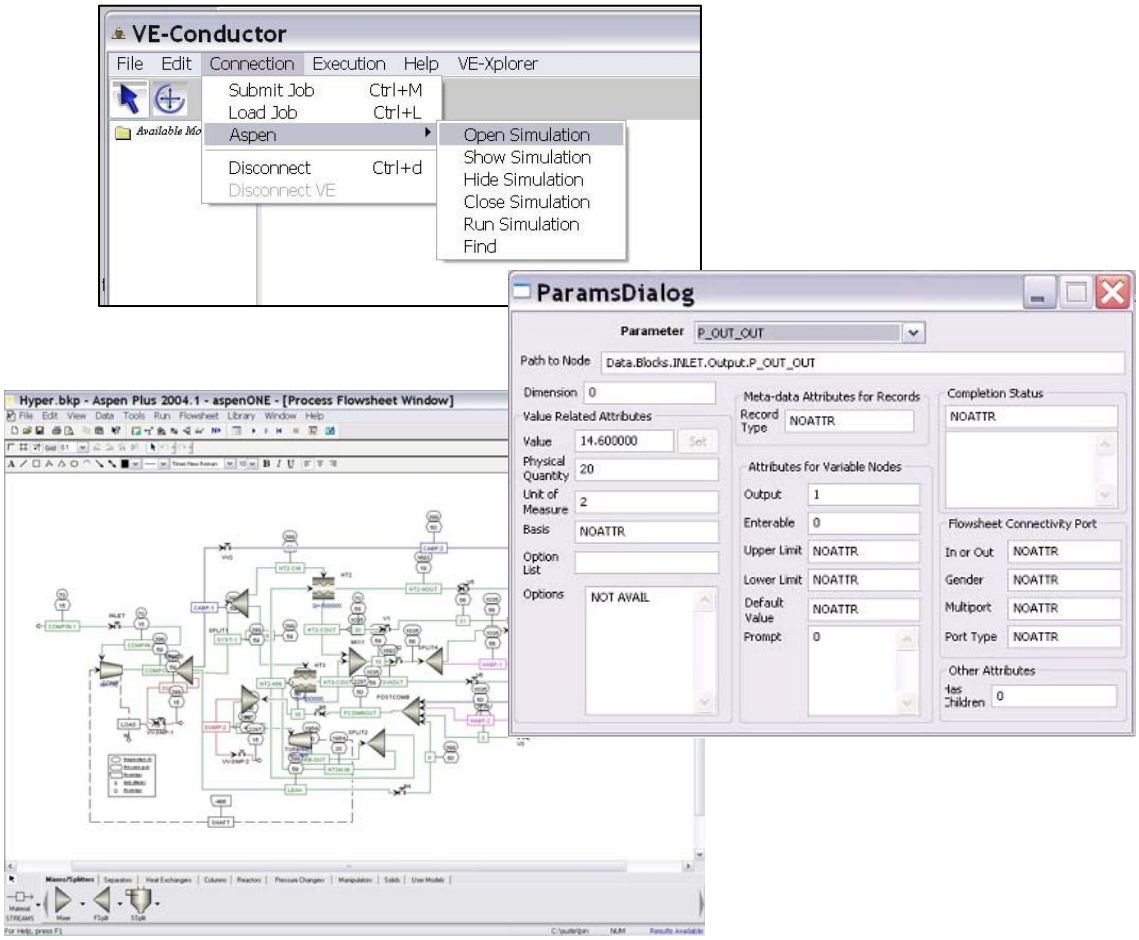

Figure 1.1.5. Selected screenshots of the coupled software.

Figure 1.1.5 shows selected screenshots of the coupled software. REI's contributions to the efforts focused in three areas:

- Software Engineering,
- AspenPlus Interfacing and
- Aspen Unit Plug-in Modifications.

Each of these is described in additional detail in the following paragraphs.

Software Engineering

A key contribution of REI to the effort was that of software engineering. REI software engineers provided significant input into the overall design and architecture of the coupled VE-Suite-APECS software. With additional inputs and refinements provided by ISU and NETL team members, a viable design plan was created and changes implemented. The software design for the VE-Suite-APECS enhancements was performed according to accepted industry standard procedures.

AspenPlus Interfacing

One of the key elements of functionality required to create the VE-Suite-APECS coupling was a wrapper (or abstraction) library for AspenPlus. To address this need, REI implemented the C/C++ Aspen Simulator Interface (CASI) library, using the prototype version as a starting point. This library provides a high-level C++ interface to the AspenPlus software. In addition to a simplified interface, the library also encapsulates the details of the AspenPlus interfacing to the library itself. While maintaining the external interface to the library (to keep from breaking existing library client code), REI continued to test and debug CASI throughout the course of the project.

Aspen Unit Plug-in Modifications

The CORBA IDL interface (VE-Open) was modified for back-end computational units to support a Query-style interface. With the Query infrastructure in-place, REI was able to implement AspenPlus-specific functionality for the Aspen Unit. Specifically, the Aspen Unit includes a command-driven AspenPlus interface engine, which receives commands through the Query interface. The engine then parses the command, compares it to a set of available commands, and carries out the required tasks using the CASI interface calls. This supported command set was further enhanced by ISU and NETL team members as additional functionality was required.

The redesigned VE-Suite-to-APECS coupling was demonstrated for Dr. Steve Zitney of NETL by NETL's Mr. Terry Jordan and ISU's Mr. Doug McCorkle following the aforementioned implementation efforts. Dr. Zitney was regularly briefed and provided demonstrations of the coupling throughout the course of the project and through to the time of this writing.

12

Follow-on CASI Library Development

The CASI library continued to be enhanced throughout the course of the project as the needs of the project evolved. These enhancements included the following:

- Adding the ability to not only open and interact with a single AspenPlus flowsheet, but also to close a sheet and load another. Enabling this functionality within CASI proved to be a difficult task given that Aspen Tech did not support C++ for the AspenPlus automation interface. The close/load functionality works from Visual Basic, which prompted the REI team to consider porting CASI to Visual Basic. However, given that the vast majority of CASI capabilities were already in place, it was decided to continue pursuing a solution to the C++ problem. In addition, the C++ CASI library performs operations much faster than could be obtained with a Visual Basic implementation. With assistance from NETL, REI was put in contact with a high-level developer at Aspen Tech who provided guidance on how to treat the close/load C++ issue. Based on these discussions REI completed implementation of the needed capability.
- Adding the functionality required to access any AspenPlus variable, including stream variables. Prior to this modification, only variables associated with blocks were accessible.
- Adding the functionality required to access a reduced set of AspenPlus variables from a special node in the AspenPlus automation interface structure. This reduced set of variables makes available the most common parameters rather than the complete set. Access to this reduced set makes it much easier for a user to locate and modify key parameters from VE-Suite.
- Upgrading CASI for compatibility with AspenPlus 2006
- Implementing single-step execution control for AspenPlus flowsheets. This feature provides CASI the capability to "force" AspenPlus to perform individual steps (blocks) within the overall flowsheet simulation as opposed to having to execute the entire flowsheet.
- Implementing support for multi-value properties. This feature provides CASI the flexibility to specify and load AspenPlus properties that contain more than just a single simple data type (i.e., single floating point value). Hence, property data can now be in almost any form (e.g., an array of coefficients for a polynomial representation or multiple species, text strings, etc.).

After REI completed the major portions of the CASI library, additional efforts for improving CASI were performed by ISU and NETL developers working on coupling VE-Suite and AspenPlus. CASI has been used heavily by the ISU and NETL teams for their efforts on VE-Suite-APECS integration. VE-Suite, communicating through CASI, has been used to successfully open and interact with flowsheets involving hundreds of calculation blocks.

During the second year of the project, REI worked with NETL and Aspen Tech personnel to investigate the possibility of modifying CASI to make use of a new Aspen Tech interface, entitled CXS, which had been designated as the replacement for the aging COM Automation Interface to AspenPlus used by CASI. Later in the project REI was informed by Aspen Tech that they had decided CXS was still in a developmental stage and thus not ready for mainstream use.

Their plans to release CXS to the public were placed on indefinite “hold”. According to Aspen Tech, the COM-based approach used by CASI will be supported for a significant time in the future. As a result, REI dropped all plans to port the CASI library to CXS.

Throughout the project, the CASI library implementation was stored on ISU’s SVN source control servers, to allow for collaborative development activities between project team members.

1.1.2 Task 1.2 Software Management

Within this subtask software management tasks were performed. This included installing and testing updated versions of AspenPlus and APECS and distributing the REI developed CASI library.

- At the start of the project REI used AspenPlus 2006. This was subsequently replaced with AspenPlus 2006 - 20.0.3595. After each installation of upgraded AspenPlus software, tests were performed to confirm the plant performance predicted with the IGCC flowsheets obtained from NETL (see Section 1.3) computed with the new and old versions of AspenPlus agreed.

- REI encountered several problems with the initial versions of APECS provided by NETL. REI worked with NETL and ANSYS/Fluent personnel to resolve these problems. The last version of APECS provided to REI (APECS version 1.05-Beta 050) contained modifications to address the identified problems.

- During the course of the project updated versions of the REI CASI library were placed on the ISU Subversion (SVN) source control servers to provide access to the software by other NETL funded researchers assisting with the integration of VE-Suite and AspenPlus. SVN is an open-source versioning software. SVN allows the source code to be viewed and administered over the internet, thus allowing the entire software development team seamless access for the common development effort.

- ROM software originally developed by ISU and enhanced by REI was also placed on the ISU SVN source control servers to facilitate collaborative efforts with other NETL funded researchers developing ROM capabilities.

1.2 Task 2 – APECS Framework Enhancements - Models

The objective of this task was to enhance selected component equipment models as needed and deliver them as CAPE-Open compliant models for use in APECS. Specific sub-tasks included:

- Task 2.1 Enhance selected sub-models within the REI gasifier models to better predict gasifier performance.
- Task 2.2 Implement CAPE-Open compliant versions of selected REI process models as needed to support simulations of the plant configurations performed as demonstrations.
- Task 2.3 Implement CAPE-Open compliant ASU models provided by project participants and/or stakeholders.
- Task 2.4 Automated Reduced Order Models.
- Task 2.5 Implement CAPE-Open compliant coupling to selected GE GateCycle models for use in APECS by users that have access to a valid GE GateCycle license.

Provided below is a description of the technical work effort for each of these sub-tasks.

1.2.1 Task 2.1 Enhance Sub-models in REI Entrained Flow Gasifier Models

The gasifier is one of the most important systems in an IGCC system because it converts a solid fossil fuel into more environmentally attractive hydrocarbon fuel or feedstock. Our modeling efforts have focused on two "generic", cylindrical, entrained flow gasifier configurations: single stage, down fired and two stage, upflow with multiple feed inlets that can be opposed or tangentially fired. Either model can use a slurry feed or a dry feed. These systems are representative of the dominant, commercially available gasifier systems. Although we have focused our efforts on pressurized, oxygen fired systems, the models can also be used to model air blown or non-pressurized systems.

REI previously developed both CFD and engineering process models for the different gasifiers [Bockelie et al., 2004]. The REI Entrained Flow Gasifier CFD models were built using *GLACIER*, REI's proprietary comprehensive two-phase reacting CFD-based code. The CFD models provide detailed information about the gasifier flowfield, slagging behavior, heat transfer, soot and tar formation, etc., but can require long run times. The REI Entrained Flow Gasifier Process models are mechanistic based, and include a coal gasification kinetics model to account for high-pressure kinetics effects, a flowing slag indicator, and tar and soot models. The process models only provide information about the gross conditions within the gasifier, but run quickly and thus can be used for scoping studies and for investigating optimal process conditions prior to running the CFD models.

The following material first provides an overview of the capabilities of *GLACIER* and the engineering process models. This is followed by detailed discussions on the improved submodels implemented into the REI entrained flow gasifier models to better predict:

- pressure dependence on emissivity properties used in radiation heat transfer calculations.
- pressure dependence on char reactivity; and
- vaporized ash behavior.

GLACIER – overview

GLACIER is a comprehensive reacting CFD code that has been used to model approximately 150 different industrial furnaces. The algorithms used in the *GLACIER* code are robust, accurate,

iterative solvers that extract the nonlinear coupling between turbulent fluid mechanics, gas-phase reaction chemistry, heat transfer (particularly radiation), particle-phase reaction, turbulent particle dispersion, and particle-wall or heat transfer surface interactions. Particle/fluid interphase coupling is included through a moving-Eulerian particle cloud tracking and source distribution technique. Computations of turbulent fluctuations include statistical distributions for all reaction and radiation properties. Reaction and radiation calculations can include any number of chemical species. *GLACIER* has the following model capabilities:

- complex 3D geometries;
- polydispersed phases of gases and particles, droplets or slurries with full mass, and momentum and energy coupling between phases;
- multiple reaction rate processes for liquid vaporization, coal devolatilization, and heterogeneous particle reactions;
- steady-state, laminar or turbulent flows;
- mixing and reaction of multiple fuels;
- full coupling between turbulent fluid mechanics, radiative and convective heat transfer, and chemical reactions;
- homogeneous combustion and gasification performed with equilibrium chemistry and turbulence-chemistry interaction accounted for with an assumed shape Probability Density Function (PDF);
- radiative heat transfer for scattering-absorbing-emitting, turbulent, sooting media;
- variable thermal boundary conditions including adiabatic, thermal resistance, heat exchanger;
- prediction of particle trajectories, concentrations and dispersion, particle deposition;
- slagging of material deposited on walls; and
- tar and soot production/destruction.

To compute pollutant emissions, vaporized metals and other trace species, finite-rate chemistry effects can be included in a post-processor mode. Further details on the enhancements to *GLACIER* for use in the REI Entrained Flow Gasifier CFD model are available in [Bockelie et al., 2002] and [Bockelie et al., 2004].

Engineering Process Models – overview

The REI Entrained Flow Gasifier Process model consists of two submodels: a zonal equilibrium submodel with heat transfer and a solid fuel (coal particle) burnout submodel. A schematic of the model for a one-stage gasifier is illustrated in Figure 1.2.1.

- The heat transfer submodel accounts for heat transfer to the ash contained in the solid fuel, and heat transfer to walls to account for backside cooling (including heat extraction); the wall heat transfer submodel only requires the wall resistance and backside temperature (e.g., steam temperature) to be specified.
- The zonal equilibrium submodel calculates the equilibrium exit gas concentration and temperature given a prescribed heat transfer through the walls. An ash viscosity submodel from the CFD gasifier slag model is used to calculate a representative ash viscosity and critical viscosity temperature and thereby provide a slagging indicator.
- The particle burnout and char recycle are required inputs to the zonal submodel obtained from the particle burnout submodel, while the gas and radiation temperatures are the required inputs into the particle burnout submodel obtained from the zonal submodel. For the one-stage gasifier, particle burnout can be entered by the user or computed. If the desired burnout is specified by the user, the particle burnout submodel is used to determine the residence time and the gross geometry needed to produce the specified particle burnout.

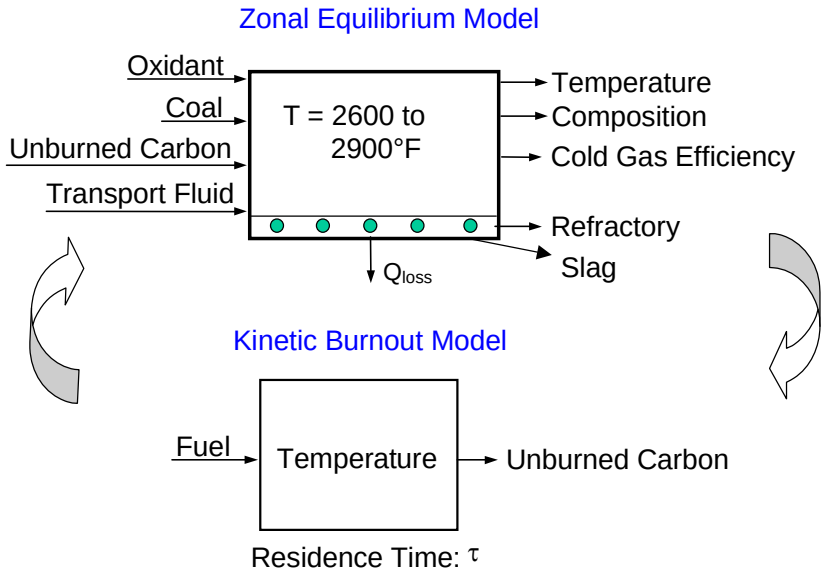

Figure 1.2.1. Schematic for the one-stage entrained flow engineering process model.

Included in the particle burnout model are soot and tar sub-models and a coal gasification kinetics model to account for high-pressure kinetics effects. The tar and soot sub-model predicts the generation/destruction of tar and soot within the gasifier, the presence of which primarily impacts local heat transfer properties. The heterogeneous reaction kinetics that describe coal gasification processes play a central role in calculations performed by the model. The wide range of conditions that exist in a commercial-scale gasifier makes it difficult to apply a simple correlation to describe the competing effects on reactions from oxygen firing, elevated operating pressure and small particle size.

High Pressure Radiation Properties of Gases

Local heat transfer rates in entrained flow coal gasifiers used in IGCC plants can be considerably higher than in water-wall boilers because of the high peak temperatures near the injectors that can be achieved with oxygen combustion, and the high partial pressures of the radiating species (CO_2, H_2O, CO, augmented locally with soot). The high heat transfer is responsible for the limited lifetime of the fuel injectors. The emissivity models for gasifiers need to be enhanced to include pressure dependence. This effect could potentially be even more important for gasifiers used in future IGCC plants that will be designed to be CO2 capture ready which will operate at system pressures (e.g., 60-70 bar) that are much higher than current practice.

A gas radiative properties model that is more accurate at higher pressure was implemented into the REI entrained flow gasifier models. The program *RADCAL* [Grosshandler, 1993], developed at NIST, was implemented as a sub-model into the gasifier models. *RADCAL* predicts the radiation intensity leaving a non-isothermal volume containing non-uniform concentrations of CO_2, H_2O, CO, CH_4, N_2, O_2, and soot. The radiative properties of the combined gases are calculated with a narrow-band model. The soot is treated as purely absorbing in the Rayleigh limit. The program was converted from a standalone code that reads an input file to a subroutine

with the composition, soot concentration, temperature, and path length as subroutine arguments. The total emissivity is then calculated.

The implementation of the *RADCAL* sub-model into the CFD model is straightforward. In the original CFD model, the gas total emissivities were calculated by correlated fits with Hottel emissivity charts. The discrete ordinates submodel (used for radiative heat transfer) within the gasifier CFD model requires the gas properties to be expressed in terms of a gray absorption coefficient, κ. This is extracted from the total gas emissivity assuming Beer's law is applicable:

$$\kappa = -\frac{1}{L}\ln(1-\varepsilon)\,. \qquad (1.2.1)$$

Example calculations using the improved gasifier CFD model are provided in the Results and Discussion section of this report (see Section 2.2.1) and in [Bockelie et al., 2007c].

Pressure Dependence on Char Reactivity

The temperature range in a gasifier can vary from 1200 to 3000 K. Hence, the gasification reaction rate can be controlled by chemical kinetics, external mass diffusion, or both. The kinetics model used to describe oxidation/gasification in a gasifier should allow for a smooth transition from the two limiting reaction regimes, as well as include the diffusion-controlled regime that lies between the two extreme conditions.

Reactant and product inhibition effects can have a significant impact on gasification rates. For example, the fractional order kinetics for CO_2 can account for the CO_2 inhibition but not the CO inhibition. Therefore, a *Langmuir-Hinshelwood* formulation was adopted as it explicitly places the product inhibition effect in the denominator as shown in the following equation for CO_2 and H_2O gasification:

$$r_s(1/s) = \frac{k_1 P_{CO_2} + k_2 P_{H_2O}}{1 + k_3 P_{CO_2} + k_4 P_{CO} + k_5 P_{H_2O} + k_6 P_{H_2}} \qquad (1.2.2)$$

where

$$k_i = k_{i0} \cdot \exp\left(-\frac{E_i}{RT}\right) \qquad (1.2.3)$$

In general, CO, CO_2, H_2, and H_2O are present in the gasification mixture. The kinetic parameters of [Muhlen et. al., 1985], [van Heek and Muhlen, 1991] were used with a single multiplication factor applied to both k_{10} and k_{20} to reproduce the carbon conversions reported by [McDaniel and Hornick, 2002]. As described by Liu and Niksa (2004), the rates for different chars can be scaled by the pre-exponential constant. In Equation (1.2.2) both the CO2 and H2O gasification are equally inhibited by the presence of CO, CO_2, H_2, and H_2O. In an earlier publication [Bockelie et al, 2006c], REI used a form of the Langmuir-Hinshelwood expressions for the CO_2 and H_2O

gasification that had different denominators. The CO_2 gasification rate was inhibited by CO_2 and CO, while the H_2O gasification rate was inhibited by H_2O and H_2 only. However, the data presented by Roberts et. al. (2005) suggest equal inhibition by CO_2 of CO_2 and H_2O gasification. Therefore, Equation (1.2.2) is a more accurate representation as demonstrated below.

Illustrated in Figure 1.2.2 is coal gasification data obtained in a laboratory scale reactor by researchers at the Center for Coal Sustainable Development (CCSD) [Roberts et al., 2005]. The plot shows the carbon conversion as a function of (reactor) residence time for several coals (different coals represented by different symbols). The data demonstrates that under gasification conditions that the volatiles are released very rapidly, which is followed by char gasification which is a much slower process. In effect, char gasification is the limiting process for gasifier performance. Or viewed differently, a better understanding of char gasification processes is needed to improve gasifier designs and performance.

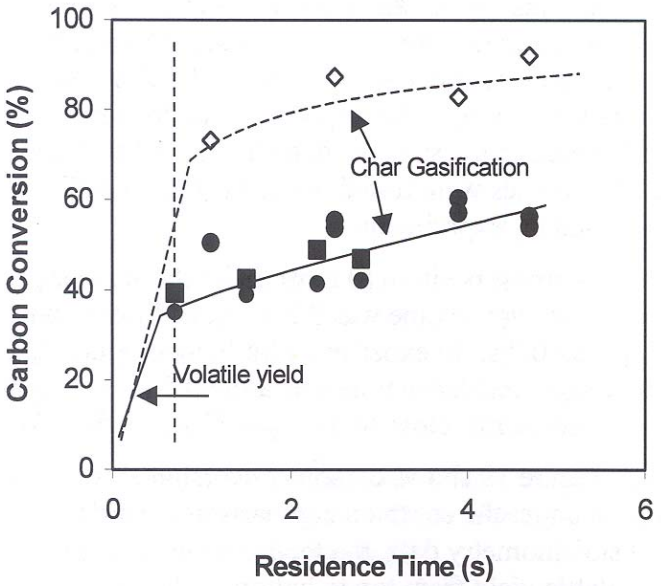

Figure 1.2.2. Carbon conversion versus residence time. Data from [Roberts et al., 2005]

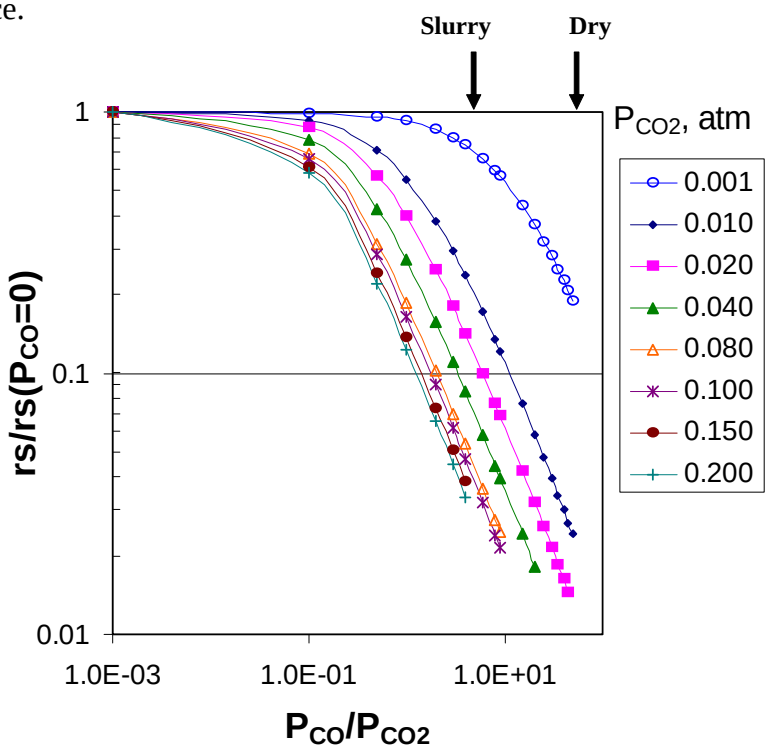

Figure 1.2.3. Coal gasification rates showing CO inhibition effect. Data from [van Heek and Muhlen, 1991].

Illustrated in Figure 1.2.3 is gasification data published in the open literature that highlights the impact of CO inhibition on coal gasification rates. Indicated are approximate locations on the plot for wet (slurry) feed and dry feed gasifiers. From the plots it can be seen that the gasification rate decreases with increased CO concentration. In addition, it can be seen that CO inhibition effects are expected to be larger for dry feed gasifiers which tend to have higher CO concentrations in the product syngas.

Example calculations for comparisons of wet (slurry) feed vs. dry feed are provided in the Results and Discussion section of this report (see Section 2.2.2) and [Bockelie et al., 2006ce].

Ash Vaporization

For a slagging gasifier, a high slag efficiency, or slag removal at the walls is needed. This requires tracking the particles to the wall using the CFD code, and determining their ability to flow down the wall from their viscosity. For ash viscosity and slag flow, the REI entrained flow gasifier models can use models based on models and correlations developed by our Australian collaborators for Australian coals [Patterson et al., 2001] or use a more general formulation that works well for a range of feedstocks [Kalmanovitch et al. 1988], [Urbain et al., 1981]. These can be used within the gasifier models to show the dependence of slag efficiency on the gasifier L/D ratio as a function of pressure (size). Improved information is also needed on the vaporization and condensation of mineral matter contained in coal. This mineral matter forms submicron ash particles that can blind filters. The transformation of the mineral matter is dependent upon many factors including the size distribution of the coal, the (local) gasification conditions, and the forms of occurrence for the elements in the coal and the interaction of different elements. Ash vaporization is augmented by the high temperatures (>3000°C) near the injector in a gasifier. REI's model for the vaporization and condensation of mineral constituents, developed for pulverized coal fired boilers [Lee et al., 2000], has been implemented into our gasifier models to carry out these analyses. In the previous study of Lee et al., values predicted by the ash vaporization model were benchmarked against single particle data from a drop-tube furnace and example calculations were performed for a commercial scale (500 MWe) coal fired electric utility boiler to investigate the impact of a low NOx boiler firing system retrofit on the predicted vaporized ash that would exit the boiler in the flue gas. As highlighted in [Lee et al., 2000], an advantage to using a CFD model for evaluating ash vaporization is that individual particle behavior can be traced back to their original fuel injectors; thus fuel injectors that contribute larger amounts of vaporized ash to the syngas exiting the gasifier can be identified. Likewise, the impact of particles passing through local pockets of high temperature gases (e.g., 1800 C) can be evaluated.

Provided below is an overview and then details of the ash vaporization model. Sufficient details are presented to allow a knowledgeable modeler to implement the model into their own tools. Example results using the model are provided in the Results and Discussion section of this report (see Section 2.2.3) and [Bockelie et al., 2008ce].

<u>Model Overview</u>

The mass of the submicron particles is dominated by the major constituents of coal mineral matter; namely, iron, silicon, aluminum, and the alkali and alkaline earth elements. These

elements are present in minerals distributed in coal partially as included mineral matter, partially as atomically dispersed elements, and partially as extraneous mineral particles. During fuel conversion, most of the mineral matter distributed in a coal particle is exposed on the surface of the char particle as it recedes during oxidation. For the conditions within an electric utility boiler, at the char surface, this mineral matter coalesces and forms one or more particles, usually in the 1 to 20 μm range; particles that will be captured with high efficiency by the air pollution control devices (APCD). A small amount of the particles, of the order of one percent of the ash in coal, will vaporize and subsequently re-condense to form submicron particles that are in the size range in which penetration through filters is high.

The ash vaporization process can be modeled by applying fundamental understanding to various transformation pathways of mineral matter as shown in Figure 1.2.4. Part of this vaporization occurs during devolatilization in which elements that are present in organometallic form, many of which are trace transition elements, are released. The refractory oxides (FeO, SiO_2, MgO, CaO, Al_2O_3) are vaporized by the reduction of the oxides to the more volatile suboxides or metal, followed by the diffusion of the suboxides or metals to the particle boundary layer where they are reoxidized and condense to form a submicron aerosol [Quann and Sarofim, 1982].

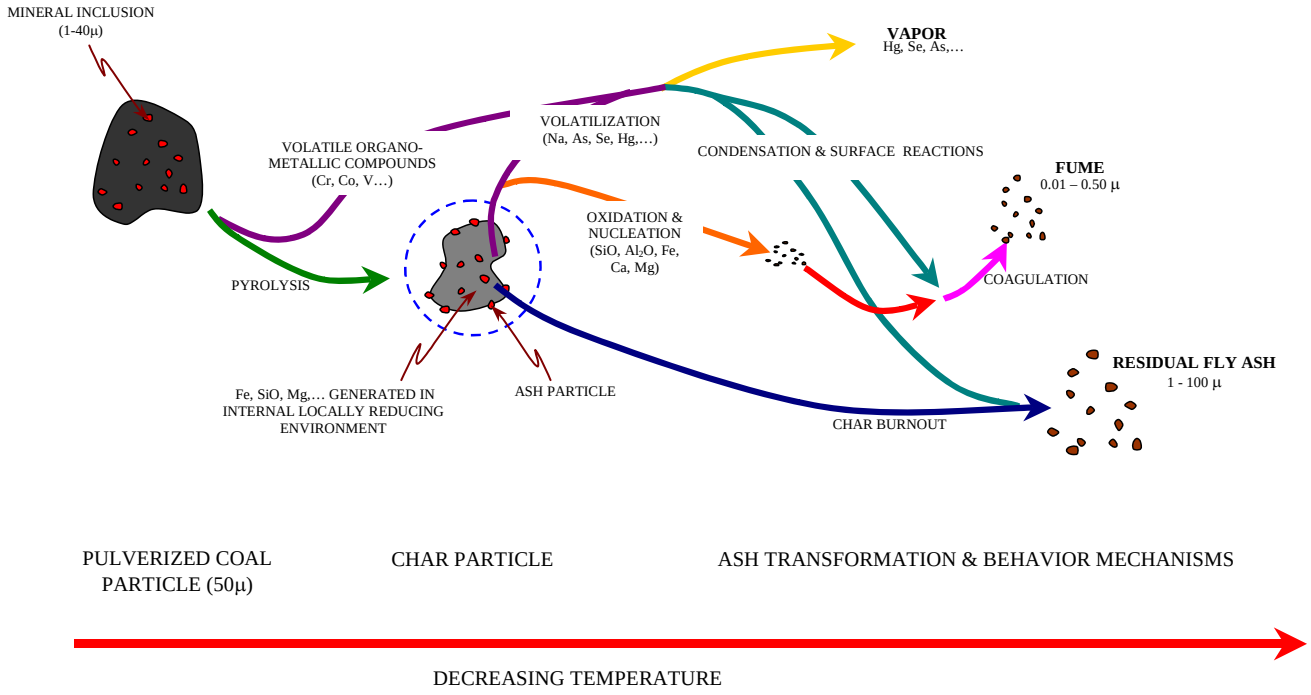

Figure 1.2.4. Schematic of mineral matter transformation during pulverized fuel conversion.

The vapor pressure of the vaporizing suboxide or metal is determined at the higher temperatures by the equilibrium of the reaction between the refractory oxide (RO) and carbon monoxide (CO) inside the particle, or

$$RO + CO \Leftrightarrow R + CO_2 \qquad (1.2.4)$$

An approximate value for the vapor pressure R of the reduced species can be obtained by assuming that the reaction in Equation (1.2.4) is at equilibrium. For this case, the vapor pressure is given by

$$P_R = K_E \frac{P_{CO}}{P_{CO_2}} \qquad (1.2.5)$$

For aluminum oxide, a slightly different formulation is needed since equilibrium considerations [Lee et al., 2000] show that the reduction reaction leading to the highest vapor pressure intermediate is:

$$Al_2O_3 + 2\ CO = Al_2O + 2\ CO_2 \qquad (1.2.6)$$

In this case the vapor pressure of the reduced species Al_2O is given by

$$P_R = K_E \left(\frac{P_{CO}}{P_{CO_2}} \right)^2 \qquad (1.2.7)$$

The application of this equation by Quann and Sarofim [1982] and more recently by Lee et al. [2000] was based on the assumption that the CO_2 partial pressure in a particle was determined by the oxidation of CO, or equal to P_R for the reaction in Equation (1.2.4) and equal to 2 P_R for the reaction in Equation (1.2.6). Haynes [2000a] has noted that the formation of CO_2 from surface reactions of carbon and oxygen and by gas phase reactions, will greatly exceed the amount produced by reaction in Equation (1.2.4). The effect of increasing the CO_2 concentration without allowing for an associated increase in temperature will be to decrease the predicted vaporization rate. Hence, the model provides a bounding value for the vaporized ash that will be contained in the syngas. Additional drop tube data is needed to improve this aspect of the model.

The vapor R of the reduced species is transferred from the surfaces of the mineral inclusions to the surface of the char particle, a process that determines the vaporization rate. The rate of vaporization when the mass transfer is taken into account is a function of the volume concentration of the minerals in the char, the mineral inclusion size, the equilibrium constant K_E, the CO/CO_2 ratio, the effective diffusivity of R through the char, and the external mass transfer coefficient. The reduced species, once exposed to oxygen in the particle boundary layer, is reoxidized and condenses to form submicron particles. The size of the submicron particles may be calculated from the mass vaporized using well-established theory on aerosol dynamics [Friedlander, 2000]. In addition, as depicted schematically in Figure 1.2.4, the more volatile salts of the alkali metals and the volatile trace metals will vaporize. These will condense downstream of the combustion zone at points where the combustion products have cooled down to their condensation temperatures. They will deposit on the surfaces of existing particles, in a manner calculable from mass-transfer-limited condensation [Flagan, 1994].

The ash vaporization model described above is run as a post-processor to the gasifier model because the feedback from the ash vaporization to the local gas temperatures, gas compositions and velocity fields will be minimal. The model calculations are performed along the trajectory for each cloud of particles contained in the model. Calculations that require local gas properties (e.g., temperature, partial pressures) use values interpolated from the local flow field.

Model Details

The ash vaporization model implemented in REI's entrained flow gasifier CFD model is based on models developed by Prof. Sarofim and his students. The model draws heavily upon single particle drop tube test described in [Quann, 1982] and [Quann and Sarofim, 1982]. As noted in [Lee, 2000], a simplified model for a single burning coal particle was developed to examine and interpret the experimental results obtained by Quann (1982). The simplified model was benchmarked to the drop tube data described above and subsequently used to provide estimates of the ash vaporization in a full boiler for low NOx firing conditions based on CFD simulation results [Lee, 2001], [Lee, Sarofim et al, 2001], [Eddings, Sarofim et al, 2001].

The model focuses on both the physical and thermochemical processes that occur in a burning coal particle. The physical processes involve the transport of inorganic vapors from the char particle, and the thermochemical processes involve the generation of volatile inorganic vapors within char particles by the reduction of refractory metal oxides.

Inherent mineral matter in coal occurs as either finely disseminated crystallites, or as inclusions with typical characteristic dimensions of 2 microns or less [Padia 1976], [Ward, 1977] embedded in the organic matrix of coal particles as in the case of silicon in quartz or clay minerals, or as elements organically bound and dispersed as in the principal occurrence of Ca and Mg in low rank coals [Quann, 1982]. The simplified model considers the existence of a uniformly-distributed array of mineral inclusions within each pulverized coal particle. As the coal ignites and the temperature rises, each inclusion of the array within a single porous char particle acts as a vapor source contributing to the overall volatilization rate of the inorganic species as shown schematically in Figure 1.2.5.

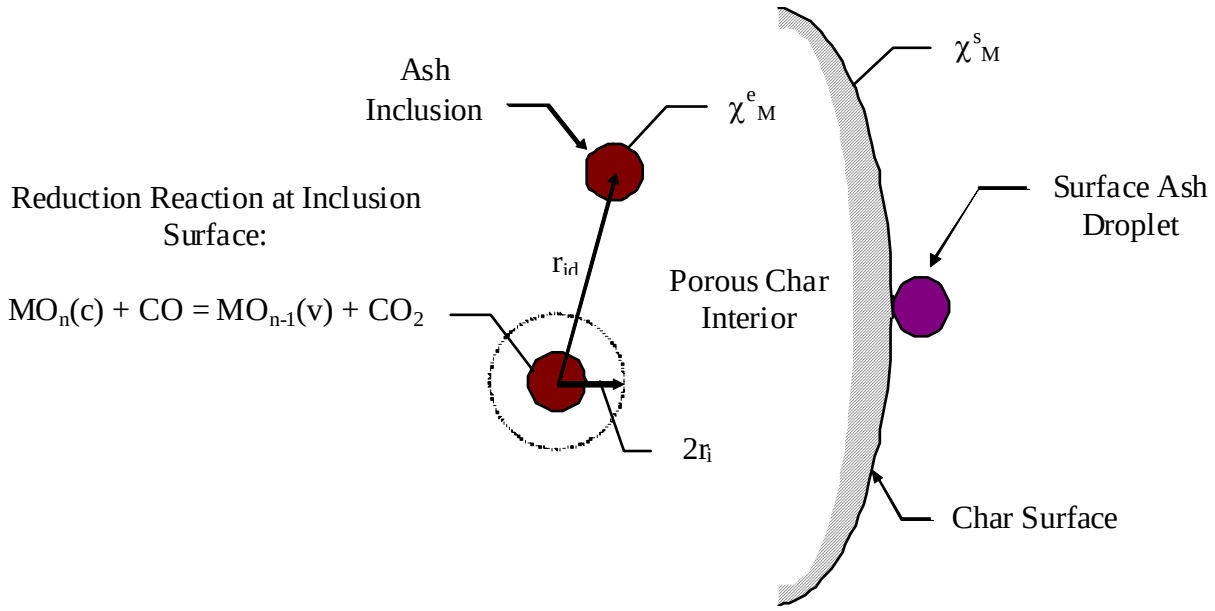

Figure 1.2.5. Schematic of the physical distributions of inclusions in a char particle.

The mineral matter within the char particle is exposed to a low oxygen potential, or reducing, condition. This occurs even though the coal particles are burning in oxygen-rich environments, and are thus the key to the thermochemical aspect of ash volatilization. The chemical reduction to more volatile forms of the refractory metal oxides within the ash will continue for as long as the char is burning. Equation (1.2.8) expresses the presence of excess carbon as:

$$\mathrm{x}M_{\mathrm{z}}O_n(c) + \mathrm{y}C \Leftrightarrow M_{\mathrm{xz}}O_{n-\mathrm{y}}(v) + \mathrm{y}CO \qquad (1.2.8)$$

In Equation (1.2.8), $M_zO_n(c)$ is the stable condensed metal oxide in the form of SiO_2, MgO, CaO, Al_2O_3, or FeO, whereas $M_{xz}O_{n\text{-}y}(v)$ is the volatile suboxide (SiO or Al_2O) or metal vapor (Mg, Ca, or Fe).

This reaction is an inherently slow process that requires the contacting of three phases. Therefore, it is more likely that the chemical reduction would progress through a series of intermediate reactions when examined at combustion timescales of less than one second [Szekely, et al. 1976]. Equation (1.2.9) and Equation (1.2.10) present the heterogeneous reactions:

$$\mathrm{x}M_{\mathrm{z}}O_n(c) + \mathrm{y}CO \Rightarrow M_{\mathrm{xz}}O_{n-\mathrm{y}}(v) + \mathrm{y}CO_2 \qquad (1.2.9)$$

$$CO_2 + C \Rightarrow 2CO \qquad (1.2.10)$$

In the current analysis, the other gaseous species, including H_2 and certain radicals, have been neglected. Although these species could act as reducing agents, the experimental system used in verifying the predictions was at lower concentrations and therefore not of primary concern. The assumption within the framework of the model is that Equation (1.2.9) occurs at equilibrium conditions at the surface of each inclusion within the char.

Based on this assumption, the equilibrium partial pressure of the metal or sub-oxide vapor, P_M^e, can be determined for Equation (1.2.9) from the equilibrium constant, Ke, at the surface of each inclusion and the partial pressures for CO and CO2. This is expressed in Equation (1.2.11) as

$$K_e = \frac{P_M^{e\,\mathrm{xz}} P_{CO_2}^{\mathrm{y}}}{a_{\mathrm{x}M_zO_n} P_{CO}^{\mathrm{y}}} \qquad (1.2.11)$$

where $a_{\mathrm{x}M_zO_n}$ is the activity coefficient. The activity coefficient is assumed to be independent of coal type and combustion conditions, so it cancels out of the equation. Equation (1.2.11) can therefore be applied to all metal oxides. For the present model, the coal is assumed to be composed of single component systems with respect to the metal oxide as opposed to multi-component systems that could result from high-temperature decomposition.

For this single-component system, assuming there is no other source of carbon dioxide to influence the surface equilibrium, the partial pressure of the inorganic vapors at the surface can be expressed as shown in Equation (1.2.12):

$$P_M^e = P_{CO_2} = (K_e P_{CO}^{y})^{\frac{1}{xz+y}} \quad (1.2.12)$$

This is accurate for the drop tube experiments performed by Quann, but must be modified for actual pulverized-coal operating units. This modification simply takes into account the CO_2 present in the system; therefore, the partial pressure for the inorganic vapors would be expressed as given in Equation (1.2.13):

$$P_M^e = \left(\frac{K_e P_{CO}^{y}}{P_{CO_2}^{y}} \right)^{\frac{1}{xz}} \quad (1.2.13)$$

As mentioned, the effect of CO_2 on vaporization will be examined in the case of actual operating units to emphasize the need for this modification. The equilibrium constant can be calculated by curve-fitting JANAF (Joint Army-Navy-Air Force) thermochemical data. The curve-fit takes the form of Equation (1.2.14) as:

$$\ln(K_e) = a + \frac{10^4 b}{T} \quad (1.2.14)$$

where a and b are the curve-fit coefficients.

The model developed assumes that the vaporization from a single inclusion can be calculated provided there is an equilibrium partial pressure for the inorganic vapor at the surface of each inclusion within the char particle. This also assumes that the inclusions are embedded in an isotropic porous medium where the characteristic dimensions for the pores are much less than the inclusion size [Quann, 1982]. Based on these assumptions the rate of vaporization for a single noninteracting (ni) isolated (I) inclusion can be expressed as in Equation (1.2.15)

$$V_I^{ni} = 4\pi c D_e r_i X_M^e \quad (1.2.15)$$

where, r_i is the radius of the inclusion embedded in the char particle, c is the concentration driving force defined by Equation (1.2.16):

$$c = \frac{P_M^e}{RT_p} \quad (1.2.16)$$

X^e_M is the equilibrium mole fraction of the inorganic vapor at the inclusion surface defined by Equation (1.2.17):

$$X_M^e = \frac{P_M^e}{P_{total}} \quad (1.2.17)$$

D_e is the effective diffusivity for Knudsen diffusion of the vapor in the porous char particle as given by Equation (1.2.18):

$$D_e = \frac{\varepsilon D_k}{\tau} \tag{1.2.18}$$

where τ is the tortuosity factor which has been assigned a value of 3.0 and ε is the porosity of the char with an assumed value of 0.462. The Knudsen diffusion coefficient expressed in Equation (1.2.19) is defined as:

$$D_k = 9700 r_p \sqrt{\frac{T_p}{MW}} \tag{1.2.19}$$

with r_p given as the pore radius in centimeters, T_p is the absolute particle temperature, and MW is the molecular weight. The diffusion coefficients are given in units of cm^2/sec.

The above equations are for a single inclusion when in reality a single char particle will contain a large number of inclusions. Therefore, it is assumed that these inclusions are statistically distributed particles interacting through the inorganic vapor field within the char. Because of the low volume fraction of inclusions in coal (~0.01), a "mean field approximation" [Felderhof and Deutch, 1976] has been employed to evaluate the profile for the 'macroscopic' mole fraction, X_M, of inorganic vapor in the porous char that results from the generation of ash vapor from a group of sources. If ρ_I is the number density of inclusions in a char particle, then the vapor mole fraction X_M, with respect to the char's radial coordinate, is determined by Equation (1.2.20):

$$cD_e \nabla^2 X + \rho_I V_I^i(r) = 0 \tag{1.2.20}$$

where V^i_I is the vaporization rate for a single inclusion and is, to a first order approximation, given by Equation (1.2.21):

$$V_I^i = 4\pi r_i c D_e \left(X_M^e - X_M \right) \tag{1.2.21}$$

Thus the vaporization rate of an inclusion is, due to interaction among a large number of inclusions, dependent on its position in the char [Quann. 1982].

The appropriate boundary conditions for this model are expressed in Equation (1.2.22) and Equation (1.2.23) where

$$\text{at } r = 0: \ \frac{dX_M}{dr} = 0 \tag{1.2.22}$$

and

$$\text{at } r = r_p: \ -4\pi r_p^2 c D_e \left.\frac{dX_M}{dr}\right|_{r=r_0} = 4\pi r_p c D_{O_2} \alpha_1 X_M^s \tag{1.2.23}$$

The factor, α_1, accounts for the Stephan flow effects brought about by diffusion-controlled combustion [Quann, 1982]. Thus, Equation (1.2.24) defines α_1,as:

$$\alpha_1 = \frac{\ell n\left(1 + X_{O_2}^{b}\right)}{1 - e^{-\frac{D_{O_2}}{D_M}\ell n\left(1+X_{O_2}^{b}\right)}} \tag{1.2.24}$$

where D_M and D_{O2} have units of cm^2/sec and are the gas diffusivities of the metal vapor and of oxygen respectively as defined by Equation (1.2.25):

$$D = 0.00100 \frac{T_p^{\,1.75}\left(\frac{1}{M_1} + \frac{1}{M_2}\right)^{\frac{1}{2}}}{P_{total}\left[\left(\sum v\right)_1^{1/3} + \left(\sum v\right)_2^{1/3}\right]^2} \tag{1.2.25}$$

with the molecular weights given by M_1 and M_2 and the atomic volumes for the species defined by v. X^b_{O2} is the mole fraction of oxygen in the bulk gas far away from the burning char particle. The second boundary condition, Equation (1.2.26), is the equality of the internal and external rate of vapor transport with X^s_M defined as the mole fraction of the vapor at the external char surface. It has been assumed that as r goes to infinity, X_M goes to zero.

Equation (1.2.19) can be interpreted as the problem of diffusion and reaction in a porous catalyst pellet [Satterfield, 1970] defined by Equation (1.2.26):

$$\frac{1}{r^2}\frac{d}{dr}r^2\frac{dX_M}{dr} + \frac{\phi_I^2}{r_p^2}\left(X_M^e - X_M\right) = 0 \tag{1.2.26}$$

where the Thiele modulus, ϕ_I, given by Equation (1.2.27):

$$\phi_I = \sqrt{3\theta_I}\,\frac{r_p}{r_i} \tag{1.2.27}$$

is solely dependent on the physical distribution, or occurrence of mineral matter. The inclusion volume fraction, v_f, is a function of the coal and ash densities and the fraction of inclusions within the char. The solution to Equation (1.2.26) for the vapor mole fraction within the char particle is expressed in Equation (1.2.28) as:

$$X_M = X_M^e\left[1 - \left(1 - \left(\frac{X_M^s}{X_M^e}\right)\frac{r_p \sinh\left(\phi_I \frac{r_p}{r_i}\right)}{r \sinh \phi_I}\right)\right] \tag{1.2.28}$$

where X^s_M, the vapor mole fraction at the char surface ($r = r_p$), defined by Equation (1.2.29):

$$X_M^s = X_M^e \left[\frac{\frac{D_e}{\alpha_1 D_{O_2}} \left(\frac{\phi_I}{\tanh \phi_I} - 1 \right)}{1 + \left(\frac{D_e}{\alpha_1 D_{O_2}} \left(\frac{\phi_I}{\tanh \phi_I} - 1 \right) \right)} \right] \tag{1.2.29}$$

Thus, the total instantaneous rate of vaporization, V_c (moles/sec) from a char particle of radius r_p is determined from Equation (1.2.30):

$$V_c = 4\pi r_p{}^2 dD_e \left. \frac{\partial X_M}{\partial r} \right|_{r=r_0} = 4\pi r_p c D_{O_2} \alpha_1 X_M^s \tag{1.2.30}$$

Whereas for noninteracting inclusions, the total vaporization rate V^{ni}_c could be expressed by Equation (1.2.31) or Equation (1.2.32) as:

$$V_c^{ni} = N_I 4\pi r_i c D_e X_M^e \tag{1.2.31}$$

or

$$V_c^{ni} = N_I V_I^{ni} \tag{1.2.32}$$

where N_I is the number of inclusions in the char particle. The value for N_I can be determined from the inclusion volume fraction, v_f, which is the product of the fraction of refractory oxides in the ash and the ratio of the ash and coal densities. Equation (1.2.33), an effectiveness factor η, is given by:

$$\eta = \frac{\frac{3}{\phi_I} \left[\frac{1}{\tanh \phi_I} - \frac{1}{\phi_I} \right]}{1 + \frac{D_e}{\alpha_1 D_{O_2}} \left(\frac{\phi_I}{\tanh \phi_I} \right) - 1} \tag{1.2.33}$$

which gives the ratio of the total vaporization rate of the char, accounting for the interaction of particles and the control of external diffusion, over that of the rate of isolated inclusions and droplets in the char. Thus the total vaporization rate can be expressed by Equation (1.2.34) as:

$$V_c = \eta N_I V_I^{ni} \tag{1.2.34}$$

The vaporization rate as given is a function of several parameters when applied to the case of a full-size boiler. These parameters include the particle sizes and temperatures, the local gas concentrations of O_2, CO, and CO_2, and the particle burnout time. In determining the fraction of ash vaporized this information is also necessary; however, the amount vaporized is the integral of this vaporization rate. This expression is given by Equation (1.2.35) as:

$$F_v = \int_0^t V_c dt \tag{1.2.35}$$

Example results using the model are provided in the Results and Discussion section of this report (see Section 2.2.3) and [Bockelie et al., 2008ce].

1.2.2 Task 2.2 Implement CAPE-Open Versions of Selected REI Process Models

In a previous NETL funded project REI developed numerous process engineering models for equipment and processes needed to simulate advanced IGCC systems [Bockelie et al, 2004]. In this task, REI has ported selected REI process models to be CAPE-Open compliant for use in AspenPlus/APECS. Original development by REI was geared towards the CORBA-based APECS framework. However, it was subsequently indicated by NETL that the support for CORBA-based CAPE-Open components would be discontinued for APECS. Hence, REI developers had to port the models previously developed to work with CORBA-APECS to the COM CAPE-Open standard. In the following, we only provide information on our efforts for porting the models to the COM CAPE-Open standard.

CAPE-Open Implementation

REI has pursued the use of a COM CAPE-Open interface to make the selected REI process models available in AspenPlus/APECS. In support of this approach, an example of a COM-based model implementation was obtained from Dr. Michael Pons (Chief Technology Officer, CAPE-Open Laboratories Network), an authority on CAPE-Open. The example was subsequently built by REI and verified to work in AspenPlus. This example had a different CAPE-Open interface compared to previous examples REI obtained from the CAPE-Open alliance. This posed certain difficulties, because the example code only demonstrated the use of global thermodynamic stream parameters (e.g., pressure, temperature, etc.) but not stream components (e.g., species). After determining how to use species in the new interface, REI was able to create a COM-based version of selected process models for AspenPlus.

Due to the somewhat limited support of the CAPE-Open standard in AspenPlus, REI had to overcome a number of obstacles while porting models to work in Aspen. The major problem was a lack of access to AspenPlus sub-stream variables from CAPE-Open. The existence of this problem has been verified with AspenPlus technical support personnel. AspenPlus IGCC flowsheets obtained from NETL use a MIXEDNC stream class consisting of three substreams: MIXED, SOLID and NC (nonconventional), where MIXED would be used for gas phase, SOLID for particles and NC for coal, slug and ash. AspenPlus has a stream class changer block which allows the user to drop empty SOLID and NC sub-streams, or add them back. This operation essentially converts the stream type from MIXEDNC to CONVENTIONAL and back and is useful when a model operates on gas phase only (e.g., OTM model) but is of no use if a model needs to operate on coal or particles. In this later case REI engineers used AspenPlus Fortran calculator blocks to communicate sub-stream information between AspenPlus and the CAPE-Open model through files on a computer hard drive. Still, this approach has certain drawbacks.

1. A full installation of the Intel FORTRAN compiler is needed to make the calculator blocks work due to the very limited capabilities of the built-in FORTRAN interpreter in AspenPlus.
2. Models implemented in this manner will always produce a warning about the lack of a mass balance for the model block because AspenPlus calculates the block mass balance before the calculator block fills block output streams with data.

Example: Use of AspenPlus Calculator Blocks For Data Exchange

Calculator blocks provide the user with the ability to use custom or proprietary models in AspenPlus flowsheets. Shown below is an example of how REI uses the Aspen Calculator Blocks for implementing the COM CAPE-Open interface for the REI Entrained Flow Gasifier Process Model. It should be noted that the AspenPlus Calculator blocks have been used in a rudimentary way - just to transfer data between the sub-streams and files on the hard drive. In effect, these files serve as input/output files for the REI Entrained Flow Gasifier Process Model.

AspenPlus Calculator blocks provide the ability to specify a mapping between any AspenPlus variable (e.g. sub-stream member values) and variables internal to the user model. An example is shown in Figure 1.2.6.

Variable name	Info. flow	Definition
ULTIM		Compattr-Vec Stream=WET-COAL Substream=NC Component=COAL Attribute=ULTANAL
PROX		Compattr-Vec Stream=WET-COAL Substream=NC Component=COAL Attribute=PROXANAL
TEMPOX		Stream-Var Stream=OXYGEN Substream=MIXED Variable=TEMP Units=K

Figure 1.2.6. AspenPlus Calculator block variable mapping used for REI Entrained Flow Gasifier Process Model.

As highlighted in Figure 1.2.7, the user model can be implemented using FORTRAN or Microsoft EXCEL.

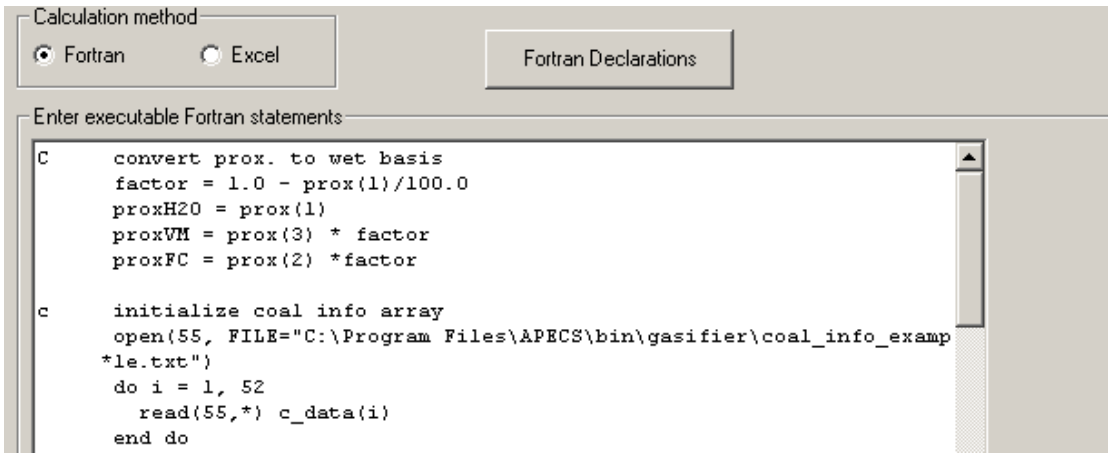

Figure 1.2.7. User FORTRAN model inside Aspen Calculator block.

For a FORTRAN based model, AspenPlus provides a built-in FORTRAN interpreter. Unfortunately, the built-in interpreter has limited functionality (i.e., only a subset of the FORTRAN language functions and operators are supported). For the gasifier model, it was determined that the AspenPlus FORTRAN interpreter was not adequate (i.e., the FORTRAN "write" statement is not available) and thus a third party FORTRAN compiler has been used. For AspenPlus the recommended FORTRAN compiler is the Intel FORTRAN 9.0 compiler. It should be noted that the FORTRAN compiler is required for gasifier model operation - the model will not function without it. Note that if the difficulties described above for CAPE-Open

accessing AspenPlus sub-streams can be solved, there would be no need to use AspenPlus Calculator blocks and thus no need for the FORTRAN compiler.

During the course of the project, REI ported the models listed below to the COM-based CAPE-Open standard for use in the NETL AspenPlus IGCC flowsheets.

- REI Entrained Flow Gasifier Process Model (one stage and two stage);
    - Further details on these models are contained in the discussion for Task 2.1 in Chapter 1 (see Section 1.2.1) and in [Bockelie et al., 2004].
- REI Carbon Bed model;
    - Further details on the model are available in [Bockelie et al., 2004].
- An OTM ASU model;
    - Further details on this model (provided by Praxair, a project team member) are provided in Chapter 1 in the discussion for Task 2.3 (see Section 1.2.3).
- REI ROM Generator.
    - Further details on the ROM Generator are provided in Chapter 1 in the discussion for Task 2.4 (see Section 1.2.4).

Example calculations performed with these four models are discussed in the Results and Discussion section of this report.

1.2.3 Task 2.3 Implement CAPE-Open Versions of ASU Models

The Air Separation Unit (ASU) is an important piece of equipment for an IGCC plant. The ASU is used to separate oxygen from ambient air in order to feed a pure stream of oxygen to the coal gasifier. In this task REI ported process models of cryogenic and Oxygen Transport Membrane (OTM) ASU models provided by Praxair, a project team member, for use in APECS. A cryogenic unit uses cryogenic distillation to separate oxygen from the other constituents in the air and represents currently available technology. In contrast, Oxygen Transport Membrane (OTM) based units represent the state-of-the-art for air separation technology that might be used in next generation IGCC plants.

The material below includes technical descriptions of the ASU models and issues addressed in porting the models for use in APECS. Example calculations using the provided ASU models within an AspenPlus flowsheet for an IGCC plant configuration studied by NETL [Klara, 2007] are provided in Chapter 3 of this report.

Cryogenic ASU Process Model

Technical Description

The cryogenic ASU model originally provided to REI by Praxair for use in this DOE project was a HYSYS based process model. HYSYS is an alternative flowsheet modeling software package used by system developers for modeling industrial plant performance. Due to the level of detail in the HYSYS model and because the model used numerous HYSYS computational blocks (sub-models), it was determined that the most effective means to implement the model into AspenPlus was to replicate the HYSYS model using similar computational blocks from AspenPlus. The AspenPlus version of the ASU model requires a network of models which includes the following:

- 3 Distillation Column (RadFrac) blocks,
- 3 Heat exchanger (MHeatX) blocks,
- 3 Heater (Heater) blocks,
- 5 Splitter (FSplit) blocks,
- 2 Compressors (Compr) blocks,
- 2 Pump blocks, and
- 3 Valve blocks.

Illustrated in Figure 1.2.8 is the AspenPlus flowsheet for the cryogenic ASU model. Block and Stream names were retained in this flowsheet.

Calculations for the processes contained within a cryogenic ASU require an accurate equation of state (EOS) to properly compute liquid and vapor properties. Technology developers for cryogenic ASU systems typically use a proprietary EOS for property evaluation. Although the basic form of the EOS might be taken from the literature (e.g., [Bender, 1970], [Bender, 1973], [Stryjek and Vera, 1986]), many of the model parameters would be adjusted to provide a better fit to proprietary data. AspenPlus provides thirteen EOS property models that are applicable to non-polar molecules such as that found in air (see Figure 1.2.9). Based on discussions with

industry personnel, REI chose to use the Peng-Robinson EOS for baseline calculations; it is similar to the Bender model, but has been used in studies available in the open literature and is available in AspenPlus.

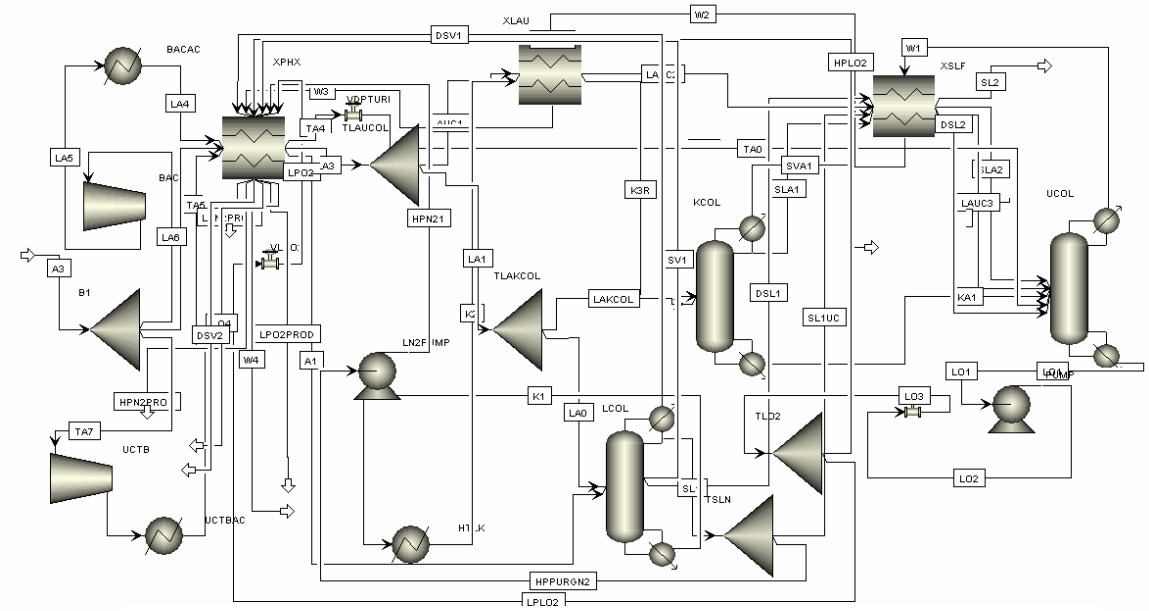

Figure 1.2.8. AspenPlus ASU network to replicate HYSYS ASU model.

Equation-of-State Property Method	K-Value Method
BWR-LS	BWR Lee-Starling
LK-PLOCK	Lee-Kesler-Plöcker
PENG-ROB	Peng-Robinson
PR-BM	Peng-Robinson with Boston-Mathias alpha function
PRWS	Peng-Robinson with Wong-Sandler mixing rules
PRMHV2	Peng-Robinson with modified Huron-Vidal mixing rules
PSRK	Predictive Redlich-Kwong-Soave
RKSWS	Redlich-Kwong-Soave with Wong-Sandler mixing rules
RKSMHV2	Redlich-Kwong-Soave with modified Huron-Vidal mixing rules
RK-ASPEN	Redlich-Kwong-ASPEN
RK-SOAVE	Redlich-Kwong-Soave
RKS-BM	Redlich-Kwong-Soave with Boston-Mathias alpha function
SR-POLAR	Schwartzentruber-Renon

Figure 1.2.9. EOS models available in AspenPlus.

Sensitivity of ASU Model Outputs to Selected EOS Model

The sensitivity of the predicted ASU performance to the selection of EOS model is shown in Table 1.2.1. For these calculations it is assumed the low pressure O2 production stream has a temperature of 61.07 F and a pressure of 72.0 psia. As can be seen from Table 1.2.1, only slight differences in predicted oxygen output concentration and flow result from these three AspenPlus models. The values predicted by the AspenPlus version of the ASI model agree to within about 5% of the values predicted by the HYSYS version of the ASU model and thus provide sufficient accuracy for the needs of this project.

Table 1.2.1. Comparison of ASU output with different EOS models.

LP O2 Prod Stream					
		ASPEN™			
EOS Model		**Peng-Rob**	**PR-BM**	**RK-ASPEN**	**RK-SOAVE**
O_2 Molar flow, lbmol/hr		**271.1**	**273.5**	**271.6**	**272.6**
O_2 Mole Fraction		**0.9594**	**0.9683**	**0.9613**	**0.9649**

The effect of air throughput on predicted values was evaluated using the Peng-Robinson EOS. Figure 1.2.10 shows the effect of the air throughput on the ASU outlet oxygen flow and concentration. For these calculations, the air stream input parameters (the A3 stream in Figure 1.4.1) are: air flow 70,370 lbmol/hr; 65.03 F; 230.0 psia; N2 mole fraction = 0.7811; Argon mole fraction = 0.0093; and O2 mole fraction = 0.2095. As seen from the plotted results, as the air flow is increased the oxygen air flow increases but the oxygen concentration decreases.

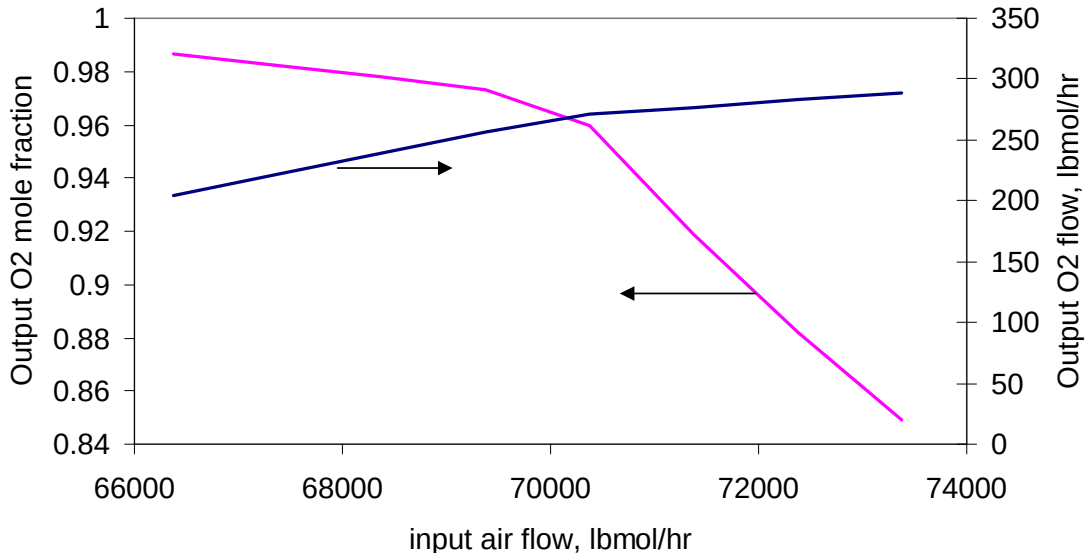

Figure 1.2.10. Predicted ASU outlet oxygen flow and concentration versus the air input flow rate.

ASU Model Implementation Into IGCC Flowsheets

The original project plan called for creating a CAPE-Open compliant ASU model. As noted above, the ASU model provided by Praxair has been converted from a HYSYS flowsheet to an AspenPlus flowsheet. Given that the model already exists in the form of an AspenPlus flowsheet, adding a CAPE-Open compliant wrapper to the model would be counter-productive. Instead, the cryogenic ASU model has been provided to NETL as an AspenPlus hierarchal library. With this approach, the model is simply a member of the library of models available to the user from AspenPlus.

The ASU model described above contains far more detail than that provided in the NETL AspenPlus IGCC flowsheets. The NETL ASU model is only a simple splitter block in which the user specifies the composition and flow rate for the streams produced for a given inlet air flow. In contrast, the detailed ASU model uses a far more detailed, and complicated, set of calculations to determine the flow rate and composition of the streams exiting the ASU.

A challenge for using the detailed ASU model within the NETL AspenPlus IGCC flowsheet is how to operate the ASU in a manner that satisfies the convergence criteria inherit with the IGCC flowsheets. The compounds that must be excluded or minimized to trace levels prior to entry to the ASU are H_2O and CO_2. These two substances, if introduced in significant amounts, will result in column drying in two of the columns. In addition, it is also important to run the ASU at high flow rates. These flow rates should exceed 20,000 lbmol/hr; smaller flow rates may lead to column drying.

The sections below provide guidance on how to import and run the ASU model within the AspenPlus IGCC flow sheet “MSCase1NPv21.bkp” provided by NETL (see discussion of Task 3 in Section 1.3). Although the approach is presented in a general manner, specific steps may require modification for other IGCC flowsheets. The following instructions assume that the NETL AspenPlus IGCC flowsheet is open and ready for execution within AspenPlus and that the user is an experienced AspenPlus modeler.

Determine Initial Estimate For Detailed Cryogenic ASU Model Input Data

The detailed ASU model requires a good initial estimate for the product streams or otherwise convergence problems can occur. A reasonable estimate can be obtained from the NETL ASU splitter block model. The following steps are recommended.

1) Eliminate the CO_2 and H_2O from the Ambient Air stream. This reduces the amount of CO_2, and H_2O entering the ASU to tolerable levels. The ambient air stream (AMBNTAIR) uses mass fractions and thus the mass fractions of the remaining species (AR, O_2, N_2) must be re-normalized (see Figure 1.2.11).
2) Execute the AspenPlus IGCC Flowsheet.
3) After a successful run, copy the results from the AIRTOASU stream into an EXCEL spreadsheet (see Figure 1.2.12). Be certain to include the Temperature and Pressure. This copied data will serve as input data for the detailed ASU model in later calculations.

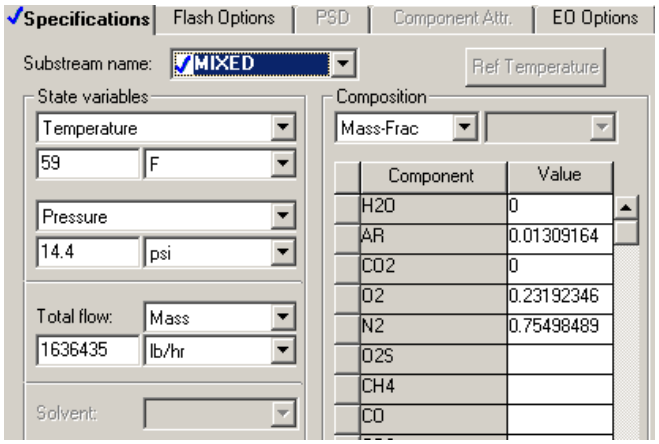

Figure 1.2.11. Normalized Components for AMBNTAIR Stream.

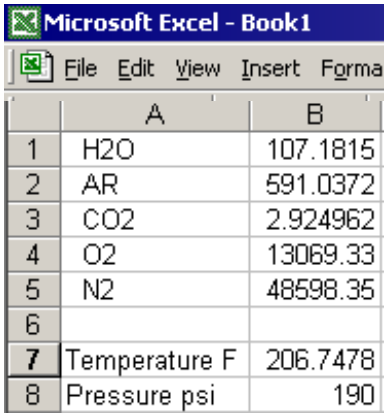

Figure 1.2.12. ASU Product stream results stored in EXCEL

Implementing the Detailed ASU Model Into the Flowsheet

1) Delete the original ASU unit contained in the flowsheeet.
2) Place the detailed ASU model in the flowsheet:
    a. Select (click on) Library in the AspenPlus menu bar.
    b. Select References. This will bring up the list of available libraries.
    c. Select the Browse button and search for the folder where the detailed ASU model library (entitled **paasu**) is located. This will create a new check box labeled **paasu**.
    d. Check the box and press OK. This will create a new tab on the model bar labeled **paasu**. Inside this tab there is a box labeled **paasu**. This is the detailed ASU model.
    e. Click on this icon and place it into the Aspen flow sheet.
3) Connect the AIRTOASU stream to a CLCHNG block called CLCHNG1. The CLCHNG block is located under the Manipulators tab in AspenPlus.
4) Create a stream called ASUFEED with its source as CLCHNG1. Do not connect the destination of this stream to a block.
5) Create a stream called FEED (see Figure 1.2.14). Copy the results from the AIRTOASU stored in the EXCEL file containing the initial guess for the ASU product stream flows (see above) and paste the results into the FEED input (see Figure 1.2.13). The stream flow rates can be copied directly from EXCEL and pasted into AspenPlus.
6) Create three output streams from the detailed ASU model and name the streams LPN2, HPN2, and O2PROD (see Figure 1.2.14). Table 1.2.2 indicates how these streams should be connected to the flowsheet streams. Insert a CLCHNG block between the created streams and the associated streams in the IGCC flowsheet. This is required because the stream class for the ASU is CONV but the stream classes for the IGCC are MIXEDNC (see Figure 1.2.14). Note that when a CONV stream is connected to a CLCHNG block and a MIXEDNC stream is then attached to that same block, sometimes the MIXEDNC stream will change classes to CONV, and vice-versa. Hence, the user check that after implementing a CLCHNG block that the streams have the appropriate class.
7) Delete the streams ASUVENT and ASU-VENT and the ASUMIX splitter block.

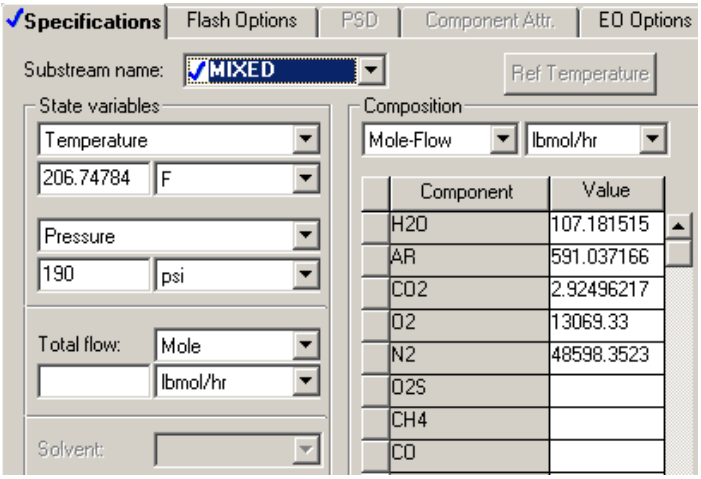

Figure 1.2.13. FEED Input for detailed ASU model.

Table 1.2.2. Detailed ASU Model Stream Connections.

	ASU Stream	Created Stream	Flowsheet Stream
Input	A3	FEED	
Output	N2PROD2	LPN2	N2PRODCT
	N2HPROD3	HPN2	HIPN2
	O2PROD2	O2PROD	O2PRODCT

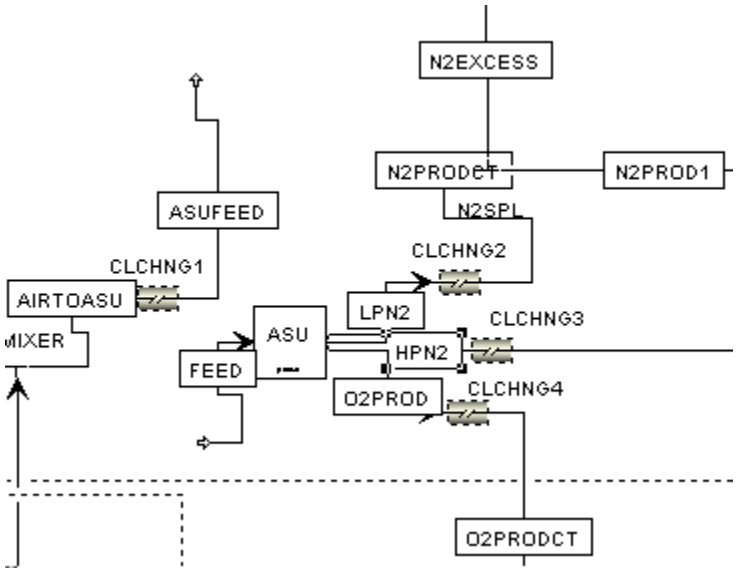

Figure 1.2.14. Detailed ASU model in flowsheet.

The reason for creating a new input for the detailed ASU model (block) that is not connected to the flowsheet is that when the flowsheet is run with the ASU using a poor initial estimate for the product flow rates, the flowsheet will not converge to a feasible solution. This can cause

problems in multiple areas of the ASU. Instead of trying to wade through all of these problems one can instead use the (nearly) correct product stream values as the input into the ASU and use the resulting solution as a gauge to see if the ASU specifications are correct. If the procedure outlined above is not performed it can be difficult to obtain a (feasible) solution.

Execute The Flowsheet

To execute the modified flowsheet the following steps are recommended.

1) Clear the streams in the ASU by performing a right-button mouse click and selecting "clear" from the list of options.
2) Select the Convergence folder and then select Sequence. Two rows in the provided tables will have to be deleted due to incomplete information (see Figure 1.2.15).

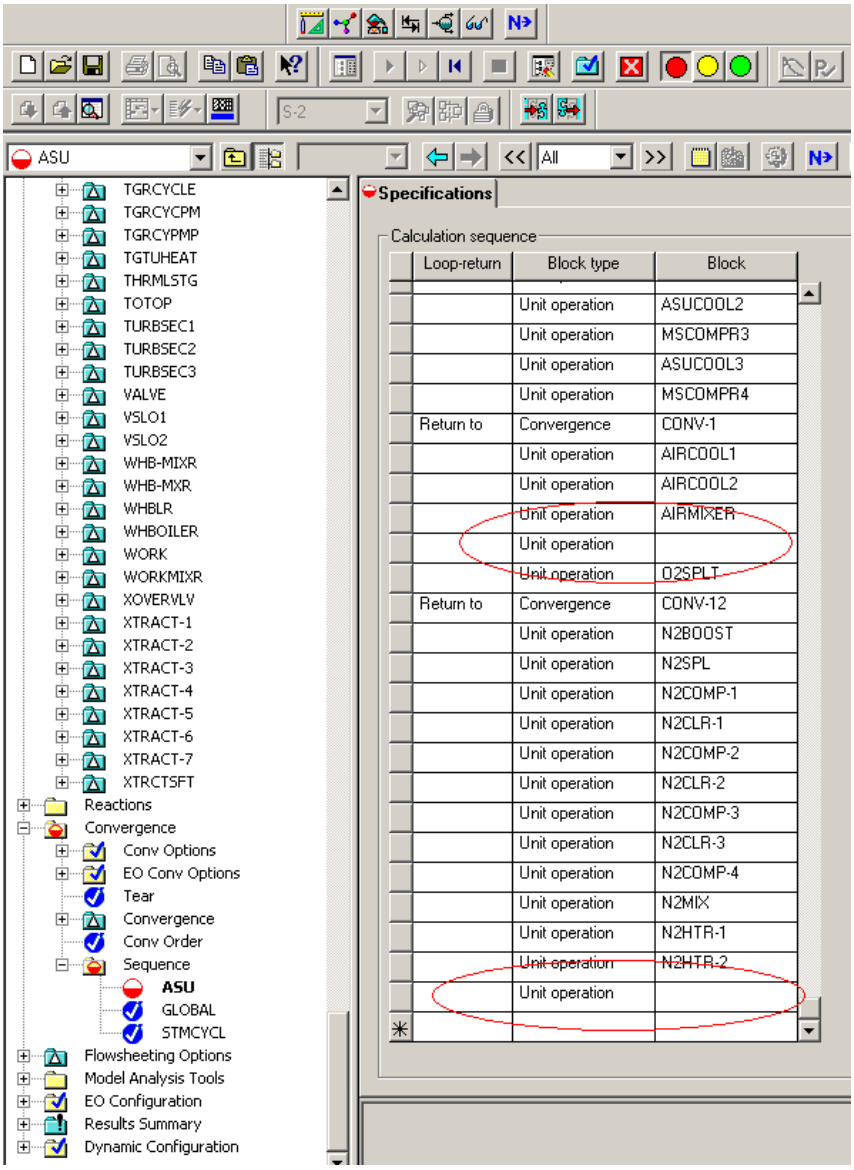

Figure 1.2.15. Convergence lines that must be deleted.

3) Select ASU Properties.
    a. select PENG-ROB for the base method in the dialog boxed for Property methods and models (see Figure 1.2.16).
    b. select Petroleum Calculation Options and set Free-water method to IDEAL (see Figure 1.2.16).
4) Execute the flowsheet.

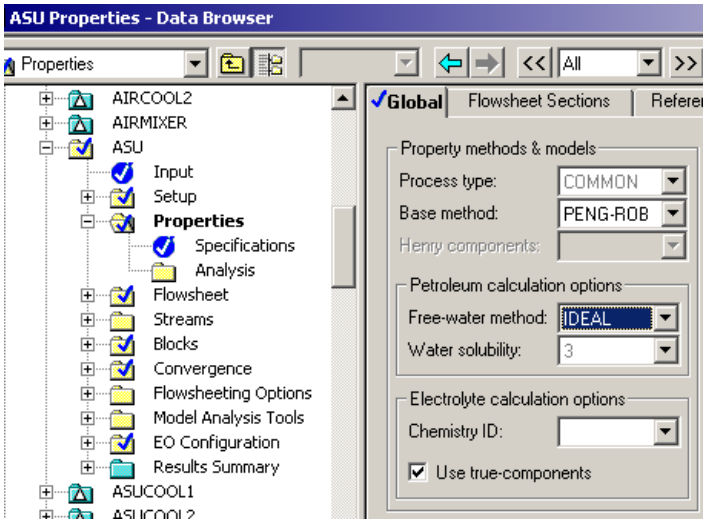

Figure 1.2.16. Detailed ASU model properties.

ASU Errors

The user must check that the ASU executes without any block errors. Oftentimes, there are block errors when first executing the ASU. These errors can be addressed by altering the Reflux ratios in the LCOL and UCOL distillation columns. These columns are located in the ASU unit and are highlighted in Figure 1.2.17. The following procedure is recommended if the Reflux ratios must be adjusted.

1) Select the UCOL column and change the Distillate Rate to a Reflux Ratio and use the value of 0.4544 (see Figure 1.2.18).
2) Select the LCOL Column and change the Reflux Ratio to 30 (see Figure 1.2.19). The UCOL and LCOL parameter changes are not the ideal settings but they should allow the ASU to operate.
3) If the ASU still has errors try adjusting the LCOL and UCOL Reflux Ratios until the ASU runs without any block errors.

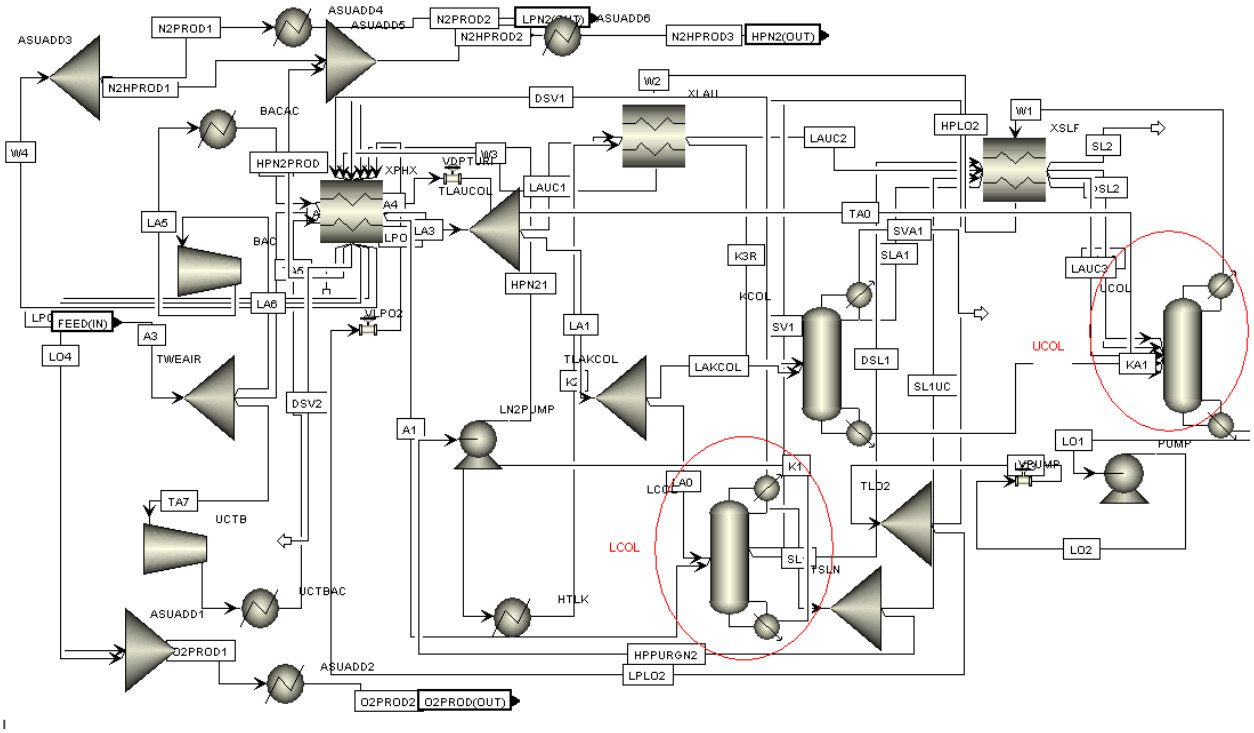

Figure 1.2.17. Location of LCOL and UCOL distillation columns in detailed ASU model.

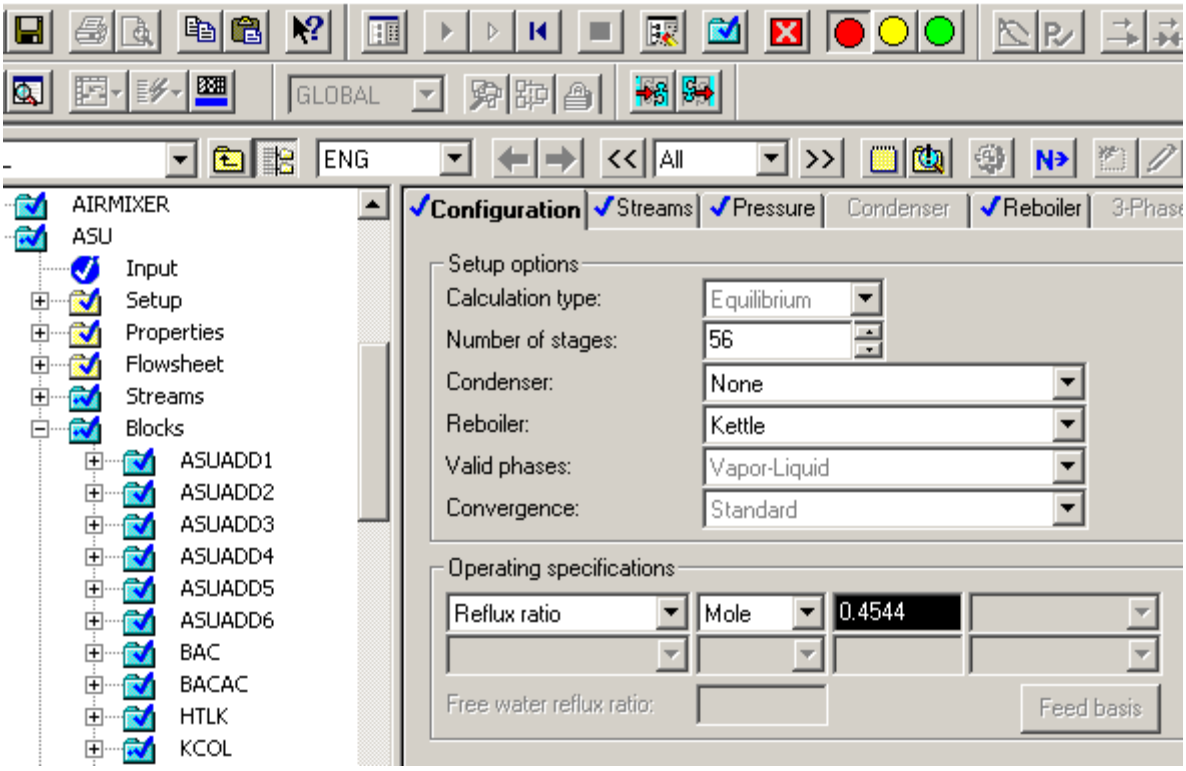

Figure 1.2.18. UCOL distillation column configuration.

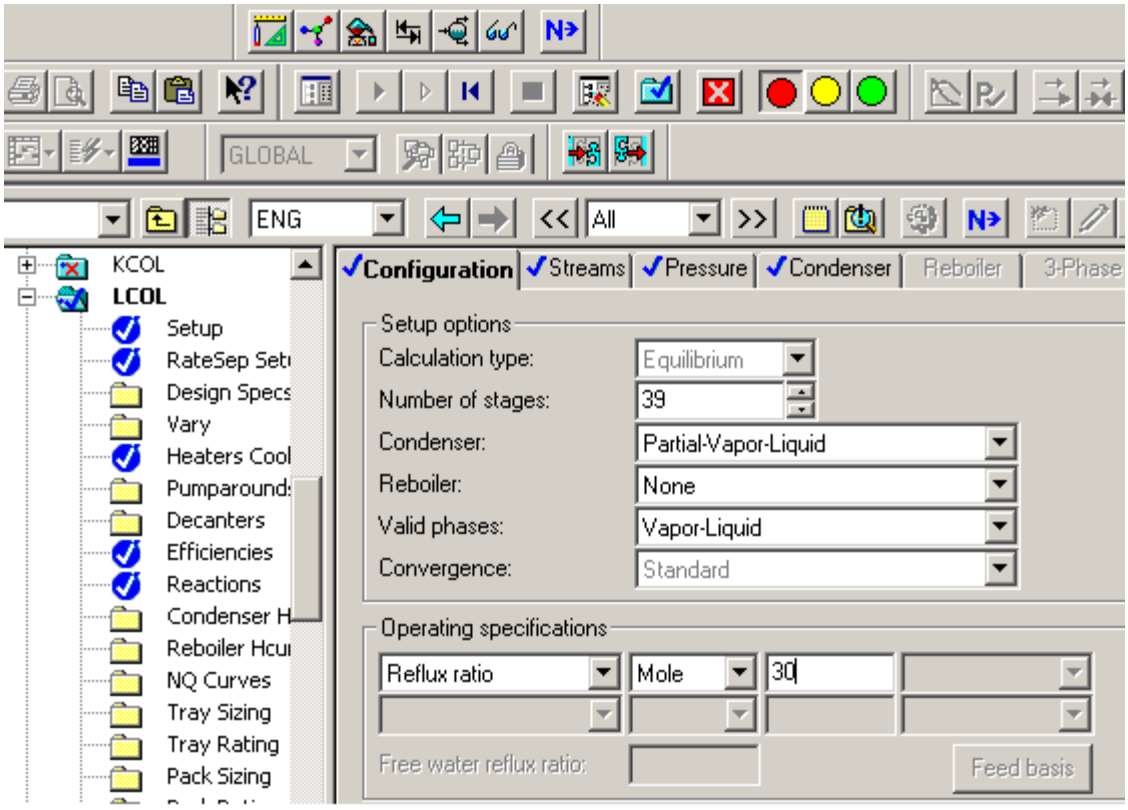

Figure 1.2.19. LCOL distillation column configuration.

Convergence Issues

1) The convergence block most directly affected by the detail ASU model is CONV12. This convergence block uses the AIRTOASU Design Specification for convergence criteria (see Figure 1.2.20). If the results show an error in CONV12 or if the solution didn't converge to the desired solution go to the AIRTOASU Design Specification and alter the tolerance to a level where a solution can converge. This may require increasing the tolerance level well above 50,000.
2) Once a solution can be obtained without any convergence issues, lower the convergence tolerance to its lowest possible level.
    a. Select the UCOL Data Browser screen. Have both the ASUAIR design specification screen and the UCOL screen open as shown in Figure 1.2.21.
    b. Alter the UCOL R-value and run the simulation. If a change in the R-value allows the flowsheet to converge then chances are that the change has lowered the convergence tolerance. Check this by lowering the convergence tolerance and rerunning the simulation.
    c. Repeat this process until you have restored the original convergence tolerance. Note that a small change in the R-value has a large impact on the convergence tolerance. The R-values may need added significant figures to converge. Figure 1.2.22 illustrates an example of the result of this iterative process.
    d. Because this is an iterative approach, it requires a trial and error procedure and thus can involve a significant amount of effort.

3) When the user has identified a Reflux Ratio that allows the flowsheet to converge the FEED stream can be erased and the ASUFEED stream can be connected to the A3 stream of the ASU (see Figure 1.2.21).
4) With the ASUFEED connected to the ASU the user can now operate the flowsheet with a functional ASU.

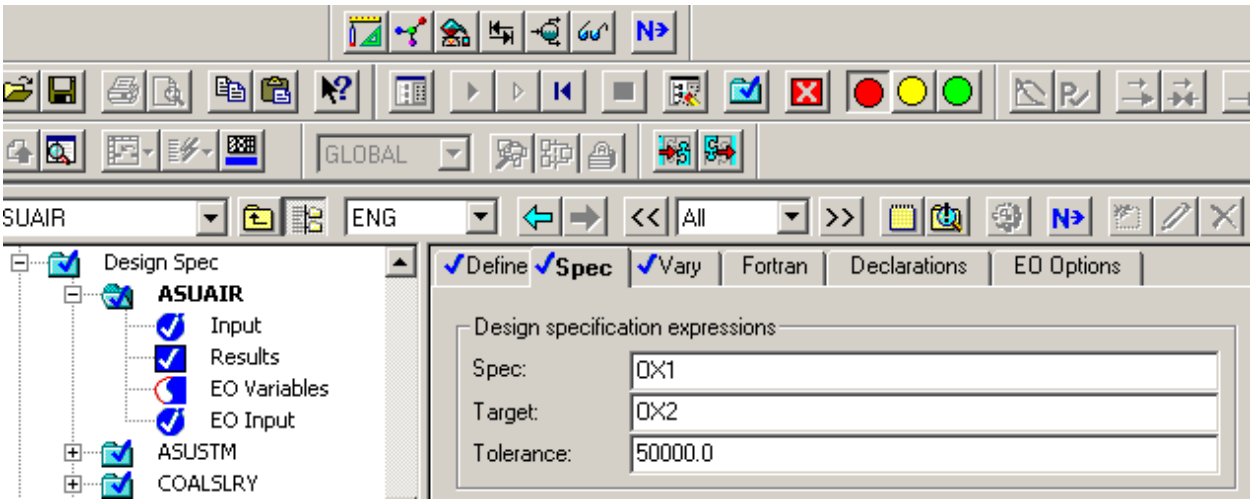

Figure 1.2.20. ASUAIR Design Specification window.

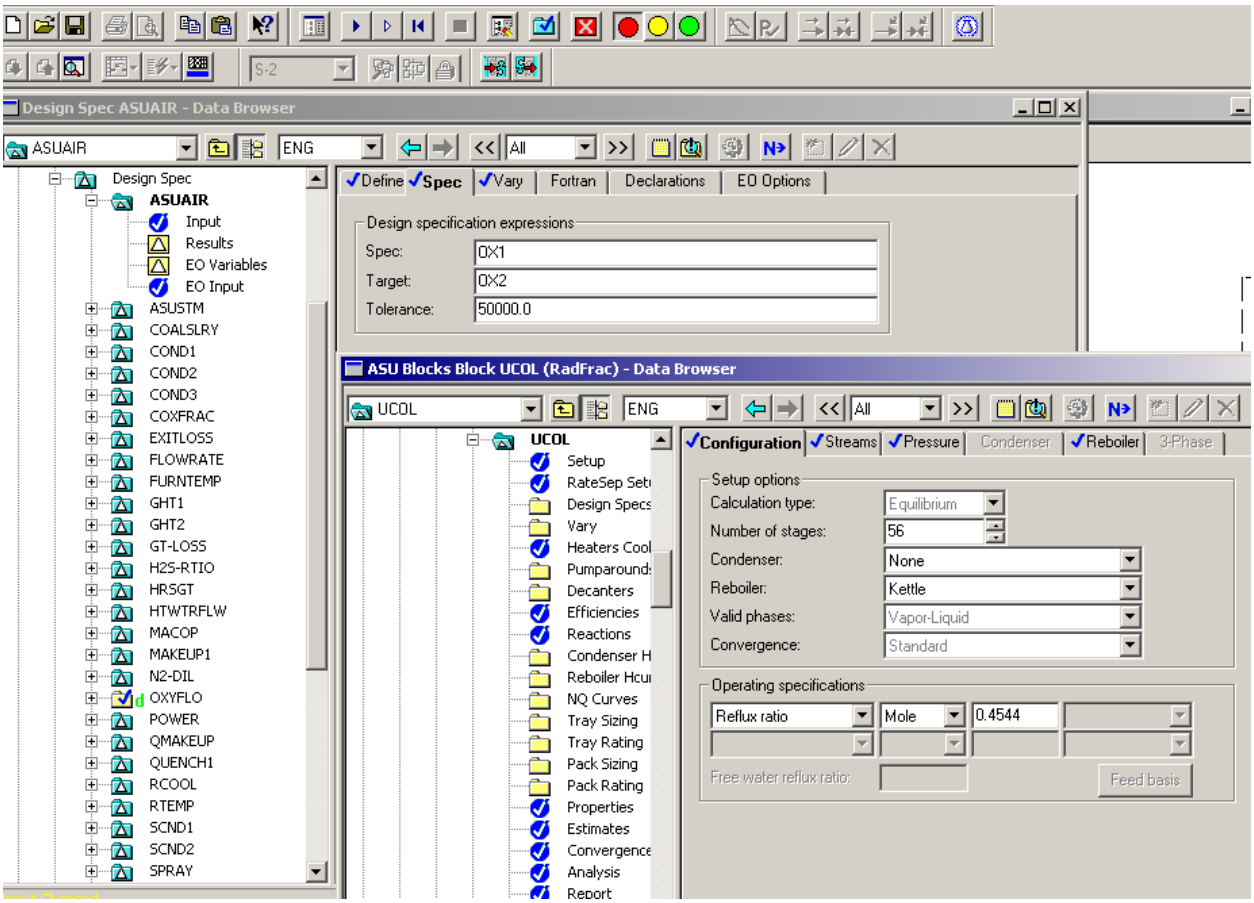

Figure 1.2.21. Screen setup with ASUAIR Design Specification and UCOL windows open.

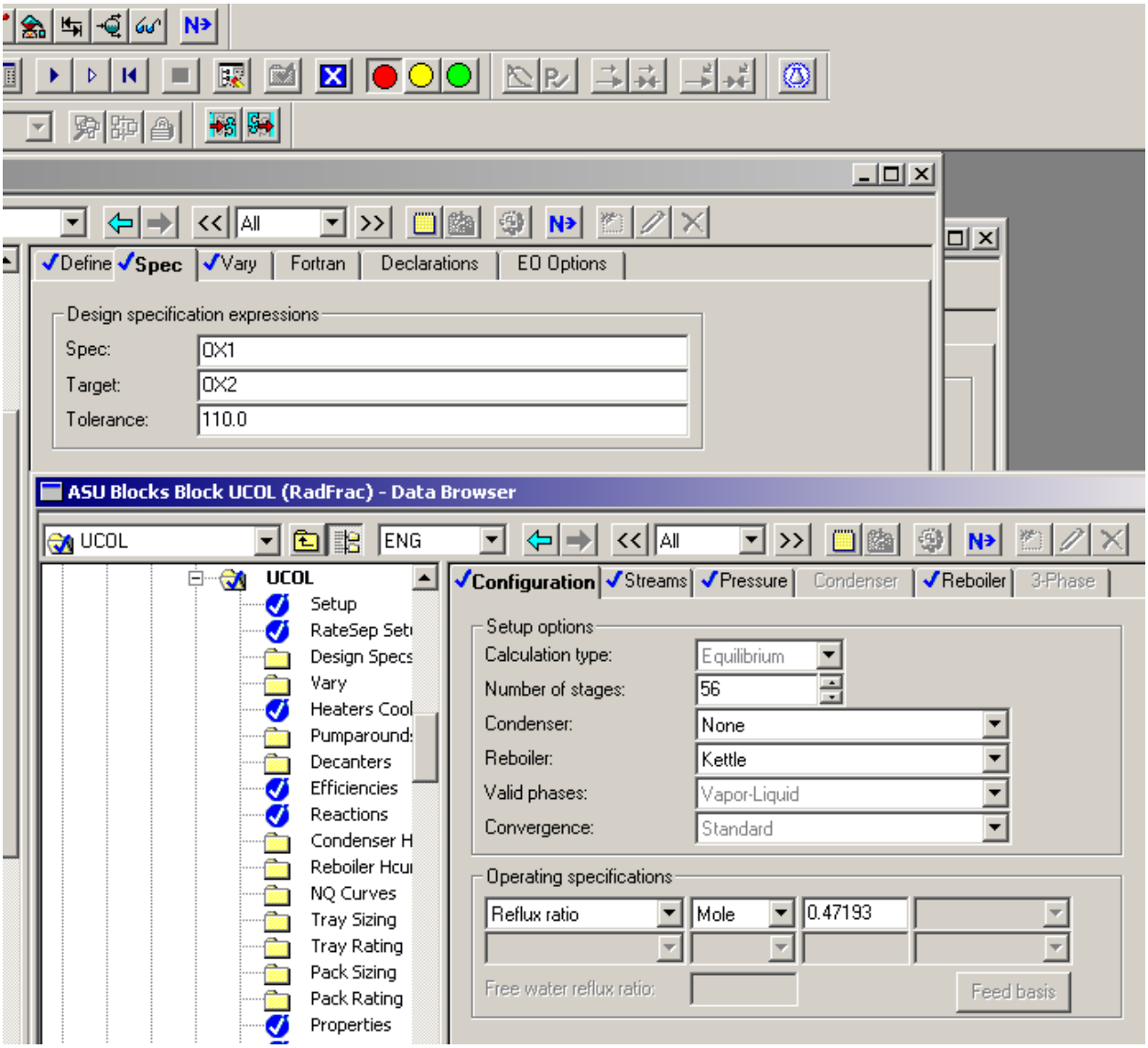

Figure 1.2.22. Example of Iterative Process.

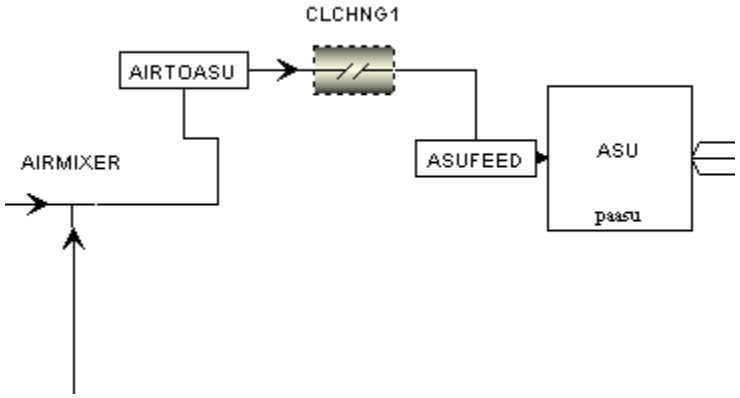

Figure 1.2.23. ASUFEED stream connected to detailed ASU model.

Example Results
Illustrated in Figure 1.2.24 are the results of the ASU implementation for the O2PROD Stream. Results may vary depending on the UCOL Reflux ratio used for model convergence.

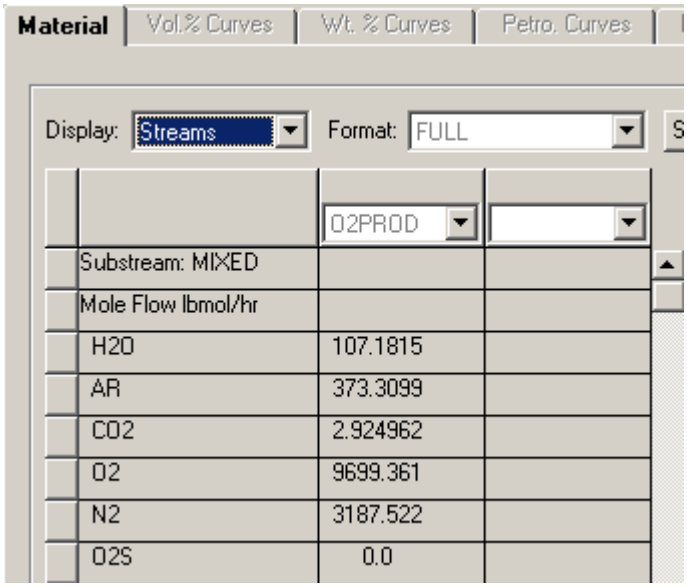

Figure 1.2.24. O2PROD stream results.

Summary
The above material provides a description of the detailed cryogenic ASU process model provided to NETL and instructions on the procedure for inserting the model into an AspenPlus IGCC flowsheet. A discussion on the impact of using the detailed ASU model on predicted plant performance is provided in Chapter 2 (see Section 2.4.1).

OTM ASU Model

REI obtained a process model for an OTM based ASU from Praxair, a project team member, for use in this project. Praxair has been developing OTM technology with support from NETL. The focus of their development efforts has been to reduce the cost and increase the efficiency of integrated oxygen-fired coal in IGCC power plants [Prasad et al., 2003].

In the following are provided an overview and detailed description of the model, implementing the model in C++, implementing the COM CAPE-Open interface and example calculations. Provided in the Results and Discussion section of this report are example calculations performed with the C++ version of the model within AspenPlus using the COM CAPE-Open interface (see Section 2.4.2).

Overview

In an OTM device, the air separation process occurs by forcing air across a mixed-conducting oxide membrane to produce oxygen (i.e., the product). Illustrated in Figure 1.2.25 is an example cross-section of a membrane. The membrane consists of a dense, gas separation layer of a mixed-conducting oxide on porous support material. Porous mixed-conducting oxide layers are applied on either the airside, oxygen product side, or both sides, to improve the rate of oxygen transfer. Each porous layer has its own thickness, pore size, porosity and tortuosity. Compressed air is supplied to the side of the membrane with the thin gas separation layer, while a low-pressure, high purity oxygen product is collected from the porous support side.

Figure 1.2.25. Cross section of an OTM using a scanning electron microscopy. Figure taken from [van Hassel, 2004].

The OTM process model provided by Praxair was a stand-alone model implemented as a MicroSoft EXCEL spreadsheet. The model represented a simplified version of a more detailed OTM model described in [van Hassel, 2004]. In general, the transfer of oxygen across an OTM is governed and limited by a number of physical processes, such as mass transfer across a boundary layer on the air side, surface exchange, ambipolar diffusion through the gas separation layer, etc. The provided model predicts key parameters of OTM performance and design, such as the oxygen flux through the membrane and membrane size using engineering approximations and correlations. Note that equipment required to supply the compressed air to the OTM and to extract the product gas (oxygen) from the OTM must be modeled with auxiliary equipment models (e.g., pumps, fans, compressors).

Model Description

The following provides a detailed description of the model inputs, equations solved, solution method and model outputs for the OTM ASU process model.

Model Inputs/Outputs

The model inputs include:

- the inlet O2 mole fraction;
- inlet and outlet pressures and pressure drops;
- OTM operating temperature; desired O2 recovery fraction; and
- desired O2 output.

The model outputs include:

- O2 flux and amount of O2 transferred;
- inlet and outlet O2 flow rates;
- model diagnostics (e.g., results of the minimization process); and
- membrane design parameters (e.g., required membrane size, membrane pinch pressure)

The user interface for the EXCEL version of the model is shown in Figure 1.2.26.

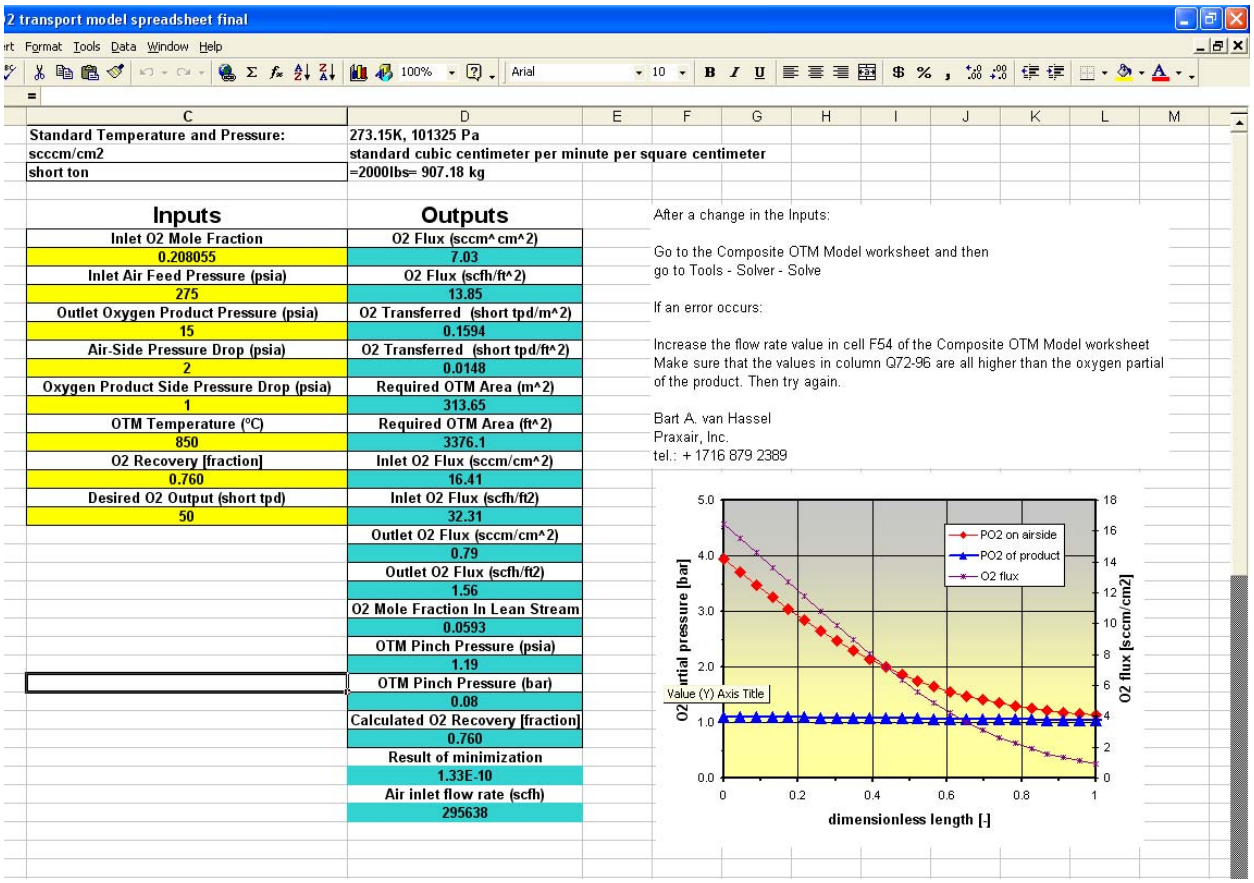

Figure 1.2.26. User interface for EXCEL version of OTM process model.

Model Equations
The equations listed below are used (solved) within the model.

1. Ambipolar conductivity is computed as:

$$\sigma = \sigma^0 e^{-\frac{E}{R}\left(\frac{1}{T}-\frac{1}{1273.5}\right)} \tag{1.2.36}$$

where

σ^0 is average ambipolar conductivity,
E is activation energy for ambipolar conductivity,
R is gas constant and
T is membrane temperature in K.

2. Then, two coefficients are computed:

$$k_p = k_p^0 e^{-\frac{E_p}{R}\left(\frac{1}{T}-\frac{1}{1273.5}\right)} \tag{1.2.37}$$

$$k_{dp} = k_{dp}^0 e^{-\frac{E_{dp}}{R}\left(\frac{1}{T}-\frac{1}{1273.5}\right)} \tag{1.2.38}$$

where

k_p^0 is a reference value and is a function of membrane temperature
k_{dp}^0 is taken to be equal to k_p^0,
E_p is activation energy and
E_{dp} is taken same as E_p so these two coefficients are equal.

3. The Knudsen diffusion coefficient of air is defined as:

$$D_{Kn,O2} = \frac{2}{3} r_p \sqrt{\frac{8RT}{\pi M_{O2}}} \tag{1.2.39}$$

where

r_p is membrane pore radius,
M_{O2} is molecular weight of oxygen.

4. Partial oxygen pressure on air side is defined as:

$$p_{O2}^{air} = p^{air} \frac{\dot{n}_{O2}^{air}}{\dot{n}_{O2}^{air} + \dot{n}_{N2}^{air}} \tag{1.2.40}$$

where

p^{air} is air pressure (in bars) and
$\dot{n}$ -s are molar flow rates of respective air components.

5. Analogously, partial oxygen pressure on the purge side is defined as:

$$p_{O2}^{purge} = p^{purge} \frac{\dot{n}_{O2}^{purge}}{\dot{n}_{O2}^{purge} + \dot{n}_{N2}^{purge} + \dot{n}_{He}^{purge} + \dot{n}_{CO2}^{purge}} \tag{1.2.41}$$

6. Then, oxygen flux from the air side is defined as:

$$J_{O2}^{air} = -RT\left(\log(p_{O2}^{if}) - \log(p_{O2}^{air})\right) \Bigg/ \left(\frac{16F^2 l_{dl}}{\sigma} + \frac{RT}{k_{dp}\sqrt{p_{O2}^{if}}} + \frac{RT}{k_p \sqrt{p_{O2}^{air}}} \right) \quad (1.2.42)$$

where

F is Faraday constant,
l_{dl} is dense layer thickness and
p_{O2}^{if} is partial oxygen pressure on the interface.

7. A characteristic length is defined as:

a. $$l_s = r_{out} \log\left(\frac{r_{out}}{r_{in}}\right) \quad (1.2.43)$$

then the oxygen flux on the purge side is defined as:

b. $$J_{O2}^{purge} = -\frac{10^5 \varepsilon}{\tau RT l_s}\left(p_{O2}^{purge} - p_{O2}^{if}\right)\left(D_{Kn,O2} + \frac{10^5 r_p^2}{16\eta}\left(p_{O2}^{purge} + p_{O2}^{if}\right)\right) \quad (1.2.44)$$

where

ε is porosity,
τ is tortuosity and
η is gas viscosity.

Solution Technique

To obtain the oxygen output of a membrane, the membrane is divided length-wise into a number of segments (steps) and oxygen fluxes on the air and purge side are computed for each step. These fluxes should match due to mass conservation.

To solve the problem, it is cast in variational form, where one tries to find a minimum of:

$$\sqrt{\sum_{all\ steps} (J_{O2}^{purge} - J_{O2}^{air})^2 + (R_{O2} - R_{O2}^{in})^2}\ , \quad (1.2.45)$$

where

R_{O2} is fraction of oxygen recovered by the membrane and
R_{O2}^{in} is the target oxygen fraction.

To find the minimum, the variables allowed to vary are p_{O2}^{if} and the volume flow rate of incoming air. Good initial guesses for these variables are required for solution efficiency and existence.

Each of the steps is initialized taking into account changes due to previous steps, except for step '0', where the input values are used. For step 'i', the oxygen molar flow rates and pressures are:

1. $$\dot{n}_{O2}^{air}[i] = \dot{n}_{O2}^{air}[i-1] - S J_{O2}^{air} \quad (1.2.46)$$
2. $$\dot{n}_{O2}^{purge}[i] = \dot{n}_{O2}^{purge}[i-1] + S J_{O2}^{purge} \quad (1.2.47)$$
3. $$p^{air}[i] = p^{air}[i-1] - dp^{air}/(N-1) \quad (1.2.48)$$

4. $p^{purge}[i] = p^{purge}[i-1] - dp^{purge}/(N-1)$ (1.2.49)

where

S is a step area,

dp -s are specified pressure drops for air and purge side and

N is the number of steps.

C++ version of OTM model

In final form, the OTM model is to be used in AspenPlus flowsheets for IGCC plant configurations. Because the original OTM model is implemented in EXCEL, there are some issues which had to be resolved to use it as a process model within AspenPlus.

- The formulation of the model is based on an error minimization problem which is solved using a native solver within EXCEL. Even though AspenPlus has some support for user-provided models written in EXCEL, it is unclear that advanced features of EXCEL (e.g., use of built-in solvers) are supported through this user-provided model interface.
- It is un-likely that advanced features of EXCEL could be utilized if the spreadsheet model uses a CAPE-Open interface.

To ensure the model provided to NETL can be implemented into AspenPlus as a CAPE-Open compliant model, REI ported the OTM process model to C++. As a result, the built-in solver used in the EXCEL version of the model was replaced with a SIMPLEX type minimization problem solution algorithm [Cormen et al., 2001], [Nelder and Mead, 1965]. The variable the model varies to achieve the minimum value of a constraint is the partial oxygen pressure on the membrane interface.

- The following provides a simple example of the SIMPLEX algorithm. For a two dimensional problem, the SIMPLEX is a triangle and the method searches for the minimum of a given function by evaluating its value at the vertices of a triangle. Given a certain set of rules, the vertex where the function value is largest is discarded and a new vertex is found. This procedure generates a sequence of triangles, with minimizing function values at the vertices. When the tolerance criteria is satisfied, the solution (i.e., minimum for the function in question) has been found.

Compare Calculations with EXCEL and C++ Versions of OTM ASU Model

Illustrated in Table 1.2.3 are the results from example calculations performed with the REI port of the Praxair Oxygen Transport Membrane (OTM) process model from EXCEL to C++ (see section 2). The calculations were performed using the default values for the model input parameters (see Figure 1.2.26). The function being minimized by the solution algorithm in the model is a balance of O2 fluxes resulting from ambipolar diffusion of oxygen ions through dense oxide film and from viscous flow of oxygen on the product (oxygen) side of the membrane. Shown in the table are values predicted by the EXCEL version of the model, the REI C++ version of the model and the error between the two models where the error is defined as:

Error = [(EXCEL model value) – (REI C++ model value)] / (EXCEL model value).

Overall, good agreement is obtained between the two versions of the model. The model results agree to 6 digits. Minor discrepancies occur due to physical constants used by the models (e.g., gas constant, Faraday constant, etc.) were used with more digits of precision in the REI C++ model as compared to the EXCEL version of the model.

Table 1.2.3. Comparison of Predicted Values For EXCEL and REI C++ Versions of OTM Process Model

EXCEL Version	REI C++ Version	Error
1.16357E+00	1.16356E+00	1.36000E-05
1.15754E+00	1.15753E+00	1.06000E-05
1.15142E+00	1.15142E+00	4.50000E-06
1.14524E+00	1.14523E+00	1.07000E-05
1.13899E+00	1.13899E+00	2.30000E-06
1.13272E+00	1.13271E+00	8.50000E-06
1.12643E+00	1.12643E+00	5.00000E-06
1.12016E+00	1.12016E+00	4.50000E-06
1.11394E+00	1.11393E+00	6.90000E-06
1.10779E+00	1.10779E+00	6.00000E-07
1.10176E+00	1.10176E+00	3.70000E-06
1.09587E+00	1.09586E+00	5.70000E-06
1.09014E+00	1.09014E+00	9.00000E-07
1.08461E+00	1.08461E+00	9.00000E-07
1.07929E+00	1.07929E+00	4.00000E-06
1.07418E+00	1.07418E+00	1.80000E-06
1.06930E+00	1.06930E+00	2.00000E-07
1.06464E+00	1.06464E+00	2.10000E-06
1.06019E+00	1.06019E+00	3.80000E-06
1.05593E+00	1.05593E+00	1.90000E-06
1.05186E+00	1.05186E+00	1.40000E-06
1.04795E+00	1.04795E+00	1.70000E-06
1.04418E+00	1.04418E+00	2.20000E-06
1.04054E+00	1.04054E+00	1.90000E-06
1.03701E+00	1.03701E+00	3.60000E-06

To gain further confidence in REI's C++ version of the OTM model additional comparisons have been performed to compare predicted values from the original EXCEL version of the model the C++ version of the model. Illustrated in Figure 1.2.27 is the predicted average O2 flux as a function of the oxygen recovery ratio. Illustrated in Figure 1.2.28 is the predicted average O2 flux as a function of membrane temperature. From the figures it can be seen that the values predicted by the EXCEL and C++ versions of the model are in good agreement.

The OTM model can also be used to provide a preliminary estimate of the size of the ASU required for an IGCC plant application. Assuming all other input parameters for the OTM model are fixed, the membrane size will grow linearly with respect to oxygen flow rate. Hence, given the amount of O2 required to operate the gasifier, membrane size required to produce this oxygen can be estimated. For example, for 9699 lbmol/hour oxygen flow rate (this number has been obtained from one of NETL IGCC Aspen flowsheets [Klara, 2007], the membrane size would be over 20,000 square meters. As a point of reference, heat exchangers used in the chemical process industry contain tube banks/bundles that provide a surface area of several

hundred square meters, implying that numerous equipment units would be required to provide the required amount of membrane surface area. Substantial optimization will be required for these systems to be installed in commercial scale IGCC plants.

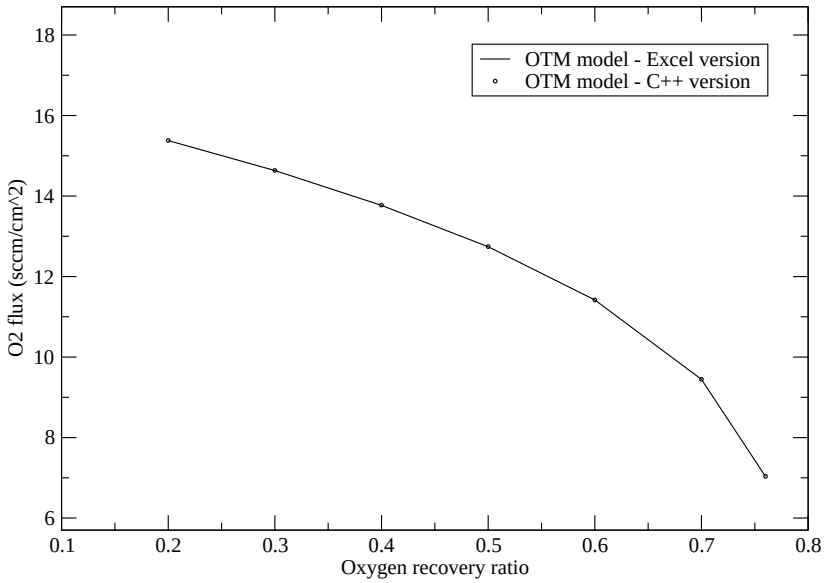

Figure 1.2.27. Average O2 Flux as a function of O2 recovery ratio.

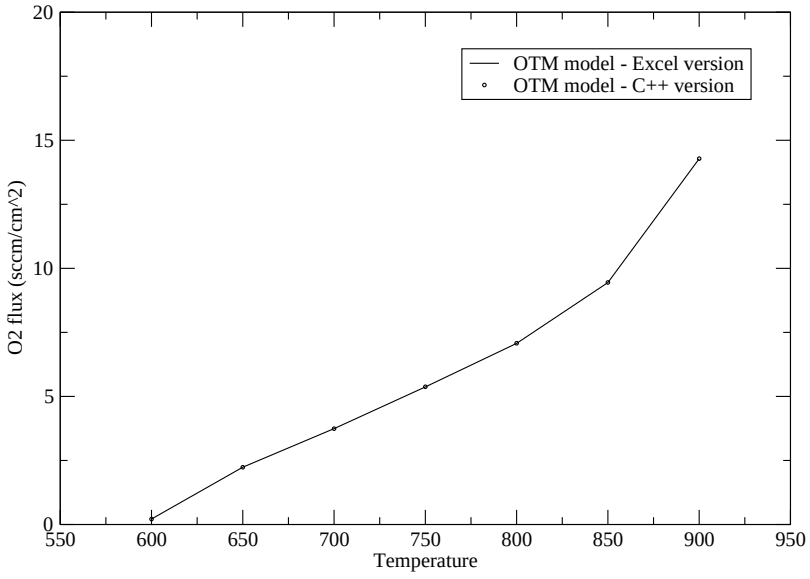

Figure 1.2.28. Average O2 Flux as a function of membrane temperature.

CAPE-Open Implementation

The OTM model provided to NETL uses a COM CAPE-Open interface. However, software tools to support generating a COM interface for models to be coupled to AspenPlus/APECS were not readily available when the work effort for the OTM model was being performed.

Two research groups developing such software were contacted by REI. Both groups presented papers in the technical session on CAPE-Open interfaces at the AIChE Annual Conference. One group is from University of Trieste, Italy [Fermeglia et al., 2007] and the other is from the US Environmental Protection Agency (EPA) [Barrett et al., 2007]. Unfortunately, the only implementation that is currently publicly available from these groups is from the US EPA [Barrett et al., 2007].

The COM CAPE-Open implementation developed at the US EPA provides the user with a template written in C# to build user process models for COFE, a CAPE-Open flowsheet environment that is part of the COCO simulation environment (COCO = CAPE-Open-to-CAPE-Open) [van Baten, 2007]. In principle, because these models are CAPE-Open compliant they can be used in any process simulation software supporting CAPE-Open standard, including AspenPlus. However, REI's experience was that the EPA template did not work in AspenPlus. Several problems were encountered. In particular, the template only seemed to support user parameters of type REAL. It was difficult to determine if the problems encountered were due to inadequacies with AspenPlus or with the EPA implementation.

Given that the higher-level CAPE-Open support tools were still largely unusable, REI instead chose to implement the OTM COM-CAPE-Open model using a template provided by Dr. Michael Pons (Chief Technology Officer, CAPE-Open Laboratories Network), an authority on CAPE-Open (see discussion for Task 2.2 in Chapter 2).

Using the aforementioned CAPE template, the OTM module has been built by REI and verified to work in AspenPlus/APECS. Due to the limited support of the CAPE-Open standard in AspenPlus, the OTM model has only been demonstrated for using simple streams because access to the components of composite AspenPlus streams (e.g., the MIXEDNC type used in the NETL AspenPlus IGCC flowsheets) from CAPE-Open is not supported by AspenPlus (this was verified with AspenPlus technical support personnel). Stream class changer blocks were employed to overcome CAPE-Open support issues in AspenPlus and make it work in NETL IGCC flowsheet.

Illustrated in Figure 1.2.29 is the User Interface for the OTM model implemented with COM-based CAPE-Open interface within AspenPlus. The model inputs for the EXCEL version of the model were the inlet O2 mole fraction, inlet and outlet pressures, inlet and outlet side pressure drops, OTM temperature, O2 recovery factor and desired amount of O2 to be output from the membrane.

- In the AspenPlus IGCC flowsheets, some of the input parameters can be deduced (extracted) from the input stream but others have to be specified by the user. The inlet pressure for the OTM model is just the inlet stream pressure, the OTM temperature is assumed to be the inlet stream temperature and the inlet O2 mole fraction is obtained from the inlet stream.

- The inlet air flow rate, air oxygen content and oxygen recovery factor are used to determine the desired amount of O2 to be produced by the OTM unit.
- The oxygen recovery factor, outlet pressure, inlet and outlet side pressure drops are user-specified parameters for the model.
- Upon successful execution, the model outputs are the O2 recovery factor (it is part of the model computation), average volumetric oxygen flux through the membrane, the membrane surface area and the model minimization result (which is an indicator of successful model computation and has to be small).
- An amount of oxygen equal to the desired membrane oxygen output is placed in the outlet stream and the remainder of the inlet stream contents is placed in waste stream.

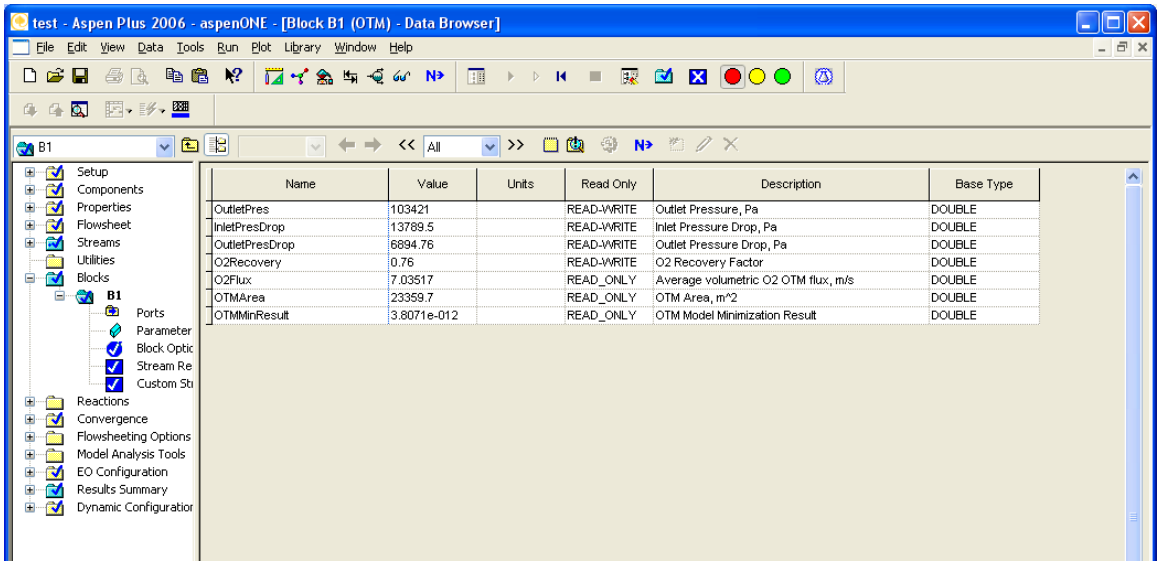

Figure 1.2.29. Input-output panel in AspenPlus/APECS for the OTM model with a COM-based CAPE-Open interface.

1.2.4 Task 2.4 Automated Reduced Order Models

In this task REI developed a standalone ROM generator that can use detailed data sets (obtained from process models, CFD models or laboratory data) to create a ROM and subsequently output (export) a CAPE-Open compliant component that encapsulates the ROM. Selection of the mathematical technique used by the ROM generator was part of the research for this task and was made in consultation with DOE to ensure there was not duplication of other available tools or NETL contracted efforts. The work effort was performed in collaboration with NETL researchers and personnel from NETL contracted projects (i.e., ANSYS/Fluent), CMU, and ISU.

In the following are provided material describing

- background information (review) on ROM methods described in the open literature;
- a POD-like method for ROM generation and ROM evaluation developed by REI and ISU in a collaborative effort; and
- the Final Deliverable to NETL for this task which included a standalone neural-net-based ROM generation tool and a COM CAPE-Open compliant ROM.

Background Information

Numerical simulation of large-scale dynamical systems using advanced computers has been an extremely useful tool for studying complex physical phenomena, in particular in the field of CFD. However, as more detail is included, the dimensionality of such modeling may increase to unmanageable levels of storage and computational requirements. There are two major limitations of large-scale numerical simulations.

1. Although such analysis can provide a large amount of temporal and spatial information of variables of interest, such data may not necessarily provide an increased level of understanding of the physics of the system.
2. Without the dedication of massive resources, numerical simulation of large-scale systems remains far too computationally expensive to be used in practical industry applications.

Thus, there is a fundamental gap between the numerical analysis fidelity and practical implementation, which suggests that computed data need to be distilled into lower-order models that can serve as the basis for additional analysis. The intention of reduced-order models (ROMs) are to provide quantitatively accurate descriptions of the dynamics of systems at a much lower computational cost, and to provide a means by which system dynamics can be readily interpreted. Hence, there is substantial interest in ROMs because of their relatively short turnaround time and acceptable levels of accuracy. However, the method for creating (generating) the ROM is still an active research area.

As noted in [Osawe et al., 2006], the approaches used to create a ROM from a CFD simulation can roughly be grouped into three categories:

- Systematic leveraging of CFD predictions; and
- Order reduction of CFD equations.
- Black box approach;

Each of these are summarized below, with the “Black Box” methods described in greater detail.

Systematic Leveraging

In the method of systematic leveraging, a simple physical model is constructed based on CFD results. Modeling real combustion systems with networks of idealized Perfectly Stirred Reactors (PSRs) and Plug Flow Reactors (PFRs) has been used for several years to model gas turbines [Swithenbank et al. 1972], [Ewan et al. 1984], electric utility boilers [Pedersen et al. 1998], [Niksa & Liu, 2002] and process equipment [Bezzo et al., 2004]. The premise is that the complex flow patterns found in a real device can be broken down into regions that are well-approximated by a PSR or a PFR. The reactors representing the regions of the flow can be connected in parallel or in series (or a combination of both) with the outflow of one or more reactors forming the inflow of another. The CFD results are used to provide knowledge of the flowfield for the characterization of mixing and chemical process in each zone. This approach also does not require a detailed knowledge of CFD equations and may have good accuracy over a greater parameter range. Its drawback is that the CFD flow field must be calculated a priori. This approach has been used extensively by the research group led by Prof. Tognotti of the University of Pisa, Italy [Falcitelli et al., 2002], [Benedetto et al., 2000].

Order Reduction (Model Reduction)

The order reduction approach, also known as model reduction, typically makes use of detailed knowledge of the differential equations of the system and can take flow physics of the systems into account. Model reduction of large-scale dynamics systems have been extensively researched in the field of circuit design, controls, structural dynamics, fluid dynamics, and Micro-electro-mechanical systems (MEMS) [Antoulas and Sorensen, 2001], [Holmes et al. 1996].

For example, consider a dynamical system described by the state equations,

$$\sum : \dot{x} = f(x,u), \quad y = h(x,u) \tag{1.2.50}$$

with the state $x(\cdot) \in R^n$, input $u(\cdot) \in R^m$, output $y(\cdot) \in R^p$, where $n >> m, p$. For simplicity, let $\sum = (f,h)$ denote the system. Then the model reduction problem becomes:

approximate $\sum = (f,h)$ with

$$\hat{\sum} = (\hat{f},\hat{h}),\ \hat{x}(\cdot) \in R^k,\ u(\cdot) \in R^m, \text{ and } \hat{y}(\cdot) \in R^p \tag{1.2.51}$$

where $k << n$, so that requirements below are satisfied:

(1) the approximation error is small and there exists a global error bound;
(2) preservation of stability and passivity;
(3) the procedure must be computationally efficient; and
(4) the procedure must be automatic, i.e., based on an error tolerance.

Black Box

In the black box approach, CFD simulations are performed over a suitable range of conditions, and the inputs and outputs are analyzed using correlation based models such as regression, artificial neural network, Principal Component Analysis (PCA), etc. This technique does not require a detailed knowledge of CFD models and is straight forward to implement. However, the model accuracy is restricted to a narrow parameter range.

Outside of typical regression and neural-net-based approaches, Black Box model reduction methods can be cast into three broad categories (see Table 1.2.4):

- Singular Value Decomposition (SVD) based methods,

- Krylov based methods, and
- hybrid methods that combine the best aspects of the SVD and Krylov approaches.

Table 1.2.4. Overview of approximation methods [Antoulas and Sorenson, 2001]

Approximation methods for dynamics systems			
Krylov	**SVD**		**SVD-Krylov**
Linear Systems		**Nonlinear Systems**	
• Realization • Interpolation • Lanczos • Arnoldi	• Balanced truncation • Hankel approximation	• POD methods • Empirical grammians	• Least squares approximation
Numerical efficiency; Applicability n>100	Preservation of stability; Global error bound; Applicability n<100		Preservation of stability; Global error bound; Numerical efficiency; Applicability n>100

SVD Methods

The SVD-based approximation methods have their roots in the singular value decomposition (SVD) and the resulting solution of the approximation of matrices by means of matrices of lower rank, which are optimal in the 2-norm. Given a matrix $A \in R^{n\times m}$, its singular value decomposition is a factorization $A = U\sum V^*$, where $U \in R^{n\times n}$, $V \in R^{m\times m}$ are unitary (orthogonal), and $\sum = diag(\sigma_1,\ldots\sigma_n) \in R^{mxn}$ is diagonal with non-negative diagonal entries call singular values: $\sigma_i = \sqrt{\lambda_i(A^*A)} > \sigma_{i+1}$. The model reduction problem is to find $X \in R^{nxm}$, rank X < rank A, such that 2-norm of the error $E = A - X$ is minimized. Schmide-Mirsky, Eckart-Young theory states that the solution of the above problems is

$$\min \| A - X \|_2 = \sigma_{k+1}(A) \qquad (1.2.52)$$

and a minimizer $X_{\min}$ can be expressed as truncated dyadic decomposition of A,

$$X_{\min} = \sigma_1 u_1 v_1^* + \sigma_2 u_2 v_2^* + \cdots + \sigma_k u_k v_k^*, \qquad (1.2.53)$$

where u_i, v_j are columns of U, V. Thus the system represented by A can be best approximated by the system represented by $X_{\min}$ with given error bound.

SVD-based approximation approaches can be applied to both linear and nonlinear dynamical systems. For linear dynamics systems, the methods of balanced truncation and Hankel norm approximation have been developed. For nonlinear systems, one straightforward way of applying SVD is as follows. Choose an input function and compute the resulting trajectory; collect samples of this trajectory at different times and compute the SVD of the resulting collection of samples. Then apply the SVD to the resulting matrix. This method is known as proper orthogonal decomposition (POD).

Note: The literature contains some "controversial" definitions for POD, SVD, Principal Component Analysis (PCA) and Karhunen Loeve decomposition (KLD). Some researcher's regard these methods as essentially the same, but which were introduced in different disciplines [Chatterjee 2000], [Holmes et al., 1996]. Some consider that POD

consists of SVD, PCA, and KLD [Liang et al. 2002]. As per the review in [Antoulas and Sorensen, 2001], for this project POD is categorized as a sub-model of SVD.

One disadvantage of POD methods is that the accuracy of reduced-order models heavily depends on the initial excitation function chosen, the time instances at which the measurements are taken; consequently, the singular values obtained are not system invariants.

Krylov-based Methods

Krylov-based approximation methods are constructed based on *moment matching* of the *impulse response* of the system $\sum$ [Bai, 2002]. For a linear dynamical system, a transfer function $G(s)$ can be obtained. Expanding its transfer function around s_0, results in

$$G(s) = \eta_0 + \eta_1(s - s_0) + \eta_2(s - s_0)^2 + \eta_3(s - s_0)^3 + \cdots. \quad (1.2.54)$$

The moments of $\sum$ at s_0 are the coefficients η_j in the above expansion. The approximation problem now consists in find $\hat{\sum}$ such that

$$\hat{G}(s) = \hat{\eta}_0 + \hat{\eta}_1(s - s_0) + \hat{\eta}_2(s - s_0)^2 + \hat{\eta}_3(s - s_0)^3 + \cdots \quad (1.2.55)$$

where for appropriate l,

$$\eta_j = \hat{\eta}_j \quad j = 1,2,\ldots,l. \quad (1.2.56)$$

Two widely used methods fall under this category, namely the Lanczos and the Arnoldi algorithms. The key to the success of these methods is that they can be implemented iteratively. These implementation methods are closely related to iterative eigenvalue computations. The drawbacks of this approach are that the resulting reduced order systems have no guaranteed error bound, stability is not necessarily preserved and some of them are not automatic.

SVD-based and Krylov-based approximation methods have distinct sets of advantages (See Table 1.2.4). Therefore substantial effort has been put into devising approximation methods which combines the best attributes of these two approximation approaches. One example is the least squares approximation proposed in [Gugercin and Antoulas, 2006].

A number of software packages are available for model reduction computations. Below are some existing software packages available online.

- Model reduction software: SLICOT [http://www.win.tue.nl/niconet]
- Eigenvalue problems solvers: ARPACK [http://www.caam.rice.edu/software/ARPACK]
- Linear algebra package: LAPACK, [http://netlib.org/lapack/]

Collaboration With ISU on ROM Capability

REI collaborated with ISU on the design and development of a Proper Orthogonal Decomposition (POD) software toolset for generalized applications. The POD software was based on work by Prof. Michael Kirby of Colorado State University [Kirby, 2000], an acknowledged expert in ROM. The POD software was originally implemented by Sunil Suram, a Ph.D. Student of Prof. Mark Bryden, at ISU.

Discussions with NETL indicated concern that the POD-based ROM approach too closely matched the work being performed by other groups funded by NETL, possibly due to the POD engine using Singular Value Decomposition (SVD) techniques – albeit at a low level in the algorithm. REI believes that the REI/ISU implementation offers some unique differences and potential advantages. As such, REI provided the ROM POD engine as an *additional* deliverable to NETL; the ROM POD engine was delivered as a stand-alone code (i.e., NOT wrapped as a COM CAPE-Open module).

For the deliverable to NETL for the ROM task, REI pursued a different approach from that used in the REI/ISU collaborative efforts. Details are provided below.

ROM Capability Delivered to NETL

The ROM capabilities developed by REI and delivered to NETL are based on multi-dimensional ROM techniques that deal only with mapping a set of scalar input variables to a set of scalar output variables. These techniques make no assumption about the fidelity of the model used to create the ROM, hence the approach works equally well for data sets from multi-dimensional data sets (e.g., CFD results) and for zero-dimensional data sets (e.g., process model results, laboratory data). It is implicitly assumed that a user of the ROM in AspenPlus is less interested with reconstruction of a full flow field and more interested with the resulting values passed to downstream equipment/processes in AspenPlus flowsheets.

REI investigated a number of different approaches for the scalar mappings (from model inputs to outputs), including MatLab, IMSL Libraries and neural networks. The best success was achieved through the use of a publicly available neural network (see below). This approach provides a good path forward for providing a CAPE-Open ROM tool kit to NETL.

For the final deliverable, REI provided NETL with two components for the ROM toolkit:

1. A stand-alone ROM generator tool, which relies on simple text file input to define the training sets. The data input to the ROM engine could come from any source, ranging from simple, zero-dimensional process models to full CFD models where averaged planer values are used to create scalar output data.
2. A CAPE-Open compliant ROM module that makes use of the ROM generated by the stand-alone engine.

The following material provides further details on the work effort performed.

<u>ROM Investigation and Example Calculations</u>

In REI's opinion, high-fidelity direct multi-dimensional interpolation of the data points required by the process flowsheet analysis (e.g. outlet temperature, pressure, etc.) is adequate for constructing the ROM. In the following we highlight the use of two multi-dimensional interpolation methods evaluated by REI:

1) Radial-Basis Function (RBF) interpolation capability available in the IMSL numerical library and
2) neural networks computed using publicly available neural network codes.

The two methods were tested using data generated from the REI Entrained Flow Gasifier Process Model for a range of oxygen:coal ratios and water:coal (i.e., slurry density) ratios. Illustrated in Table 1.2.5 is the predicted exit temperature from the gasifier model.

Table 1.2.5. Gasifier Exit Temperature (K) as a Function of H2O/Coal and O2/Coal Ratios

	O2/Coal				
H2O/Coal	**0.4**	**0.6**	**0.8**	**1**	**1.2**
0.00	1230.647	1353.886	1557.222	2318.072	2914.5
0.25	1172.92	1281.055	1379.284	1557.222	2173.757
0.50	1125.936	1230.647	1313.237	1396.913	1557.222
0.75	1084.916	1190.588	1267.054	1336.293	1409.938
1.00	1047.74	1156.389	1230.647	1293.167	1353.886

Radial Basis Function Interpolation

One method evaluated by REI was a Radial Basis Function (RBF) interpolation method [ARANZ, 2008]. RBF is used to interpolate (large) scattered data point sets in two or more dimensions. Several applications in graphics, geophysics, reconstruction of surfaces and learning use interpolation methods based on RBFs. There is a significant theory on RBF interpolation [Buhmann, 2000].

RBF interpolation is available as a part of the IMSL C library developed by Visual Numerics [Visual Numerics, 2008]. This method computes a least-squares fit to multi-dimensional scattered data with basis functions for this operation restricted to be of radial function type. The resulting fit is a weighted linear combination of radial basis functions. The quality of the fit depends on the number of radial functions used for the basis and the location of their centers.

Using the 25 data points contained in Table 1.2.5 a RBF representation was generated. When evaluated at the point (0.1, 0.5), the predicted gasifier exit temperature is 1206.71, which results in a relative error of 4.6%. This error is larger than desired but possibly adequate for flowsheet calculations. As described below, a neural network can perform the same interpolation but with a smaller error.

A complication with this approach is that the IMSL implementation for the RBF function fit is saved in an IMSL-defined data structure. This does not allow for separate ROM creation and evaluation stages.

The above information indicates RBF provides a feasible approach to generate a ROM that would provide adequate accuracy and computational speed for flowsheet simulations. However, as described below the neural network approach provides a less complicated path forward for completing the ROM task for this project. Further use of RBF was not pursued.

Neural Network - Background

A neural network is an interconnected assembly of simple processing elements or nodes, whose functionality is loosely based on the animal neuron. A good introductory reference is [Hertz., 1991]. A representative schematic of a neural network is shown in Figure 1.2.30. The neural network consists of input nodes, output nodes and layers of hidden nodes between the input and output nodes. The processing ability of the network is due to the layering of these computational nodes that are linked to one another through weighted connections. These inputs enter the network, are attenuated or amplified by adjustable weights and the resulting signals are summed and processed through a nonlinear function to give an output from each node. The two input nodes shown in the figure are blank because they simply pass the inputs unchanged to be attenuated or amplified by the weights of the first layer of hidden nodes. The number of nodes per layer and the number of layers depend on the number of input and output streams and the desired accuracy. The number of input nodes is simply the number of degrees of freedom used in the optimization.

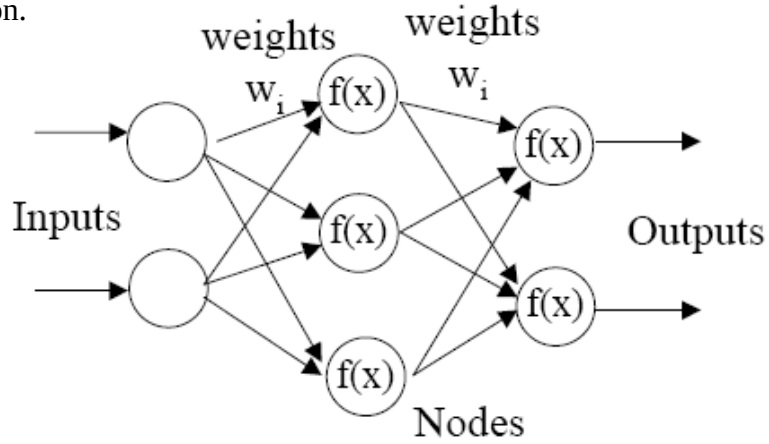

Figure 1.2.30. Schematic representation of an artificial neural network

Neural Network Based Interpolation Using Quickprop

Initially, REI performed the ROM calculations with Quickprop, a public domain neural network code [Quickprop, 2008]. The ROM was trained using the 25 data points shown in Table 1.2.5. For a O2/Fuel ratio of 0.5 and a H2O/Fuel ratio of 0.1 the ROM predicts an exit temperature value of 1221.46 and the REI entrained flow gasifier process model predicts a value of 1265.448. Hence, the value predicted by the ROM has a relative error of 1.5%. The error in the exit temperature predicted by the neural network will decrease if higher resolution datasets are used to train the ROM.

Although the Quickprop neural network code worked well for the small test problem described above (i.e., interpolate from 25 points), additional tests demonstrated it was not appropriate for applications requiring interpolation from a large data set (e.g., 25,000 data points); unacceptably long computational times occurred when using large data sets. Hence, an alternative neural network code was obtained.

Neural Network Based Interpolation Using FANN Library

REI selected the FANN (http://leenissen.dk/fann/) neural network library to complete the ROM task. Several criteria were used in this decision.

- The FANN library is publicly available and implemented in C, which makes its integration with a C++ CAPE-Open wrapper less problematic.
- Calculations demonstrated this package can handle large datasets.
- ROM creation and evaluation stages are easily separated.
- Multiple training algorithms are available based on the back propagation principle; that is, inputs are propagated forward through the network and then the error is propagated backward while weights are adjusted to reduce the error. Algorithms available include Qprop and Rprop.
    - The Qprop algorithm is based on a local quadratic 1D approximation of the error function. In some cases, this approximation can lead to large updates to the weights, slowing down the training.
    - The Rprop algorithm uses the "sign" of the partial derivative of the error with respect to the weight for the weight update; this helps to avoid excessively large updates to the weights such as can occur in Qprop.
- Last, the FANN library supports two modes for network topology (configuration) selection: user-specified and automatic (cascade training) based on training error reduction.

Data Selection For ROM Demonstration

Even though the ROM creation and evaluation codes are generic in regards to the data they operate on, a particular model has to be selected for ROM demonstration in AspenPlus to be able to tie the ROM inputs and outputs to stream variables in AspenPlus. REI based the ROM example on the REI Entrained Flow Gasifier Process Model for a one stage gasifier..

Six parameters were chosen as ROM input parameters:

- Gasifier pressure = 7065060 Pa (69.7 atm)
- Coal (as received) mass flow rate = 66 kg/s (6286 tpd)
- Oxygen temperature = 370 K
- H2O temperature = 292 K
- Oxygen/coal ratio = 0.9
- H2O/coal ratio = 0.4

with their base values shown above being gasifier operating parameters taken from the existing AspenPlus IGCC flowsheets obtained from NETL. To create a data matrix for the ROM, five values were selected for each parameter from the following range (relative to the base condition for the first four):

- Gasifier pressure: 0.5 - 1.5
- Solid fuel (as received) mass flow rate: 0.5 - 1.5
- Oxygen temperature: 0.8 - 1.2
- H2O temperature: 0.8 - 1.2
- Oxygen/fuel ratio: 0.4 - 1.2
- H2O/fuel ratio: 0.0 - 1.0

Seventeen variables have been chosen for the output:

- Syngas temperature
- Syngas, ash and slag mass flow rates
- Syngas composition

Because different solid fuel types are hard to parameterize, a separate ROM has been created for each fuel type (i.e., four ROMS total):

- Illinois #6
- Pittsburg #8
- Petcoke
- Wyodak (PRB coal)

In summary, the ROM training data has:

- 6 inputs, 17 outputs
- 15625 data points
- 64 extra data points to check training
- 4 datasets for 4 solid fuel types

An example of the data used for the ROM is shown in Figure 1.2.31. The figure shows the syngas temperature plotted as a function of the H2O/fuel and O2/fuel ratios for Illinois#6 and Pittsburg #8 coals.

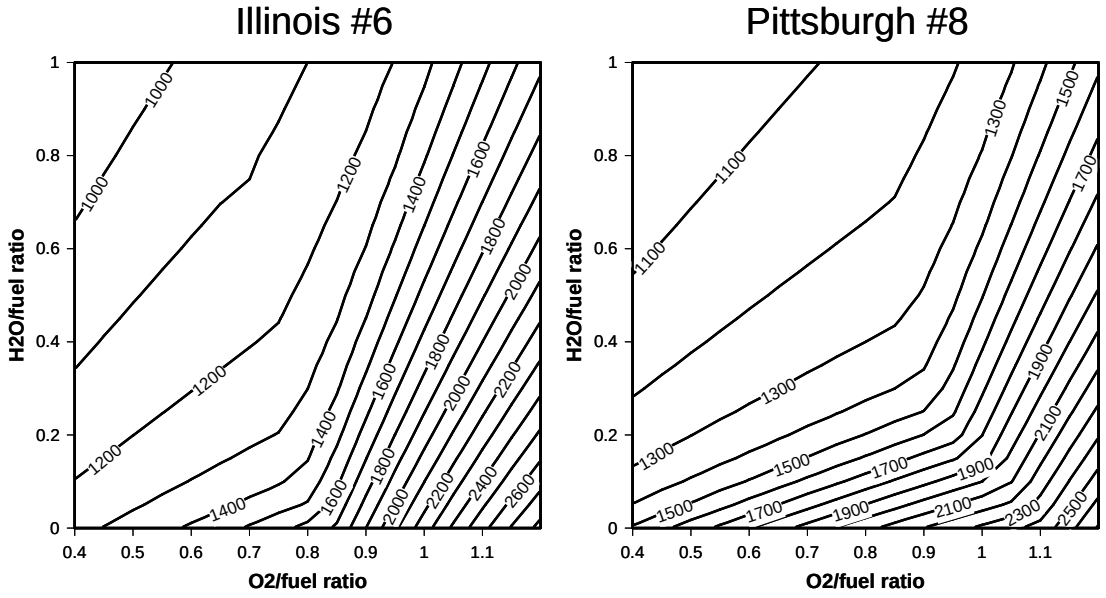

Figure 1.2.31. Example of data used for ROM.

FANN ROM training

Data from the REI Entrained Flow Gasifier Process Model was used to train the ROM that is based on the FANN library. Artificial neural networks (ANN) usually operate on data on the intervals [-0.5, 0.5] or [0, 1] and thus the data was normalized to lie in the interval [0,1]. The quality of the ANN greatly depends on the network topology, or more precisely the number of internal layers and number of neurons in these layers. Selecting a good network topology *a priori* is a hard task. Hence, cascade training was used. Depending on the fuel type, 50 to 70 neurons were used with their type automatically selected to minimize the mean square error (MSE). The number of neurons used in the cascade training was enough to achieve a MSE of about 0.05. Also, because 64 extra datasets were generated for each coal type in addition to those used for training, the resulting ANN were verified on these datasets to ensure satisfactory ANN prediction capability. As an example, the MSE for Illinois #6 training datasets was 0.009, and on 64 extra datasets it was 0.022.

ANN is not an exact curve fit and thus one should not expect that it fit the training data exactly. Instead, under proper training ANN should have the capability to predict data values for inputs not explicitly used in the training. Thus, if one continues to increase the ANN size by adding more neurons, it can lead to overtraining – i.e., the ANN would reproduce the training data with higher and higher precision but the ANN predictive capability would be lost. To increase the predictive capability of the ANN, greater input variable resolution (i.e. more training data) is required. The 64 extra data points mentioned above were used to ensure the ANN is not over-trained.

Another point to note is that the MSE is an average error measure. Hence, ANN will reproduce (predict) data with that same level of accuracy on average, but the error could be higher ("bad") or lower ("good") for individual data points. This is illustrated in Figure 1.2.32, where two data sets and ANN predictions are shown. Both of these data points are from a set of 64 extra data points. Hence, this is an example of the ANN prediction capability. The MSE for this dataset was 0.022.

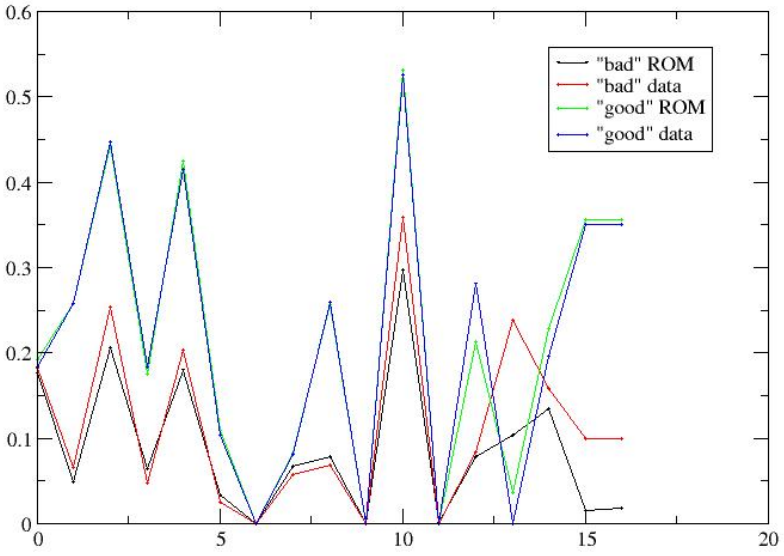

Figure 1.2.32. Example of ROM prediction capability on individual data points.

COM CAPE-Open ROM implementation

The standalone ROM generator tool automatically creates a ROM with a COM CAPE-Open interface. Illustrated in Figure 1.2.33 is the ROM in AspenPlus. The only input parameter for the ROM is the fuel type – all other values are obtained from the streams in the flowsheet. The ROM performs (simple) checking of the input data and if any input variable is out of range for the ROM a fatal error is triggered. Because the ROM is based on the REI Entrained Flow Gasifier Process Model, AspenPlus calculator blocks similar to the ones used for the gasifier model are used to implement the ROM into the AspenPlus IGCC flowsheets obtained from NETL. Likewise, as per the gasifier models the Intel FORTAN compiler is required for model operation and mass balance warnings are produced by AspenPlus due to the use of the calculator blocks (see discussion for Task 2.2 in Section 1.2.2).

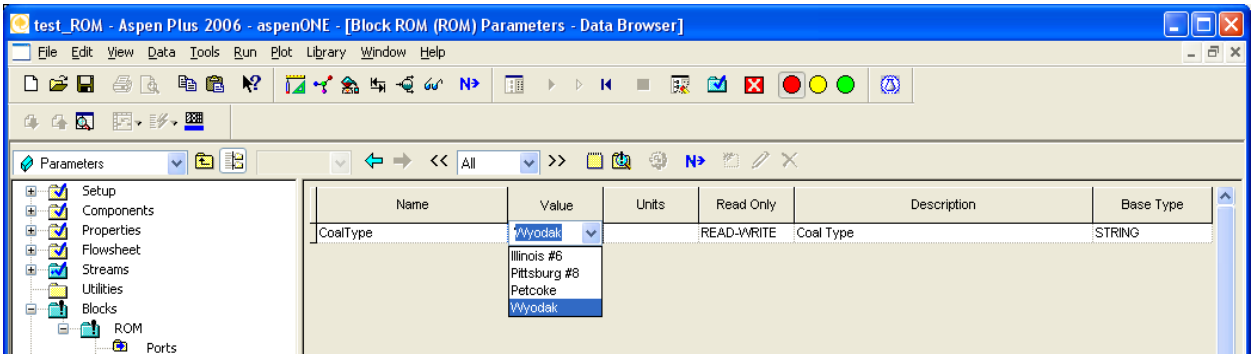

Figure 1.2.33. REI ROM input parameters with COM CAPE-Open interface.

Example calculations using the ROM in an AspenPlus IGCC flowsheet are presented in the Results and Discussion section of this report.

1.2.5 Task 2.5 Implement CAPE-Open compliant coupling between APECS and selected GE GateCycle Models

This subtask involves implementing a CAPE-Open compliant coupling to selected GateCycle models for use in CAPE-Open frameworks. GE GateCycle is a process modeling tool widely used in the power generation industry for thermal efficiency studies. (To access this capability the user must have a valid GE GateCycle license). REI was assisted in this task by Dr. Mike Erbes and his colleagues at Enginomix. Dr. Erbes was the original author and architect of GateCycle and thus is intimately familiar with GateCycle.

Model Description

The GE GateCycle 7FB gas turbine model was chosen as the GE GateCycle model to be fitted with a CAPE-Open wrapper. Development of the 7FB model was sponsored by DOE NETL and implemented by Wyatt Enterprises. The GE GateCycle 7FB model consists of the following equipment models:

- evaporation cooler;
- compressor;
- splitter;
- combustor;
- mixer;
- 3 expanders;
- duct; and
- generator.

Illustrated in Figure 1.2.34 is the network of models that represent the 7FB gas turbine model within the GE GateCycle software.

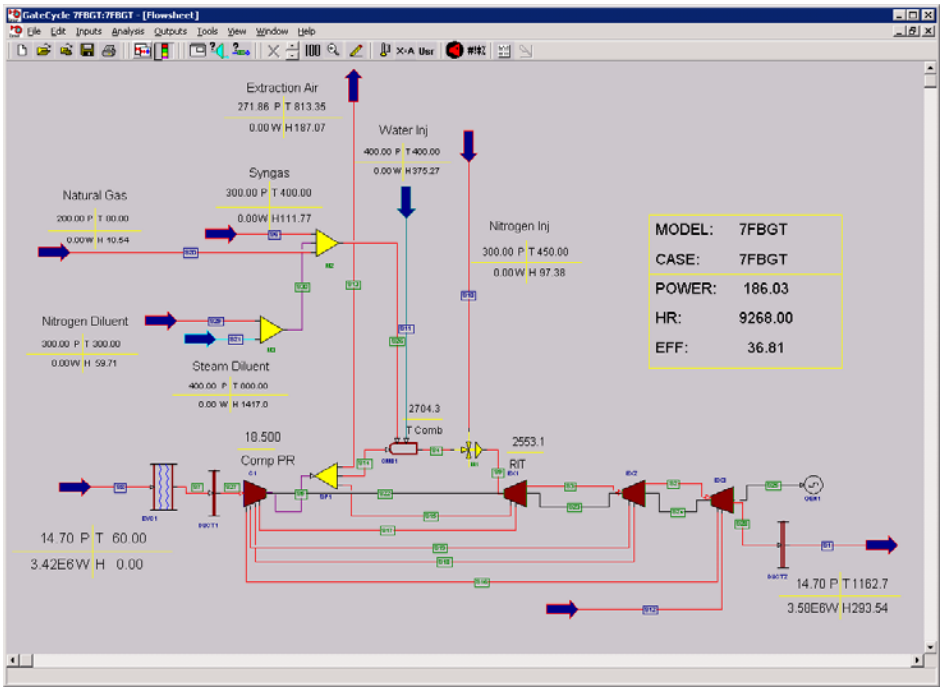

Figure 1.2.34. GE GateCycle 7FB model flowsheet.

Illustrated in Figure 1.2.35 are the model input and output parameters. Briefly, the model inputs include parameters such as the flow rate and composition of the syngas and incoming air flow and the model outputs include the predicted net power produced and exhaust gas composition and flow rate.

Model Inputs
Ambient Temperature
Ambient Pressure
Ambient Relative Humidity
Ref Temp (F) for Btu/Scf
Ref Press (psia) for Btu/Scf
Outlet Flow
Outlet Pressure
Outlet Temperature
Lower Heating Value
Outlet H-C ratio for hydrocarbons
Outlet Argon
Outlet Carbon Dioxide
Outlet Carbon Monoxide
Outlet Carbonyl Sulfide
Outlet H2O
Outlet Hydro Carbons
Outlet Hydrogen
Outlet Hydrogen Sulfide
Outlet Nitrogen
Outlet Oxygen
Outlet Sulfur Dioxide
Outlet Pressure
Outlet Temperature
Outlet Flow
Outlet Pressure
Outlet Temperature
Outlet Flow
Outlet Pressure
Outlet Temperature
Outlet Flow
Outlet Pressure
Outlet Temperature
Outlet Flow
Inlet Duct Pressure Drop
Exit Duct Pressure Drop
Compressor Overall Pressure Ratio
Desired Polytropic Efficiency
Desired Input Air Flow Rate
CDP Air Extraction Flow Rate
Combustion Efficiency
Combustor Fractional Pressure Drop
Max. Temp. Limit
Fuel Compr. Efficiency
Fuel Nozzle DP
Expander Stage Polytropic Efficiency
Expansion Ratio
Desired Nozzle Cooling Fraction of Inlet
Rotor Cooling Fraction
Input Metal Temperature - Nozzle 1
Input Metal Temperature - Rotor 1
Expansion Ratio
Nozzle Cooling Fraction of Inlet
Desired Rotor Cooling Fraction
Input Metal Temperature - Nozzle 2
Input Metal Temperature - Rotor 2
Nozzle Cooling Fraction of Inlet
Desired Rotor Cooling Flow Rate
Input Metal Temperature - Nozzle 3
Input Metal Temperature - Rotor 3

Model Outputs
Plant Net Power
GT Shaft Power
GT Generator Losses
Fuel Gas Compression Work
Net Cycle LHV Efficiency
Net Cycle LHV Heat Rate
Outlet Pressure
Outlet Temperature
Outlet Flow
Inlet Enthalpy
Outlet Pressure
Outlet Temperature
Outlet Flow
Inlet Enthalpy
Inlet Flow
Compressor Overall Pressure Ratio
Isentropic Efficiency
Polytropic Efficiency
Compressor Power Used
Exit Temperature
Inlet Duct Pressure Drop
Outlet Duct Pressure Drop
Overall Generator Efficiency
Step (polytropic) Efficiency
Isentropic Efficiency
Expansion Ratio
Expander Power Output
Rotor Inlet Temp.
Inlet Pressure
Nozzle Cooling Flow
Rotor Cooling Flow
Expander Inlet Flow Area
Nozzle Cooling Effectiveness - Stg 1
Nozzle Metal Temp - Stg 1
Rotor Cooling Effectiveness - Stg 1
Rotor Metal Temp - Stg 1
Step (polytropic) Efficiency
Isentropic Efficiency
Expansion Ratio
Expander Power Output
Rotor Inlet Temp.
Inlet Pressure
Nozzle Cooling Flow
Rotor Cooling Flow
Expander Inlet Flow Area
Nozzle Cooling Effectiveness - Stg 2
Nozzle Metal Temp - Stg 2
Rotor Cooling Effectiveness - Stg 2
Rotor Metal Temp - Stg 2
Step (polytropic) Efficiency
Isentropic Efficiency
Expansion Ratio
Expander Power Output
Rotor Inlet Temp.
Inlet Pressure
Nozzle Cooling Flow
Rotor Cooling Flow
Expander Inlet Flow Area
Nozzle Cooling Effectiveness - Stg 3
Nozzle Metal Temp - Stg 3
Rotor Cooling Effectiveness - Stg 3
Rotor Metal Temp - Stg 3

Figure 1.2.35. GE GateCycle 7FB model input and output parameters.

Benchmark Theoretical And 7FB Model Combustion Calculations

The combustor in the 7FB model uses a simple complete reaction model. Only a limited number of species (i.e., CO, CO2, H2, H2O, N2, O2, H2S, SO2, CH4) are included in the incoming gaseous streams. This could impact the accuracy of combustion calculations performed with the model. Hence, to benchmark the 7FB combustor model, comparative computations have been performed using

a) idealized reactions and
b) full chemical equilibrium as computed by the REI Reaction Engineering Kinetics Solver (REKS), a tool developed by REI for performing chemical equilibrium and chemical kinetics calculations.

All calculations were performed using the same inputs. A comparison of the values predicted using idealized (theoretical) reactions, REKS and the 7FB model (run in AspenPlus) are shown in Table 1.2.6. Overall, the predicted values are in agreement (1-2% error), indicating the GE GateCycle combustor model as implemented in AspenPlus is adequate for flowsheet evaluations of system performance.

Table 1.2.6. Compare Combustion Products Predicted by 7FB vs. other Combustion Models.

species	% Difference (theoretical vs. 7FB)	Theoretical (mole frac.)	7FB (mole frac.)	REKS equilibrium (mole frac.)	% Difference (REKS vs. 7FB)
O2	2.1%	8.5916E-03	8.6056E-03	8.5916E-03	0.2%
CO2	0.0%	6.3413E-02	6.2209E-02	6.3413E-02	1.9%
H2O	0.2%	5.0989E-02	5.0135E-02	5.0989E-02	1.7%
N2	2.1%	7.1638E-01	7.1752E-01	7.1638E-01	0.2%
Ar	2.5%	1.6063E-01	1.6153E-01	1.6063E-01	0.6%

Examples calculations for using the GE GateCycle 7FB model with a COM-based CAPE-Open compliant coupling to AspenPlus is provided in the Results and Discussion section of this report (see Section 2.6).

COM CAPE-Open Implementation

REI and Enginomix, a project team member, collaborated closely to implement the 7FB model as a CAPE-Open-compliant COM component. The GE GateCycle Automation Program Interface (API) (entitled GCAPI) interface has been used to create C++ software to

- pass all 7FB input parameters to GE GateCycle,
- execute the 7FB GE GateCycle flowsheet, and
- pass back model outputs.

Illustrated in Figure 1.2.36 is a schematic diagram of the COM CAPE-Open compliant GE GateCycle 7FB model. The figure illustrates the various software layers of the module's architecture. At the highest level is the COM CAPE-Open wrapper. From this CAPE layer, the GateCycle API wrapper is used to communicate with and control GE GateCycle from within the GCAPI layer. A challenge in developing the GCAPI code is that the key functionality of the GE GateCycle automation API is largely undocumented.

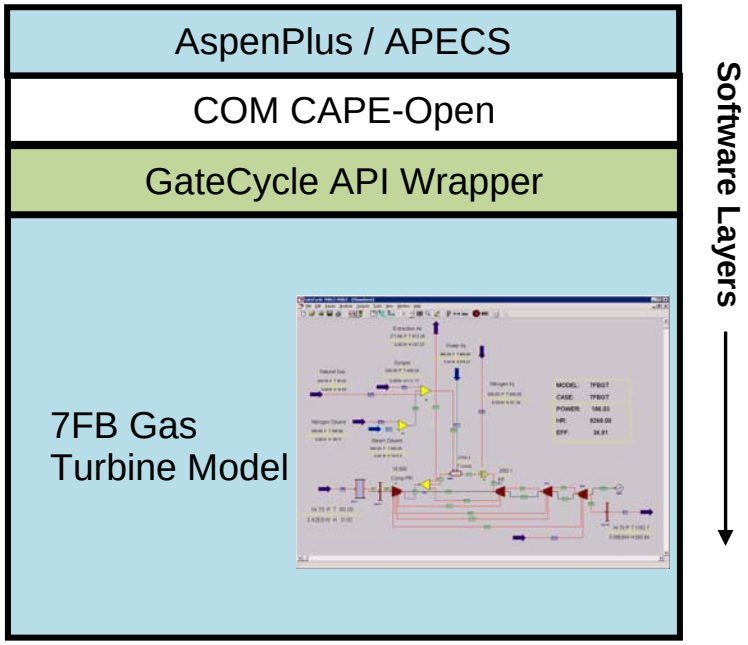

Figure 1.2.36. Schematic of COM CAPE-Open interface for GE GateCycle 7FB model.

To make the GE GateCycle 7FB CAPE-Open model available to AspenPlus/APECS users, it was decided for simplicity to keep most internal parameters for the 7FB model fixed and allow the AspenPlus/APECS user to modify only a limited subset of the model parameters. Hence, model inputs such as the syngas and air composition and flowrates are extracted from input streams in the flowsheet and the model computes the net power produced by the turbine, along with exhaust gas composition and flowrate which are passed to the output stream.

REI and Enginomix worked with NETL to define the details for user interaction for the models. Specifically, on decision on which parameters (input and output) for 7FB model to expose via the CAPE-Open interface. Based on a review of the setup and configuration of the 7FB model performed by Enginomix and REI, a software interface specification document was developed and provided to NETL for comment prior to starting the software implementation efforts.

Early in the project it was learned that a new version of GE GateCycle (V6) was to be released which could potentially use a different COM interface. Based on discussions between Enginomix and industry personnel it was determined that release of the new version of GE GateCycle was “on-hold” indefinitely. Hence, all work performed for this project is based on V5.61 of the GE GateCycle software system.

1.3 Task 3 – Demonstration

The improved simulation capability of APECS was demonstrated through selected test problems. To facilitate the example calculations, REI obtained a set of AspenPlus flowsheets for IGCC plant configurations with and without CO2 capture originally developed by NETL [Ciferno, 2006ab] and described in detail in [Klara, 2007]. REI's efforts focused on implementing COM-based CAPE-Open versions of REI process models, an AspenPlus based cryogenic ASU model, a COM-based CAPE-Open version of an OTM ASU process model, COM-based CAPE-Open ROM models and a COM-based CAPE-Open coupling between APECS/AspenPlus and a GE GateCycle model for a turbine. The ASU process models were obtained from Praxair, a project team member (see the discussion for Task 2.3 in Section 1.2.3) for implementation into the NETL AspenPlus IGCC flowsheets.

1.4 Task 4 – Program Management, Reporting and Technology Transfer

The following material highlights notable events performed as part of the Program Management task in the project, followed by a section highlighting Technology Transfer activities performed during the project to ensure the knowledge developed as a result of this project was transferred to scientists and engineers at NETL and in industry.

Programmatic Items

- Conference calls were held with:
    - REI, NETL and ISU personnel to coordinate the efforts of REI, ISU, NETL and other NETL funded projects implementing software enhancements to APECS.
    - REI, NETL, ISU, ANSYS/Fluent and CMU personnel to coordinate REI's efforts with those of these groups and other NETL funded projects that are developing ROM capability.
    - Enginomix, a project team member, to discuss software requirements to implement a CAPE-Open compliant coupling between APECS and the GE GateCycle process simulator flow sheet.
    - Praxair, a project team member, to discuss software requirements and capabilities for a model of a cryogenic Air Separation Unit (ASU) and a model of an Oxygen Transport Membrane (OTM) ASU that Praxair provided to REI for use in this project.

- On December 14, 2005, a meeting of the Advisory Panel for this project was conducted at the REI offices in Salt Lake City, Utah. Meeting participants included personnel from NETL (S. Zitney), EPRI (N. Holt), an expert in greenhouse gas issues (H. Herzog), Enginomix (M. Erbes), electric utilities (AEP, AmerenUE), a technology developer (Praxair) and REI (M.Bockelie, A.Sarofim, D.Swensen, M.Denison).
    - The purpose of the meeting was to obtain input from industry on the functionality and capability to include in simulation tools to assess the performance of advanced power plant systems and to identify CO2 capture ready IGCC plant

configurations and problems of interest to industry for use in our demonstration calculations (see Task 3 in this section).

- In the meeting, formal and informal presentations and discussions included:
  - Advanced Processing Modeling R&D at NETL
  - REI project overview
  - Gasification and IGCC – Status, Challenges, Design Issues and Opportunities
  - Simulation Requirements To Evaluate CO2 Capture Systems
  - Power Plant Modeling for IGCC Systems Analysis
  - Advanced & Oxy-fuel Systems - Near Term & Long Term
  - Process Modeling - Needs and Requirements - Industry View
  - Roundtable Discussions
    - plant configurations to assess (configurations, assessment goals)
    - process simulation needs (functionality) to include in plant simulator / assessments
- Summary notes from the meeting and all presentations were provided to meeting attendees on CDs and the summary notes were reported in [Bockelie et al, 2006a]. Further details on many of the topics discussed in the meeting can be found in [Holt, 2005], [Shah, 2005] and the proceedings of the Gasification Technologies Conference 2005 that is available on the Gasification Technologies Council web page [http://www.gasification.org].

- A member of the REI technical staff attended an advanced AspenPlus training course held at NETL in Morgantown, WV during April 26-28, 2006. The class covered the basics of using AspenPlus along with discussions of more advanced capabilities including optimization and user-defined block functionality. In addition to the AspenPlus training, attending the meeting provided REI the opportunity to meet face-to-face with personnel from NETL and other organizations that are developing software for use in the APECS framework. During the visit, discussions were held with NETL personnel on the VE-Suite-to-APECS coupling and other technical issues pertinent to this project. During the visit a demonstration of the prototype coupling of VE-Suite-to-APECS was provided to NETL personnel.

- A contractually required Annual Project Review meeting was held at NETL in Morgantown, WV on February 28, 2007. Meeting attendees included management and technical personnel from NETL and technical personnel from other NETL funded projects assisting in the development of APECS. In the meeting, REI presented an overview of our progress on the different project tasks. Topics discussed included models used by REI, the VE-Suite-to-APECS coupling, REI's CASI library, APECS development and support (current, future), difficulties encountered using APECS and the IGCC flowsheets obtained from NETL that REI has used within this project.

- A nine month no-cost extension for this project was requested by REI and granted by NETL. The no-cost extension resulted in a project end-date of September 19, 2008.

- All project Milestones were completed on time.

- All software deliverables (software infrastructure, models) were delivered to NETL.

- The project was successfully completed on June 18, 2008.

Technology Transfer:

- A paper that describes the enhanced REI entrained flow gasifier model using improved gasification kinetics was presented at the Clearwater Conference 2006 [Bockelie et al, 2006c] and Pittsburgh Coal Conference 2006 [Bockelie et al, 2006e]. Included were descriptions of model implementation and comparisons to commercial scale coal gasifier performance data from an IGCC plant. Example calculations were provided for investigating product/reactant inhibition effects on gasification rates; using an increased operating temperature to improve carbon conversion; and scaling the gasifier size to achieve high carbon conversion when operating at elevated pressures expected for IGCC plants with CO2 capture. The conference presentations highlighted the impacts on performance of wet (slurry) feed versus dry feed gasifier designs.

- REI, with Alstom and Praxair, provided a tutorial on CO2 capture for advanced power systems at the Clearwater Conference 2006 [Sarofim et al, 2006].

- Modeling results from this project were included in the Plenary Lecture provided by Prof. Terry Wall (University of Newcastle) at the Combustion Institute International Symposium [Wall, 2006].

- Two papers that describe software tools and software development issues for CAPE-Open and process modeling were presented at the 3rd Annual U.S. CAPE-OPEN Conference [Erbes et al., 2006], [Swensen et al, 2006]. Included were discussions on modeling power plants vs. chemical plants, using CAPE-Open to couple different process simulator packages and an overview of the goals, methods, tools and models being used in this project.

- A paper describing modeling techniques and results from this project was presented at the Clearwater Conference 2007 [Bockelie et al, 2007c]. The paper highlighted REI's role for the development of APECS and REI's experiences using APECS. Example results for using AspenPlus flowsheets developed by NETL for evaluating IGCC plant configurations with and without CO_2 capture were modified to use the detailed cryogenic ASU model provided by Praxair for use in this project. A comparison of the gasifier model contained in the NETL IGCC flowsheets and the REI entrained flow gasifier process model was provided.

- Information and modeling results generated within this project were included in a lecture presented to power plant engineers/managers and researchers from the Republic of Korea [Bockelie, 2007]. The lecture included background material on IGCC systems, including FutureGen, coal gasification and modeling tools / methods for evaluating IGCC plant configurations. The lecture was part of a combustion short course provided by REI. There were nineteen attendees from Korea.

- A presentation co-authored by REI and NETL was provided by REI at the 4th CAPE-Open US Conference which was held in conjunction with the AICHE Annual Meeting held in Salt Lake City, Utah in November, 2007 [Swensen et al., 2007]. The presentation focused on REI development efforts and experiences with implementing CAPE-Open solutions for the Department of Energy's NETL for Advanced Power Systems Modeling. Specific presentation topics included: project background and motivation; an overview of CAPE-Open technologies; an overview of APECS Technologies; implementation details for APECS CORBA CAPE-Open components; and an overview of models targeted for integration with APECS.

- Project team members participated in a public meeting entitled "The Future of Coal In A Carbon-Constrained World" sponsored by the University of Utah Institute for Clean and Secure Energy [UofUtah, 2008]. The meeting included several key note speakers discussing issues on green house gas emissions and the potential solutions provided by IGCC and other advanced power generation systems.

- Project team members participated in a public meeting for an IGCC Working Group hosted by a local electric utility that was evaluating the potential development of an IGCC plant.

- A paper that describes the enhanced REI Entrained Flow Gasifier model and the ash vaporization sub-model implemented as part of this project was presented at the Clearwater Coal Conference 2008 [Bockelie et al, 2008c] and at the Pittsburgh Coal Conference 2008 [Bockelie et al., 2008e]. Included were detailed descriptions of model implementation and example calculations for one and two stage slurry feed gasifiers and a one stage dry feed gasifier.

Chapter 2. Results and Discussion

In the following are provided example modeling results and discussion for

- NETL AspenPlus IGCC flow sheet calculations;
- REI Entrained Flow Gasifier Models:
    - pressure dependence on emissivity properties used in radiation heat transfer calculations;
    - pressure effects on carbon conversion;
    - an ash vaporization model;
- CAPE-Open versions of selected REI process models:
    - REI Entrained Flow Gasifier Process Model;
    - REI Carbon Bed Model;
- AspenPlus version of a Cryogenic ASU model;
- CAPE-Open version of an OTM ASU model;
- REI ROM generator; and
- CAPE-Open coupling between GE GateCycle and APECS.

2.1 NETL AspenPlus IGCC Flow Sheet Calculations – Slurry Feed with and without CO_2 Capture

NETL has provided REI with AspenPlus networks (flow sheets) that are being used by NETL to analyze IGCC plant configurations with and without CO_2 capture. NETL has performed their analyses using networks that contain proprietary models/data/model-inputs and with networks that use only non-proprietary information. The results reported by NETL [Ciferno, 2006ab] have been based on the networks that contain proprietary models/data/model-inputs. The files provided to REI use only non-proprietary information (denoted by "NP" in the file names). These networks are intended to be used for evaluation of REI models implemented as part of the current effort.

The two networks used here (called Case 1 and Case 2) involve slurry feed gasification. Case 1 is for a conventional IGCC plant without CO_2 capture and Case 2 is for the same plant configuration suitably modified to include CO_2 capture.

Included in the plant configuration are models for cryogenic ASU, wet (slurry) feed gasifier (GE/Texaco style), syngas cooler/quench, particulate removal, water gas shift reactor, syngas cooler, CO2 removal (2 stage Selexol process), fuel gas reheat for the gas turbine, conventional cycle power island, and CO2 compression. The AspenPlus network of Case 1 consists of 263 blocks and 493 streams (see Figure 2.1.1) while the network of Case 2 consists of 293 blocks and 549 streams (see Figure 2.1.1). As can be seen from Figures 2.2.1 and 2.2.2, the networks are quite complicated. The required run times were roughly 15 minutes on a 2.2 GHz desk top computer.

Table 2.1.1 lists the key results of the two cases compared with results presented by NETL at the May 2006 Clearwater Conference. The results computed by REI (Case 1, Case 2) are somewhat different from those computed by NETL (Case 1 NETL, Case 2 NETL) because the NETL results are based on proprietary models/data/model-inputs whereas the values computed by REI were generated using non-proprietary information. Nevertheless, the same trends can be seen. Note that the addition of CO_2 capture results in a significant drop in net plant efficiency.

Table 2.1.1. Comparison of key results from AspenPlus IGCC models.

Net Plant Performance	Units	Case 1	Case 2	Case 1 NETL	Case 2 NETL
Auxiliary Load	kWe	121,632	138,960	125,000	178,000
Net Plant Power	kWe	651,118	599,930	644,000	563,000
Net Plant Efficiency (HHV)		38.89%	34.72%	38.60%	32.60%
Net Plant Heat Rate (HHV)	Btu/kWhr	8,774	9,827	8,832	10,463
Coal Feed Flowrate	lb/hr	489,685	505,381	489,685	505,381

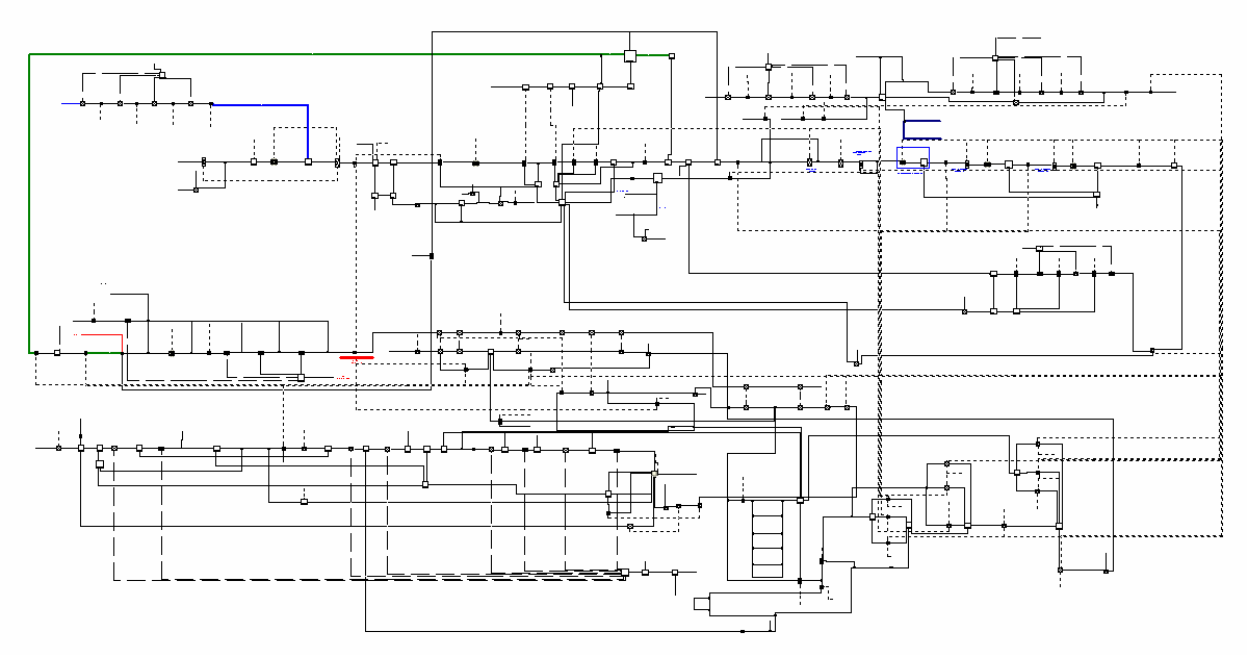

Figure 2.1.1. AspenPlus network for Case 1 – IGCC plant without CO2 capture.

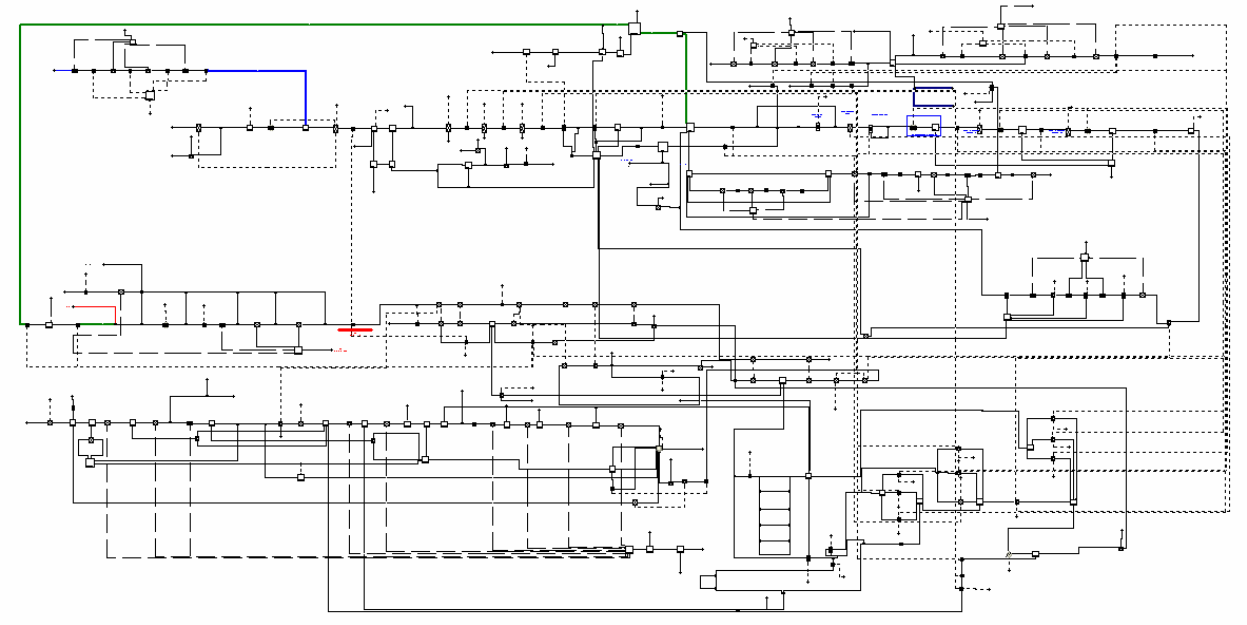

Figure 2.1.2. AspenPlus network for Case 1 – IGCC plant with CO2 capture.

2.2 REI Entrained Flow Gasifier Model

In the following sections are provided example results for the enhancements to the REI entrained flow gasifier model.

2.2.1 Pressure Dependence on Emissivity Properties

Using the gasifier model enhancements described in Chapter 1 (see discussion for Task 2.1), a sensitivity study has been performed to investigate the impact of using *RADCAL* to better simulate the pressure dependence on emissivity properties in heat transfer calculations. To perform the study, comparative simulations were performed for the same process conditions for the wet (slurry) feed gasifier and dry feed gasifier using the improved properties model and the original model. In the following, the plots labeled "Hottel Chart" indicate simulations performed with the original model and plots labeled "RADCAL" indicate simulations performed using the improved properties evaluation model.

Illustrated in Figure 2.2.1 to Figure 2.2.3 are comparisons for the wet (slurry) feed gasifier. Figure 2.2.1 shows the comparison of the gas temperature distribution for a one-stage slurry feed gasifier. The gas temperatures are somewhat higher toward the exit of the gasifier when using *RADCAL*. Figure 2.2.2 contains a comparison of the predicted gas emissivity. Figure 2.2.3 shows a comparison of the wall surface temperatures. The wall temperatures are slightly higher for the case of using *RADCAL*.

Illustrated in Figure 2.2.4 to Figure 2.2.6 are the same comparisons but with a dry feed gasifier. In the dry feed cases there is essentially no liquid water in the coal feed and higher gas temperatures can be achieved since energy is not required to vaporize the liquid water in a slurry. The walls must typically be cooled for dry feed gasifiers to prevent the refractory surfaces from being thermally damaged. In the dry feed gasifier, the water vapor concentration within the gasifier is small. Therefore the differences in predicted temperatures using the improved model (i.e., *RADCAL*) versus the original model (i.e., Hottel Charts) off are much smaller (see Figure 2.2.4 and Figure 2.2.5). The differences in radiative properties between using *RADCAL* and the Hottel correlations are more pronounced with water vapor than with CO_2 or CO.

Summary

The above results highlight the improved prediction capability provided by including the pressure dependence on the emissivity properties used in radiative heat transfer calculations. The enhanced model is applicable for wet (slurry) feed gasifiers and dry feed gasifiers, but possibly more useful for wet feed systems due to the inherently greater moisture content in the syngas. Although the improvements in the predicted heat transfer are subtle, they are important. Thermal damage of equipment surfaces within the gasifier due to overheating (e.g., fuel injectors, refractory walls) continues to be an important challenge for improving gasifier performance.

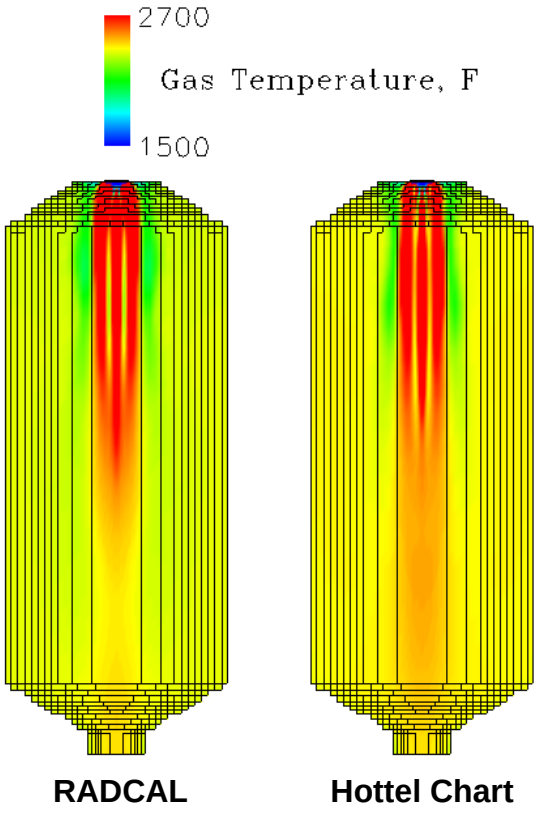

Figure 2.2.1. Effect of *RADCAL* on predicted gas temperature for a slurry feed gasifier.

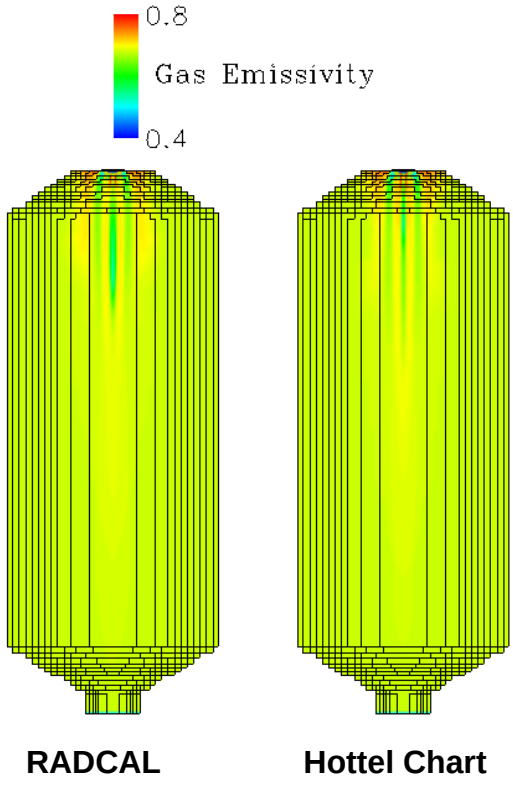

Figure 2.2.2. Effect of *RADCAL* on predicted gas emissivity for a slurry feed gasifier.

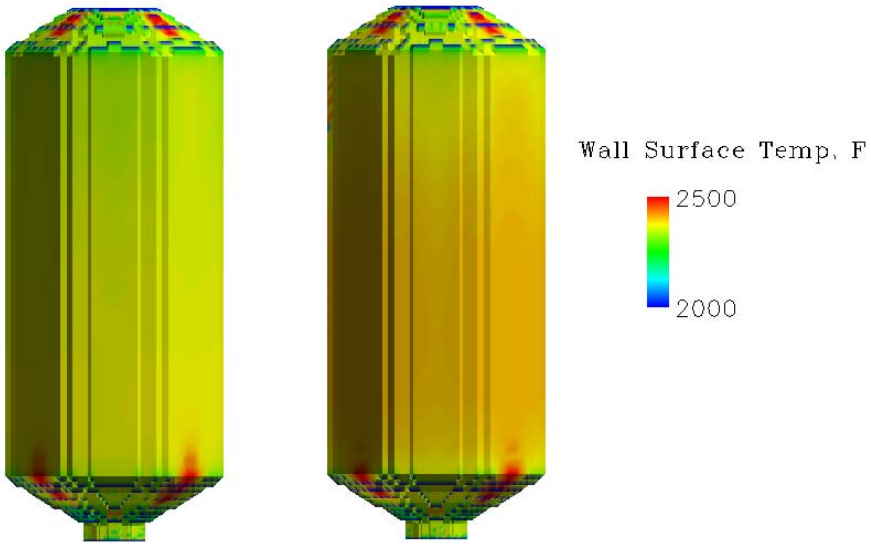

Figure 2.2.3. Effect of *RADCAL* on predicted wall surface temperature for a slurry feed gasifier.

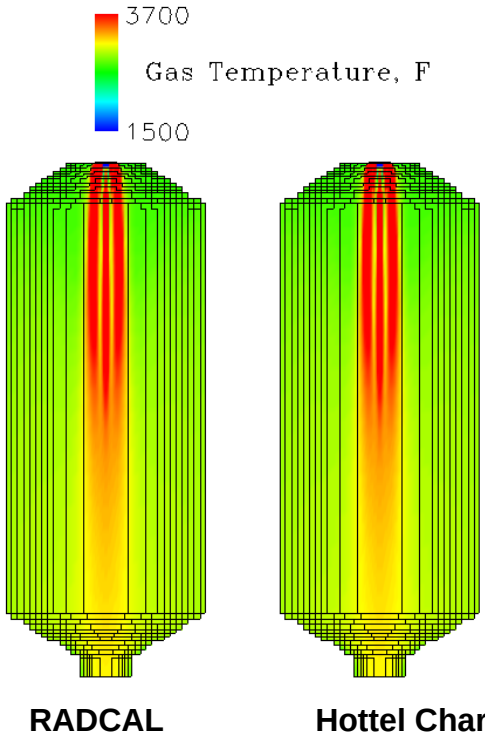

Figure 2.2.4. Effect of *RADCAL* on predicted gas temperature for a dry feed gasifier.

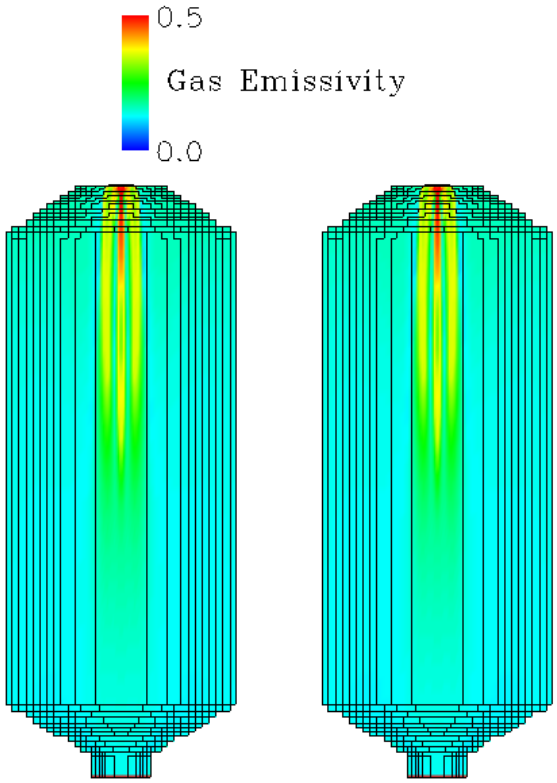

Figure 2.2.5. Effect of *RADCAL* on predicted gas emissivity for a dry feed gasifier.

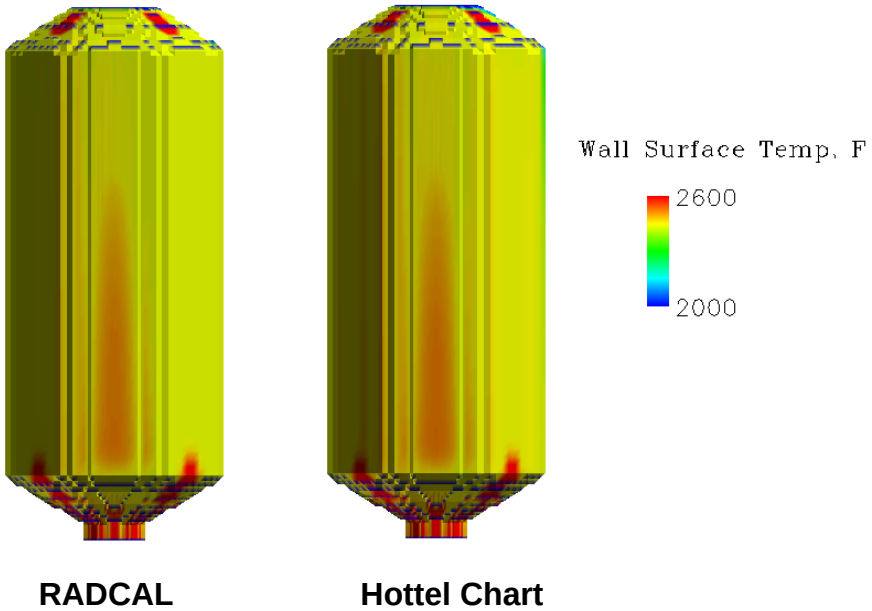

Figure 2.2.6. Effect of *RADCAL* on predicted wall surface temperature for a dry feed gasifier.

2.2.2 Pressure Effects on Carbon Conversion

In the following is a comparison of model results for gasifier performance for a wet (slurry) feed and dry feed gasifier performed with improved gasification kinetics that account for reactant and product gas inhibition effects as described in Chapter 2 (see discussion for Task 2.1).

Wet (Slurry) Feed Gasifier Description

The gasifier modeled in this study is a "generic" one-stage downfired unit. The process conditions and gross gasifier geometry used for these simulations are also summarized in Figure 2.2.7. The shape of the single-stage gasifier is based on information for a pilot scale facility [Schneyer et al., 1982] and then scaled for commercial-scale systems. We assume a L/D ratio of 2, where L is the length of the main chamber and D is the internal diameter to the refractory surface. Based on simple plug flow calculations, results in a gas residence time for the gasifier of about 3.5 seconds. The single-stage gasifier contains a single nozzle positioned at the top and center of the reactor through which the oxidant stream and coal-water slurry mixture are injected into the gasifier. See [Bockelie et al., 2004] for details.

Firing Conditions

- System Pressure = 27 atm.
- 2200 tpd Bituminous
  - 5% H_2O, 8% ash
- Slurry Feed: 65% solids (wt.)
- Oxidant (wt %)
  - 95% O_2, 5% N_2
- O_2 : C (molar) = 0.49
- Inlet Stoichiometry ~ 0.52

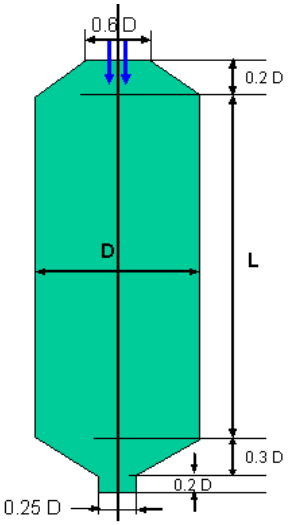

L/D = 2, D = 3.19 m

Figure 2.2.7. Schematic of one-stage, slurry-feed, downflow gasifier and process conditions.

Dry Feed Gasifier Description

Illustrated in Figure 2.2.8 is a schematic and process conditions for a single-stage upflow, dry-feed gasifier that uses a water jacket to cool the refractory. The configuration is representative of the gasifier being used at the IGCC plant at Puertellano, Spain. The gasifier is assumed to have a diameter of about 1.7 m and a L/D ratio slightly less than two (where L is the length of the constant diameter section). The firing system consists of four fuel injectors in a diametrically opposed pattern located near the bottom of the gasifier. It is assumed that no gas exits through the slag tap at the bottom of the reactor, and thus all flue gas must exit through the top opening. The gasifier employs a dry-feed system – N_2 is used for the solids transport gas. The fuel injectors are assumed to be simple "concentric pipes" through which all solids and gases enter the gasifier. We have assumed an inlet velocity for the solids of 8 m/s. The stoichiometry at the gasifier inlets is ~0.4. The gasifier uses a water jacket to provide backside cooling to the

refractory. The objective of the backside cooling is to create a “frozen” or “solid” slag layer on the hot-side refractory surface to protect the refractory from the corrosive nature of the molten slag. Compared to slurry feed the O2 to carbon ratio (as well as SR) can be lower since heat for water vaporization is not needed For further details on the dry feed gasifier configuration, see [Bockelie et al, 2004].

Firing Conditions

- System Pressure = 27 atm.
- 2200 tpd Bituminous
  - 5% H2O, 8% ash
- Oxidant (mole %)
  - 95% O_2 , 5% N_2
- 10% additional N_2 carrier gas
- O2 : C (molar) = 0.44
- Inlet Stoichiometry ~ 0.48

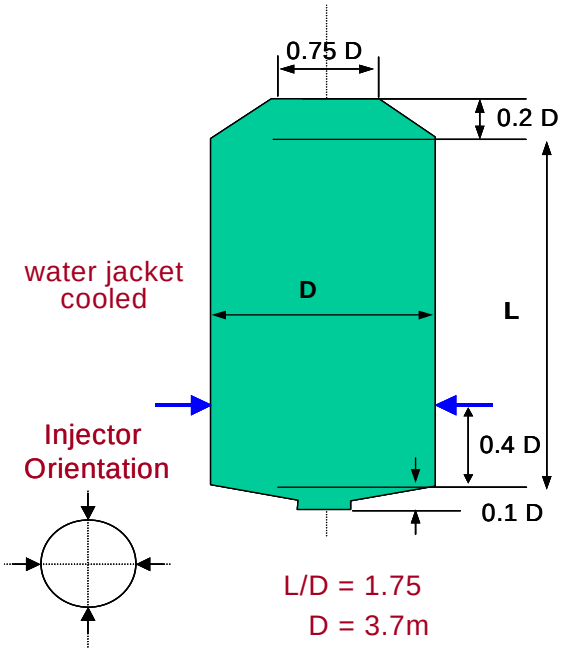

Figure 2.2.8. Schematic of single-stage, up-fired gasifier and summary of process conditions.

Illustrated in Figure 2.2.9 are the gasification rate and CO mole fraction profiles for the wet (slurry) feed gasifier (top) and dry feed gasifier (bottom). The calculations were performed using the process conditions shown in Figures 3.2.7 and 3.2.8, with the exception that the system pressure was set to 70 atm. to simulate the performance for the expected operating conditions for an IGCC plant with CO2 capture. From Figure 2.2.9 it can be seen that

- the gasification rates decrease as the CO concentration increases, although a decrease in gas temperature also accounts for the drop in gasification rate with time;
- the gasification rate due to water vapor (steam) is much greater than that of CO2; and
- the dry feed gasifier requires longer to achieve the same level of burnout as the wet feed gasifier due to the higher CO concentration in the dry feed gasifier syngas.

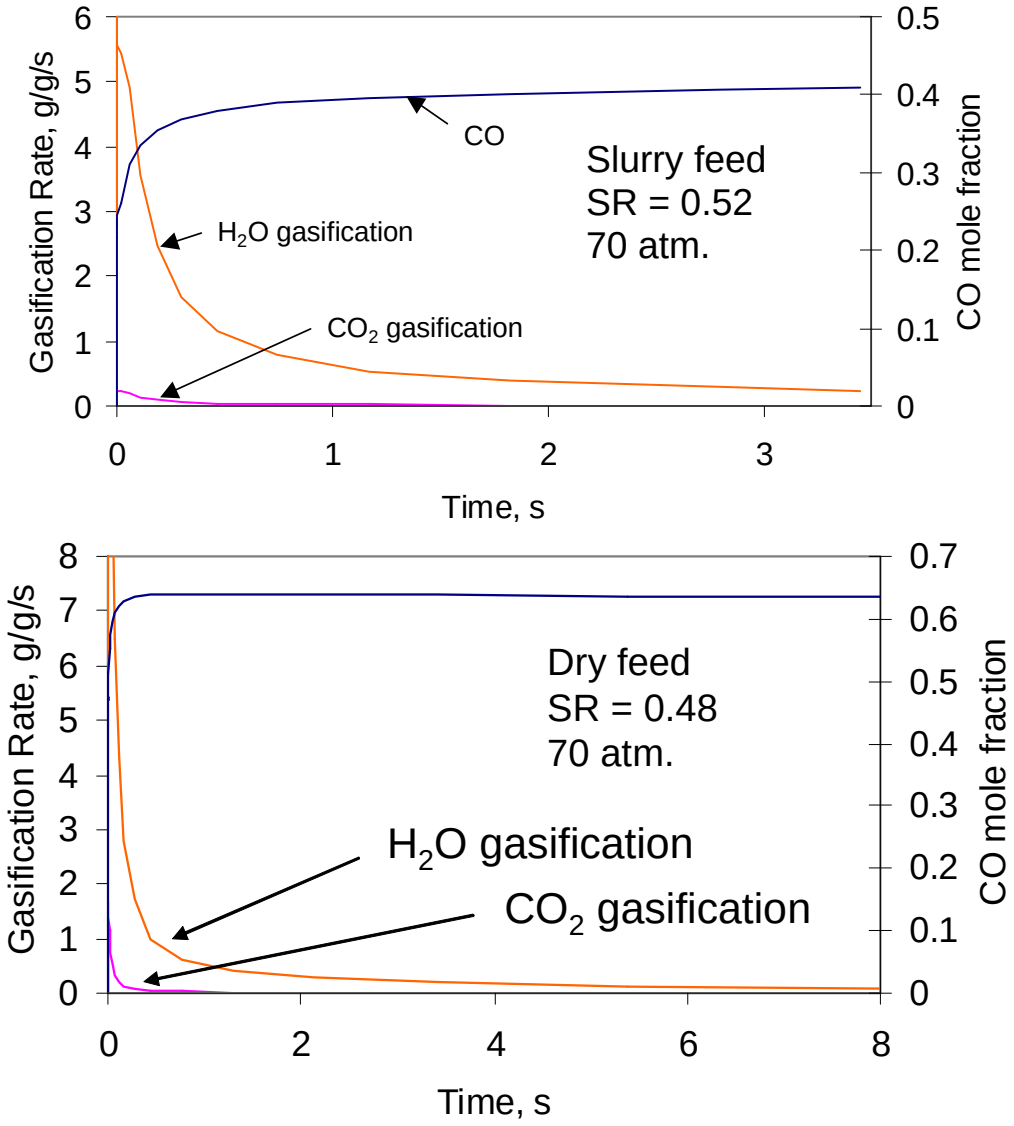

Figure 2.2.9. Calculated gasification rates and CO concentration versus residence time for a wet (slurry) feed gasifier (top) and dry feed gasifier (bottom) operated at similar process conditions.

Illustrated in Figure 2.2.10 is the predicted carbon conversion versus residence time in the gasifier at 70 atm pressure for selected stoichiometric ratios. The solid lines are the predicted performance for the wet feed gasifier and the symbols (red dots) are the predicted performance for the dry feed gasifier. The profiles were calculated using the particle burnout portion of the gasifier process model with the slurry flow rate fixed. The stoichiometric ratio was varied by varying the oxygen flow rate.

From Figure 2.2.10 it can be seen that the conversion begins very rapidly during oxidation and initial gasification while the local gas and particles are hot. Once the oxygen is depleted the much slower gasification reactions take over and the conversion levels off with increasing CO concentration, which inhibits the gasification reactions. Increasing the temperature via increasing

oxygen (i.e., increasing the stoichiometric ratio) improves the burnout but eventually the temperatures would become hot enough to decrease refractory life for the wet feed gasifier. In contrast the dry feed gasifier uses a water cooled membrane wall that allows for higher gasifier temperature operation and thereby can mitigate the CO inhibition effects described above. Last, it should be noted that the higher temperatures are achieved at the cost of cold gas efficiency of the syngas.

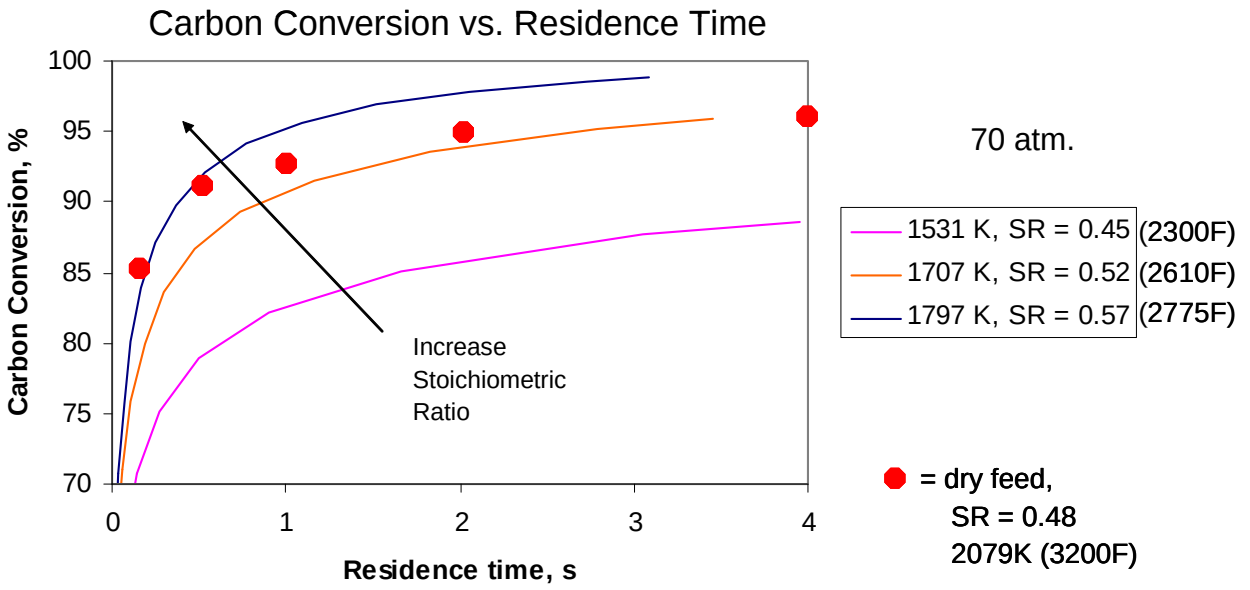

Figure 2.2.10. Predicted carbon conversion vs. residence time for selected stoichiometric ratios (70 atm.) for a wet (slurry) feed gasifier (solid lines) and a dry feed gasifier (symbols).

Summary

The above calculations highlight the importance of including gasification reactant/product inhibition effects in the gasification rate for entrained flow gasifier models. In regards to performing calculations to improve gasifier performance and/or scale-up, the above results indicate:

- heterogeneous kinetic effects determine operating temperature of the gasifier and the gasifier volume (size);
- to increase carbon conversion, it is more effective to increase the operating temperature (e.g., stoichiometric ratio) rather than increasing the gasifier volume because of the inhibition by CO of gasification rates at high carbon conversion;
- inhibition effects could complicate scale-up for higher pressure operation (e.g., CO2 capture ready plants);
- gasification rate due to moisture dominates the gasification rate due to CO2; and
- slurry feed gasification rates are higher than dry feed because of higher H2O concentrations (this can be compensated for by operation at higher temperatures with cooled refractory walls).

2.2.3 Ash Vaporization Model

The ash vaporization model described in Section 1.2.1 has been used to investigate ash vaporization for one and two stage entrained flow gasifiers. Illustrated in Figure 2.2.11 is a description of the coal (Illinois #6) and ash composition used for the example calculations. The slurry feed cases were performed for the following firing conditions: 3000tpd coal; slurry = 74 wt% solids; oxidant = 95 wt% O2, 5 wt% N2; and the oxidant flow rate determined by specifying an Oxygen:Carbon ratio = 0.40 (molar basis). The dry feed gasifier calculations were performed for the following firing conditions: 2600tpd coal; N2:coal ratio of 0.075 (lb/lb); oxidant = 76 wt% O2, 11 wt% H2O, 10 wt% N2; 3 wt% Ar and the oxidant flow rate determined by specifying an Oxygen:Carbon ratio = 0.46 (molar basis). The system pressure is assumed to be (about) 1000 psia.

Coal (Illinois #6, Dry)

C (wt%, dry)	68.93
H (wt%, dry)	4.87
O (wt%, dry)	8.95
N (wt%, dry)	1.49
S (wt%, dry)	2.67
Ash (wt%, dry)	13.09
Total (wt%, dry)	100.0
HHV (Btu/lb, dry)	12,470

Ash Chemistry (SO3-free)	
SiO2	52.90%
Al2O3	22.31%
TiO2	1.06%
Fe2O3	16.82%
CaO	2.52%
MgO	0.81%
Na2O	0.86%
K2O	2.57%

Figure 2.2.11. Coal and Ash Description.

Illustrated in Figure 2.2.12 are representative particle trajectories for a one-stage down-fired entrained flow gasifier (see gasifier geometry shown in Figure 2.2.7). Shown are the predicted conversions of different refractory oxides along the particle trajectory for a representative particle size. Shown in the plot the fraction of SiO, Mg, Na and total ash vaporization that occurs along the length of the particle trajectory. In the plots, blue indicates a low value and red is a high value. Similar plots can be generated for any size particle or any of the vaporized ash compounds tracked by the model. From the plots it can be seen that initially there is no vaporized ash but as the particles move through the gasifier vaporization occurs and that a different amount of vaporization can occur for different ash compounds and for different trajectories. That is, the local flow field conditions through which the particles pass impacts the amount of ash vaporization that occurs.

Illustrated in Figure 2.2.13 are representative particle trajectories for a one-stage up-fired, dry feed entrained flow gasifier (see gasifier geometry shown in Figure 2.2.8). The complex, re-circulating pattern exhibited by the particles is due to the flow patterns generated by the assumed fuel injector configuration (i.e., four opposed jets). As per the slurry feed gasifiers, it can be seen that the ash vaporization process is impacted by the local flow field conditions that exist within the gasifier.

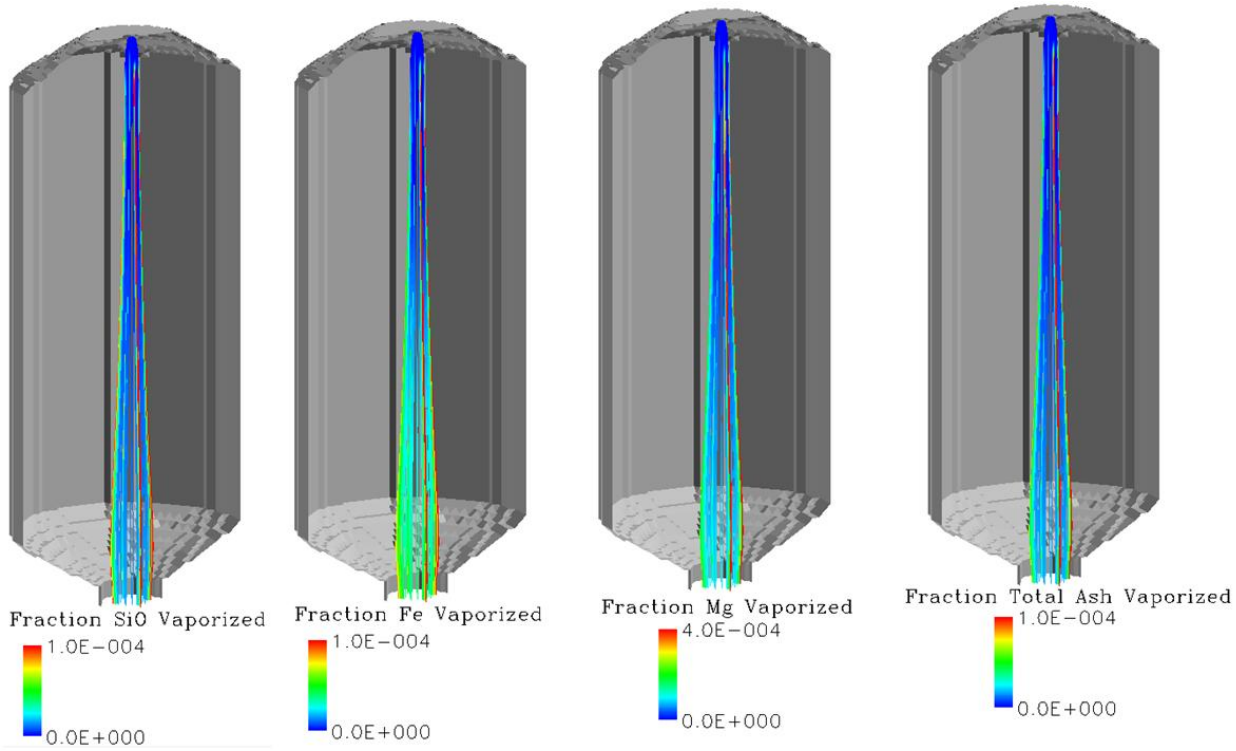

Figure 2.2.12. Ash vaporization in one-stage down-fired gasifier (25- 60 micron diameter particles).

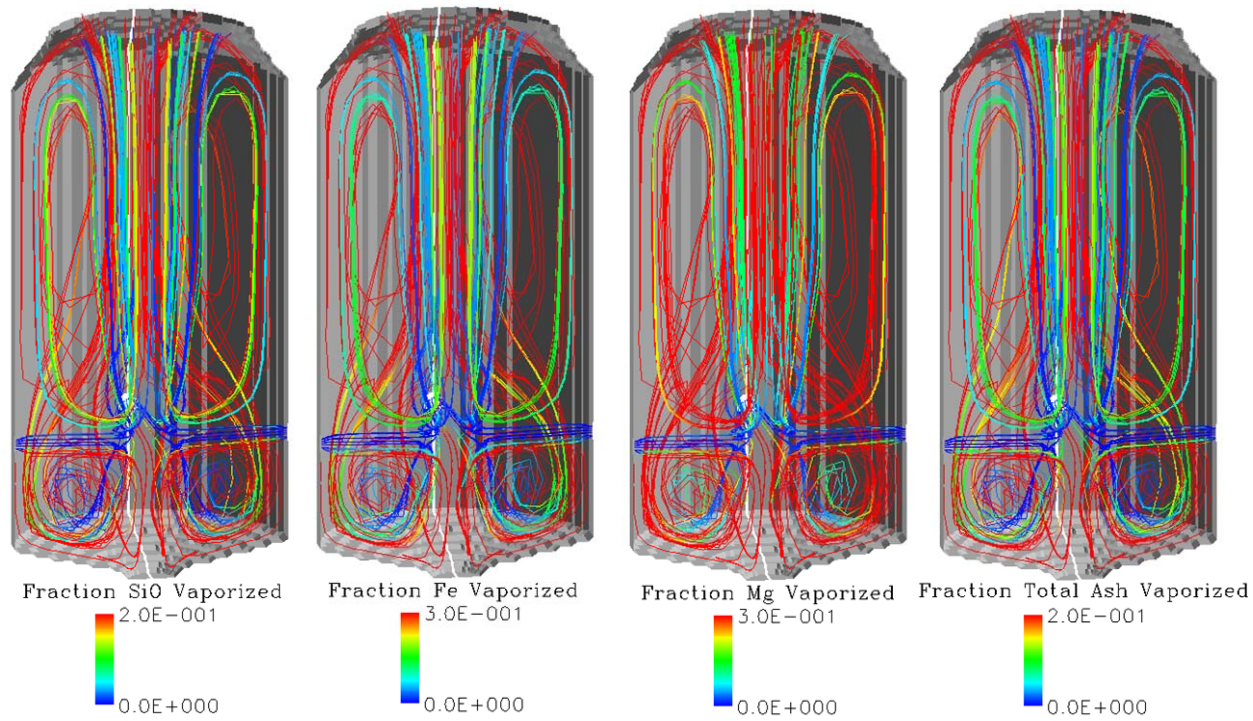

Figure 2.2.13. Ash vaporization in one-stage up-fired dry feed gasifier (25 - 60 micron diameter particles).

The ash vaporization calculations have also been performed for a two-stage, up-fired slurry feed entrained flow gasifier. The gross gasifier geometry and process conditions are summarized in Figure 2.2.14. The shape of the two-stage gasifier is based on information contained in a series of articles by Chen et al. (1999, 2000) that describe modeling studies and scale-up for a pressurized, air-blown entrained flow gasifier designed to operate at 2000 tons/day of coal. Additional assumptions used to determine the size of the gasifier were that the gasifier should provide about a two second residence time for the gases (assuming idealized flow) and has a length to diameter ratio (L/D) of about ten. The two-stage gasifier contains three levels of symmetrically placed injectors. The fuel injectors are assumed to have a simple annular passage (concentric pipes) that does not produce a spray action. The bottom two levels of injectors are oriented as per a tangential-firing system to create a strong swirling flowfield that spirals upward along the axis of the gasifier. The upper-level injectors are oriented opposed to each other. All of the oxidant and 78% of the coal is uniformly distributed amongst the fuel injectors in the first stage and the remaining coal is uniformly distributed across the injectors in the second stage. No oxidant is injected into the upper stage. For further details, see [Bockelie et al., 2004].

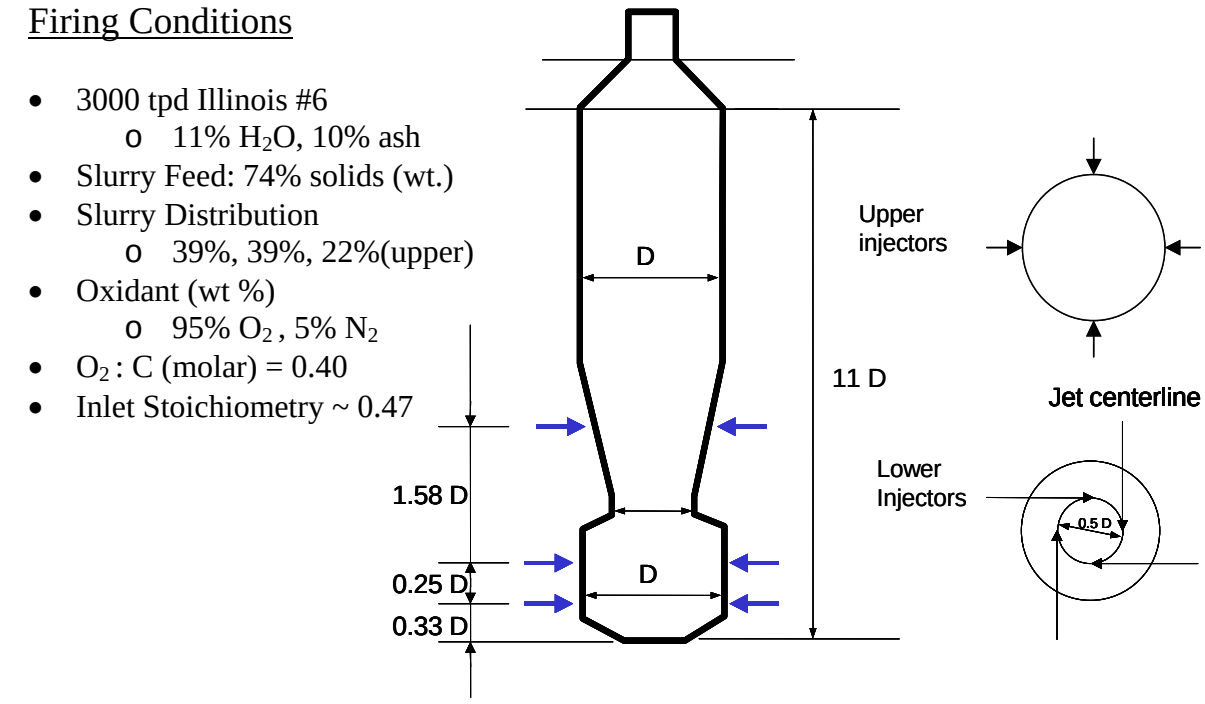

Figure 2.2.14. Schematic of two-stage upflow configuration and process conditions.

Illustrated in Figure 2.2.15 are representative particle trajectories for a two-stage up-fired slurry feed entrained flow gasifier. The highly swirling flow pattern observed in the particle trajectories is due to the assumed fuel injector configuration (i.e., T-fired in Stage 1). As per Figure 2.2.12, it can be seen that the ash vaporization process can be a very localized process.

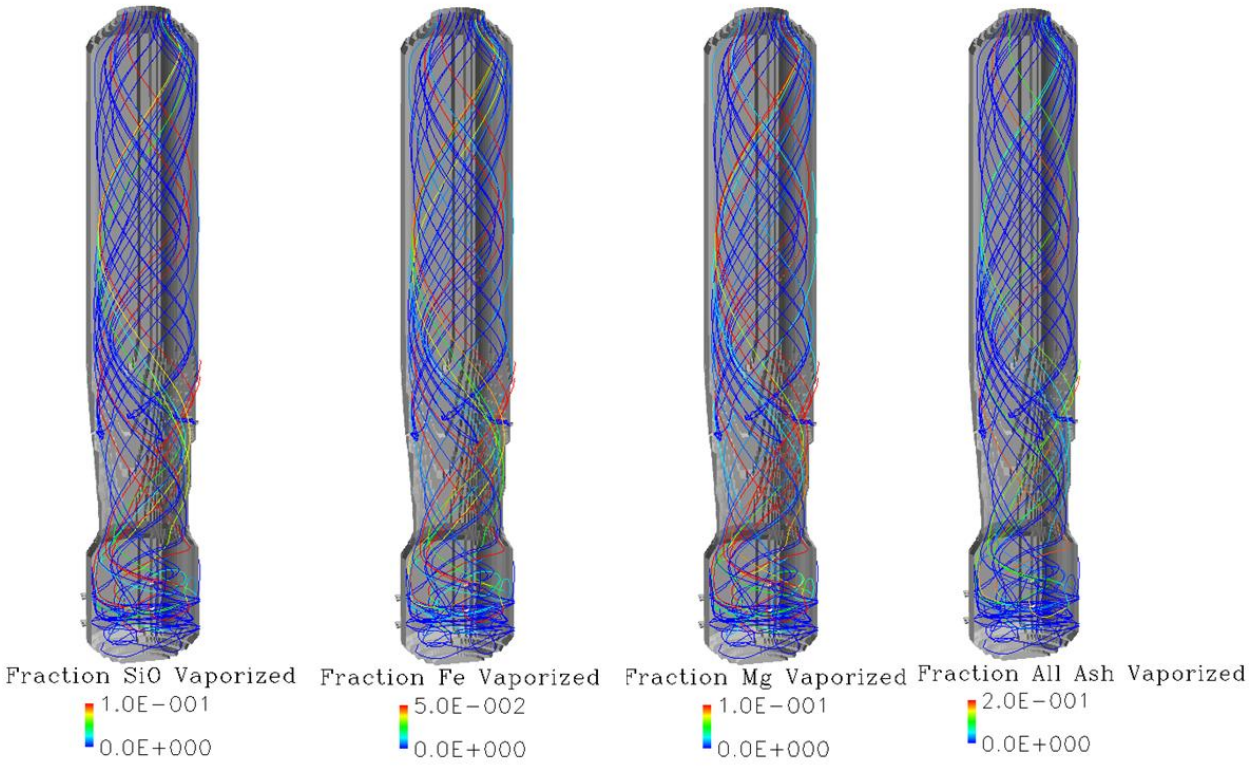

Figure 2.2.15. Ash vaporization in two-stage up-fired gasifier (25- 60 micron diameter particles).

For illustration purposes, shown in Figure 2.2.16 is a simpler version of the information contained in Figure 2.2.15. Shown in Figure 2.2.16 are the average ash vaporization (Si, Mg, Na, total) and average (bulk) particle temperature as a function of residence time in the two stage slurry feed gasifier for selected trajectories that correspond to particles with the lowest and highest amount of ash vaporization. The plots indicate that Fe, Si have noticeable higher vaporization rates than Mg, high temperatures result in more ash vaporization and that ash vaporization does not occur if the temperatures are too cold.

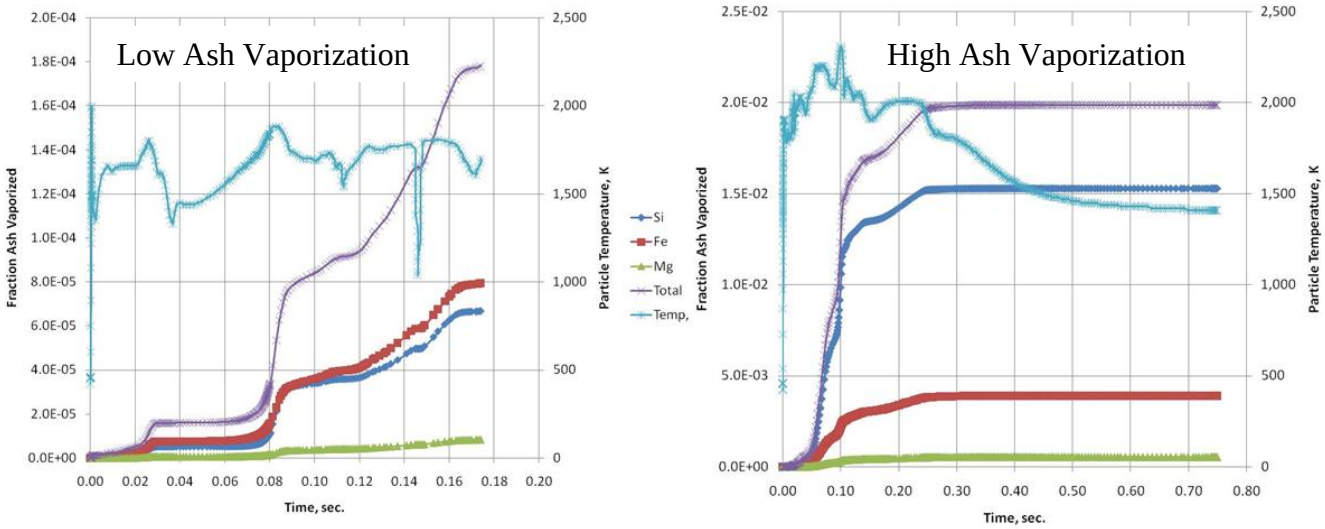

Figure 2.2.16. Ash vaporization in two-stage up-fired gasifier for particles with low ash vaporization (left plot) and high ash vaporization (right plot).

Illustrated in Figure 2.2.17 is a summary of the predicted ash vaporization within the different gasifiers investigated above. Shown are the mass fractions for vaporized ash (i.e., ratio of the mass of vaporized ash in syngas exiting the gasifier to the mass of incoming mass ash) for Si, Fe and Mg compounds in the coal ashes. In this comparison one should focus on the relative amounts of predicted vaporization rather than the values shown. The trends shown in the plot indicate that the dry feed gasifier will have a noticeably higher amount of vaporized ash in the syngas at the gasifier exit, due to the higher operating temperatures that occur in a dry feed gasifier. In addition, the results indicate that Si will be the largest contributor to the amount of vaporized ash.

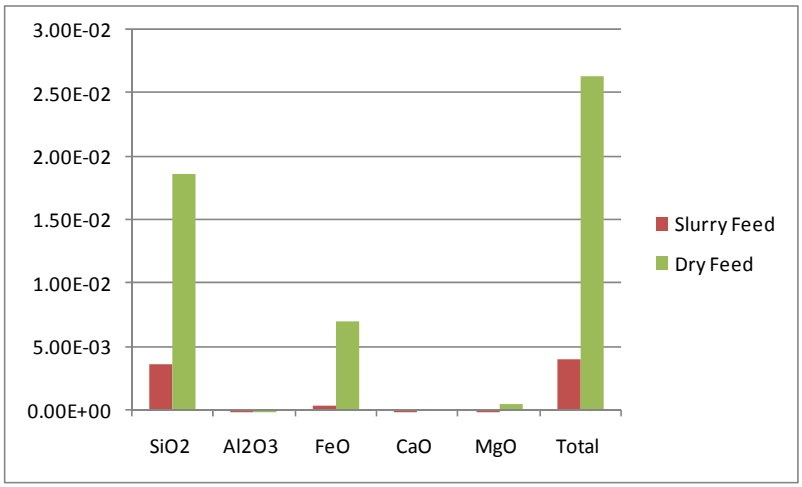

Figure 2.2.17. Predicted ash vaporization (mass fraction) for slurry feed and dry feed entrained flow gasifiers.

Summary

The above results highlight the information that can be obtained from a model for ash vaporization that can be implemented into coal gasifier models. The computed values provide insights into the impact on vaporized ash exiting the gasifier due to changes in gasifier operation and/or design. Although the calculations were performed for generic configurations of commercially available entrained flow gasifiers, the results indicate that gasifiers with (locally) higher operating temperatures will have a higher amount of vaporized ash in the syngas exiting the gasifier. The vaporized ash could potentially cause operational problems for equipment downstream of the gasifier.

2.3 CAPE-Open Versions of Selected REI process models

In the following are described example calculations performed using COM-CAPE-Open versions of the REI One and Two Stage Entrained Flow Gasifier Process Models and the REI Carbon Bed Process Model.

The REI Entrained Flow Gasifier Process Model can be run in either design mode or specified geometry mode. In addition, it can perform as a one or a two stage gasifier. To determine the particular NETL needs, the gasifier operation mode in the NETL IGCC flowsheets was examined, and it was decided that REI should provide a one stage gasifier model configured to run in design mode with 100% burnout because this model would be a direct replacement for the gasifier used in IGCC flowsheet. The two stage gasifier model has also been delivered to NETL and is also discussed below.

2.3.1 REI Entrained Flow Gasifier Process Model (One Stage Gasifier)

REI initially implemented the one stage gasifier model as a CORBA-CAPE-Open APECS model, and later ported it to COM-CAPE-Open for compatibility with next-generation releases of APECS. Illustrated in Figure 2.3.1 is a portion of an IGCC flowsheet modified to use the REI Entrained Flow Gasifier Process Model.

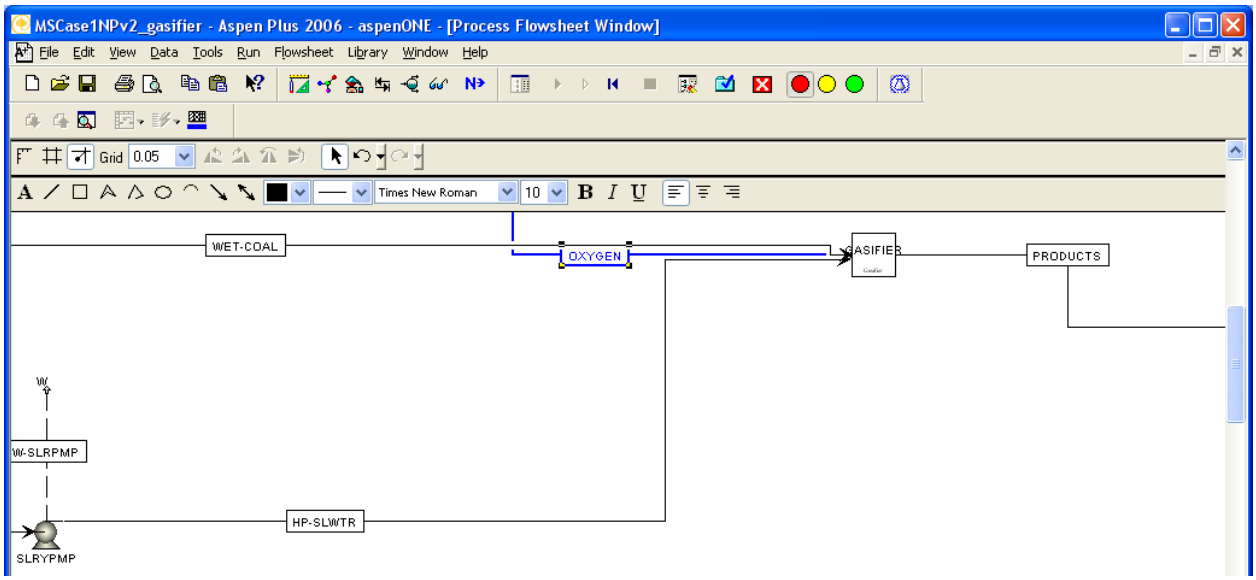

Figure 2.3.1. Gasifier in IGCC flowsheet.

In Figure 2.3.1, the original names for the streams have been retained:

- the OXYGEN stream provides oxygen;
- the WET-COAL stream provides dry coal (note that the stream name does not properly describe the information contained in the stream);
- HP-SLWTR provides water for the coal slurry; and
- the PRODUCTS stream contains syngas - a product of the gasifier.

The input parameters for the gasifier model that must be entered by the user are the pressure drop across the gasifier and the coal particle size distribution. All other parameters for the model (e.g. coal chemical composition) are obtained from the input streams in the flowsheet. The AspenPlus user interface is used to specify the input parameters (see Figure 2.3.2).

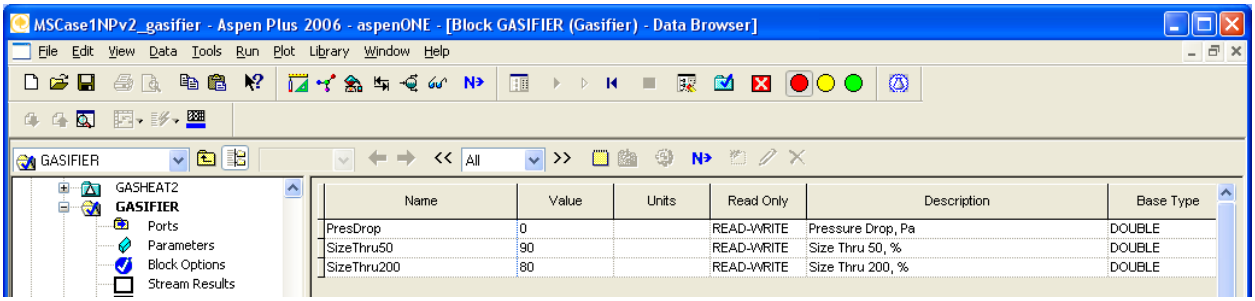

Figure 2.3.2. Example of using AspenPlus COM interface to specify inputs for REI Entrained Flow Gasifier Process Model.

There is an issue with the gasifier model running in AspenPlus, as with all other REI models implemented using calculator blocks. AspenPlus produces a warning message about the mass balance being broken around the gasifier block. This happens solely due to the fact that this mass balance computation happens before the downstream calculator block has a chance to return gasifier model results to AspenPlus. This warning should be ignored.

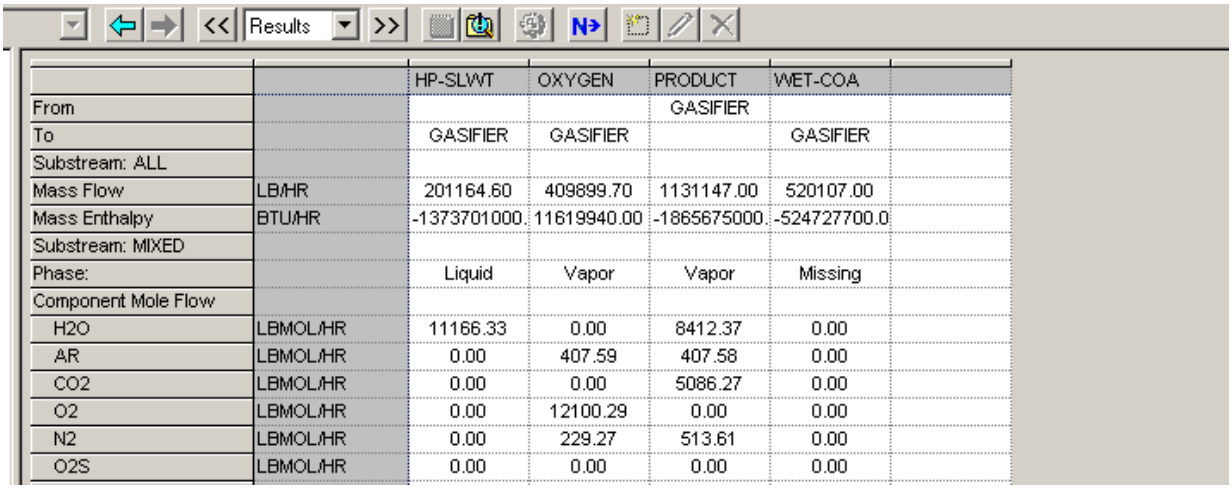

		HP-SLWT	OXYGEN	PRODUCT	WET-COA
From				GASIFIER	
To		GASIFIER	GASIFIER		GASIFIER
Substream: ALL					
Mass Flow	LB/HR	201164.60	409899.70	1131147.00	520107.00
Mass Enthalpy	BTU/HR	-1373701000.	11619940.00	-1865675000.	-524727700.0
Substream: MIXED					
Phase:		Liquid	Vapor	Vapor	Missing
Component Mole Flow					
H2O	LBMOL/HR	11166.33	0.00	8412.37	0.00
AR	LBMOL/HR	0.00	407.59	407.58	0.00
CO2	LBMOL/HR	0.00	0.00	5086.27	0.00
O2	LBMOL/HR	0.00	12100.29	0.00	0.00
N2	LBMOL/HR	0.00	229.27	513.61	0.00
O2S	LBMOL/HR	0.00	0.00	0.00	0.00

Figure 2.3.3. Example results from REI Entrained Flow Gasifier Process Model as displayed from the PRODUCTS stream within AspenPlus.

After model execution, the results are placed in the RESULT stream. The results are the properties of the syngas produced by the gasifier (e.g., syngas temperature, syngas composition) and can be viewed using standard procedures available in AspenPlus for viewing stream information (see Figure 2.3.3).

To use the REI Entrained Flow Gasifier Process Model in the AspenPlus IGCC flowsheet obtained from NETL, several modules (equipment models) in the flowsheet to represent the gasifier, and some convergence loops had to be disabled for the flowsheet to run without errors; some of the changes were required even though the REI model did not appear to influence the problematic loops. Given all these modifications, the IGCC flowsheet has been run and the results are illustrated in Figure 2.3.4.

3	**Gross Plant Power Output**			**Initial**	**diff.**
4	Gas Turbine Gross Power	513,380	kW_e	463940	-49,440
5	Sweet Gas Expander Gross Power	8,410	kW_e	8340	-70
6	Steam Turbine Gross Power	326,060	kW_e	300470	-25,590
7	**Total**	**847,850**	kW_e	772750	-75,100
8	**Auxiliary Load**				0
9	Coal Handling	670	kW_e	630	-40
10	Coal Milling	1,360	kW_e	1280	-80
11	Coal Slurry Pumps	450	kW_e	420	-30
12	Slag Handling and Dewatering	300	kW_e	280	-20
13	Air Separation Unit Auxiliaries	2,000	kW_e	2000	0
14	ASU Main Air Compressor	63,760	kW_e	59610	-4,150
15	Oxygen Compressor	12,250	kW_e	11530	-720
16	Nitrogen Compressor	30,025	kW_e	22803	-7,222
17	Sulfur Removal	3,146	kW_e	2962	-184
18	Tail Gas Recycle Compressor	910	kW_e	1070	160
19	Boiler Feedwater Pumps	5,690	kW_e	4880	-810
20	Condensate Pumps	270	kW_e	250	-20
21	Flash Bottoms Pump	200	kW_e	200	0
22	Circulating Water Pump	3,580	kW_e	3290	-290
23	Cooling Tower Fans	1,790	kW_e	1650	-140
24	Gas Turbine Auxiliaries	2,310	kW_e	2105	-205
25	Steam Turbine Auxiliaries	1,155	kW_e	1053	-102
26	Claus Plant Auxiliaries	231	kW_e	211	-20
27	Miscellaneous Balance-of-Plant	3,465	kW_e	3158	-307
28	Transformer Losses	2,470	kW_e	2250	-220
29	**Total**	136,032	kW_e	121632	-14,400
30	**Net Plant Performance**				0
31	Auxiliary Load	136,032	kW_e	121632	-14,400
32	Net Plant Power	711,818	kW_e	651118	-60,700
33	Net Plant Efficiency (HHV)	40.03%		38.89%	-1.14%
34	Net Plant Heat Rate (HHV)	8,524	Btu/kWhr	8774	250
35	Coal Feed Flowrate	520,107	lb/hr	489685	-30,422
36	Thermal Input[1]	1,778,229	kW_{th}	1674216	-104,013
37	Oxygen Flowrate	375,497	lb/hr	416677	41,180
38	Condenser Duty	1,610	MMBtu/hr	1480	-130

Figure 2.3.4. Example results of the IGCC flowsheet run with REI One Stage Entrained Flow Gasifier Process Model replacing the default gasifier.

2.3.2 REI Entrained Flow Gasifier Process Model (Two Stage Gasifier)

REI has also ported the REI Entrained Flow Gasifier Process Model for a two stage gasifier to the COM-CAPE-Open standard. Internally, both models are based on the same code, but they require a different number of input and output ports. Thus it was decided to create separate models for each gasifier to simplify usage with CAPE-Open.

Illustrated in Figure 2.3.5 is a portion of IGCC flowsheet modified to use this REI gasifier model. As per the one stage gasifier model, calculator blocks are employed to perform data exchange between the model and AspenPlus sub-streams.

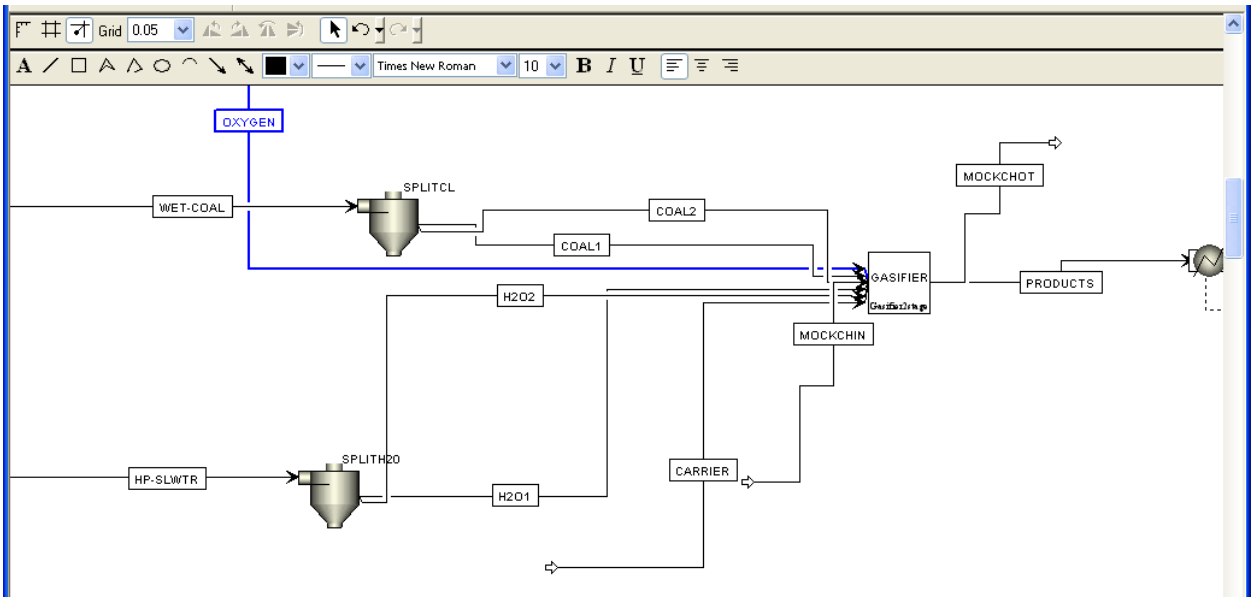

Figure 2.3.5. REI Two Stage Entrained Flow Gasifier Process Model in IGCC flowsheet.

The two stage gasifier requires the same inputs (ports) as the one stage gasifier. In addition the two stage gasifier has the following ports:

- Atomizing (or carrier) gas (Nitrogen) inlet for 2nd stage
- 2nd stage dry coal inlet
- 2nd stage water inlet
- Recycled char inlet
- Char outlet

Usually the coal slurry split is 90% to Stage One and 10% Stage Two. To incorporate the two stage gasifier model into the existing IGCC flowsheet two splitter blocks were used (SPLITCL and SPLITH2O) to split the coal and water streams in 90% - 10% portions. The second stage also requires atomizing gas for the slurry fuel injectors (for dry feed this would be carrier gas) which is assumed to be nitrogen. The flowrate is usually the same as the flowrate of dry coal entering second stage. Hence, this amount of nitrogen is supplied through the carrier inlet port. However, because this flowsheet has been created mostly to illustrate model use, a source for the nitrogen production is not included in the IGCC flowsheet.

Currently, the model is set up to run with 100% burnout, but burnout is a user parameter in this model. If burnout is not 100%, some unburned product in form of char would be produced. However, since current flowsheet has no support for char (no "char" variable), the char produced in this case will not be included in flowsheet computations. If there is a support for char in the flowsheet, then produced char can be accounted for and recycled either by feeding it back to gasifier through corresponding recycled char port, or by some other means. Calculator blocks responsible for data transfer between model and Aspen sub-streams would have to be modified accordingly. Char ports have been created for this model, but currently they don't accept or produce any flow, and streams connected to them are just mock-up streams with zero flowrates.

The model is set up to run with 100% burnout, but burnout is a user parameter in this model. If the burnout is not 100%, some unburned product in the form of char would be produced. Unfortunately the NETL IGCC flowsheets have no support for char (no "char" variable) and thus the char produced would not be included in the flowsheet computations. If there were support for the char stream in the flowsheet, then the char could be accounted for and recycled either by feeding it back to the gasifier through a corresponding char recycle port, or by some other means. Calculator blocks responsible for the data transfer between the model and AspenPlus sub-streams would have to be modified accordingly. Char ports have been created for this model, but currently they cannot receive or produce any flow and streams connected to the char ports are just mock-up streams with zero flow rates.

As noted above, burnout is the only extra user specified parameter for the two stage gasifier. Also, given the similarities of the implementation of the one and two stage gasifier models, all the issues discussed for the one stage model are applicable to the two stage model as well.

To incorporate the REI Two Stage Entrained Flow Gasifier Process Model into the AspenPlus IGCC flowsheet obtained from NETL required modifications to the flowsheet similar to those described for the one stage gasifier model (e.g., disabling certain convergence loops). The IGCC flowsheet has been run using the model and the results are presented in Figure 2.3.6.

Gross Plant Power Output			**Initial**	**diff.**
Gas Turbine Gross Power	518,710	kW_e	463940	-54,770
Sweet Gas Expander Gross Power	8,660	kW_e	8340	-320
Steam Turbine Gross Power	313,230	kW_e	300470	-12,760
Total	**840,600**	kW_e	772750	-67,850
Auxiliary Load				0
Coal Handling	670	kW_e	630	-40
Coal Milling	1,360	kW_e	1280	-80
Coal Slurry Pumps	450	kW_e	420	-30
Slag Handling and Dewatering	300	kW_e	280	-20
Air Separation Unit Auxiliaries	2,000	kW_e	2000	0
ASU Main Air Compressor	63,760	kW_e	59610	-4,150
Oxygen Compressor	12,250	kW_e	11530	-720
Nitrogen Compressor	31,377	kW_e	22803	-8,574
Sulfur Removal	3,146	kW_e	2962	-184
Tail Gas Recycle Compressor	910	kW_e	1070	160
Boiler Feedwater Pumps	5,560	kW_e	4880	-680
Condensate Pumps	260	kW_e	250	-10
Flash Bottoms Pump	200	kW_e	200	0
Circulating Water Pump	3,420	kW_e	3290	-130
Cooling Tower Fans	1,710	kW_e	1650	-60
Gas Turbine Auxiliaries	2,290	kW_e	2105	-185
Steam Turbine Auxiliaries	1,145	kW_e	1053	-92
Claus Plant Auxiliaries	229	kW_e	211	-18
Miscellaneous Balance-of-Plant	3,436	kW_e	3158	-278
Transformer Losses	2,450	kW_e	2250	-200
Total	136,923	kW_e	121632	-15,291
Net Plant Performance				0
Auxiliary Load	136,923	kW_e	121632	-15,291
Net Plant Power	703,677	kW_e	651118	-52,559
Net Plant Efficiency (HHV)	39.57%		38.89%	-0.68%
Net Plant Heat Rate (HHV)	8,623	Btu/kWhr	8774	151
Coal Feed Flowrate	520,107	lb/hr	489685	-30,422
Thermal Input[1]	1,778,229	kW_{th}	1674216	-104,013
Oxygen Flowrate	416,053	lb/hr	416677	624
Condenser Duty	1,540	MMBtu/hr	1480	-60

Figure 2.3.6. Results of IGCC flowsheet with REI Two Stage Entrained Flow Gasifier Process Model and OTM ASU model.

2.3.3 REI Carbon Bed Model

Another process model REI implemented in the COM-CAPE-Open standard is the Carbon Bed model. Model details can be found at [Bockelie et al, 2004]. In AspenPlus, the model operates on conventional streams and thus stream class changes would have to be used if the model is to be used in the AspenPlus IGCC flowsheets obtained from NETL.

The model works as a separator, removing a predefined amount (99%) of Hg and HgCl2 from the input stream and placing it in the output stream. The rest of input gas is placed in the output stream. The model also computes design parameters for the carbon bed. Figure 2.3.7 shows the Carbon Bed model parameters in AspenPlus.

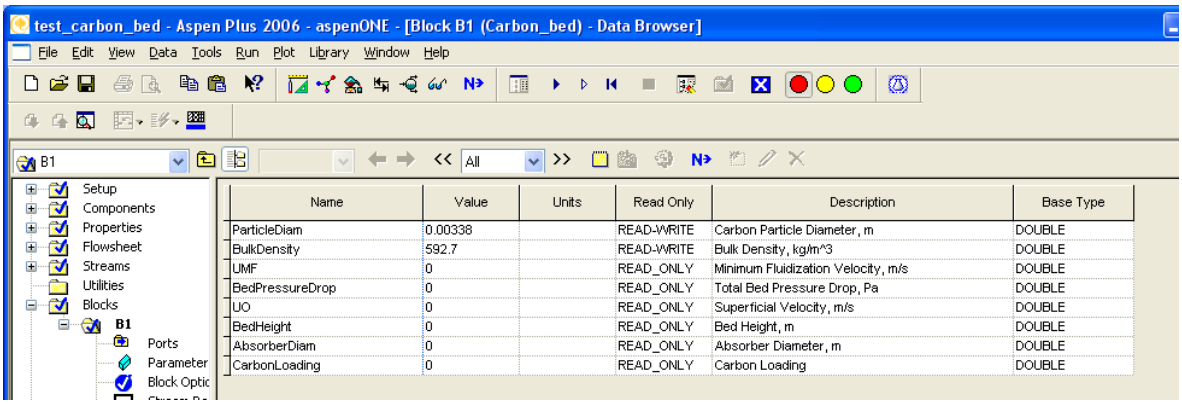

Figure 2.3.7. REI Carbon Bed model parameters in AspenPlus.

2.4 Implement CAPE-Open Versions of ASU Models

In the following are described example calculations performed with the NETL AspenPlus IGCC flowsheets using the detailed ASU models provided by Praxair, a project team member, for use in this project. Further details on the cryogenic ASU model and the OTM ASU models are provided in Chapter 1 (see discussion for Task 2.3 in Section 1.2.3).

2.4.1 Example calculations with NETL IGCC flowsheet using detailed cryogenic ASU model

The example calculations use information from the AspenPlus IGCC flow sheets obtained from NETL (see discussion for Task 3 in Section 1.3 of Chapter 1 and Figure 2.1.1 and Figure 2.1.2). NETL has provided REI with "public versions" of the flowsheets. Two of the networks (called Case 1 and Case 2) use a slurry feed gasifier. Case 1 is a conventional IGCC without CO_2 capture and Case 2 involves CO_2 capture. Example calculations are provided with both plant configurations. The computations were performed with AspenPlus 2006. The detailed ASU model was implemented into the AspenPlus IGCC flowsheets using the procedure described in Chapter 1 (see discussion for Task 2.3 in Section 1.2.3).

Results
Illustrated in Figure 2.4.1 and Figure 2.4.2 are, respectively, comparisons of the overall plant performance predicted with the original IGCC flowsheet and the modified IGCC flowsheet that employs the detailed ASU model for Case 1 and Case 2. Shown is a snapshot of a spreadsheet window containing a table that summarizes the differences for the Gross Plant Power Output, Auxiliary Load and Net Plant Performance. Under the heading of Auxiliary Load, several equipment operations and processes are listed that highlight different parasitic load losses. The columns labeled NETL, REI and DIFFERENCE are the predicted values for the IGCC flowsheet with the original ASU model, the IGCC flowsheet with the detailed ASU model, and the difference between the two predicted values (Difference = REI value – NETL value), respectively.

From Figure 2.4.1 and Figure 2.4.2 it can be seen that the two ASU models predict about the same overall plant performance for these conditions. Small differences are predicted for the power consumption for the Air and Nitrogen compressors and power generated by the steam turbine. The differences in the predicted overall plant efficiency (differences in the fourth significant digit) are within the error tolerances of the models and should be ignored.

Comments
1. Performing the flowsheet calculations described above highlighted the need to use care when initializing the detailed ASU model. The model is not overly robust. The iteration loop used within the model requires good initial estimates to obtain convergence.
2. The detailed ASU is not capable of modeling air streams with significant amounts of water. It is necessary to separate the incoming water such that there are only trace amounts entering the ASU unit.

3. The convergence criteria for the NETL AspenPlus IGCC spreadsheets as provided was prescribed ("hardwired") in the flowsheet to too small a value. To converge the model, the desired flow rate the tolerances for selected streams had to be adjusted.
4. The procedure for performing flowsheet simulations using the detailed ASU model provided in Chapter 1 (see Task 2.3) should be followed.

	A	B	C	D	E	F	G
1							
2	**MSCase1NPv2**						
3	**Gross Plant Power Output**			**NETL**	**REI**	**DIFFERENCE**	
4	Gas Turbine Gross Power	463,940	kW,	463,940	463,940	0	kW,
5	Sweet Gas Expander Gross Power	8,340	kW,	8,340	8,340	0	kW,
6	Steam Turbine Gross Power	300,510	kW,	300,470	300,510	40	kW,
7	**Total**	**772,790**	kW,	**772,750**	**772,790**	40	kW,
8	**Auxiliary Load**					0	
9	Coal Handling	630	kW,	630	630	0	kW,
10	Coal Milling	1,280	kW,	1,280	1,280	0	kW,
11	Coal Slurry Pumps	420	kW,	420	420	0	kW,
12	Slag Handling and Dewatering	280	kW,	280	280	0	kW,
13	Air Separation Unit Auxiliaries	2,000	kW,	2,000	2,000	0	kW,
14	ASU Main Air Compressor	59,080	kW,	59,610	59,080	-530	kW,
15	Oxygen Compressor	11,530	kW,	11,530	11,530	0	kW,
16	Nitrogen Compressor	22,258	kW,	22,803	22,258	-545	kW,
17	Sulfur Removal	2,962	kW,	2,962	2,962	0	kW,
18	Tail Gas Recycle Compressor	1,070	kW,	1,070	1,070	0	kW,
19	Boiler Feedwater Pumps	4,890	kW,	4,880	4,890	10	kW,
20	Condensate Pumps	250	kW,	250	250	0	kW,
21	Flash Bottoms Pump	200	kW,	200	200	0	kW,
22	Circulating Water Pump	3,290	kW,	3,290	3,290	0	kW,
23	Cooling Tower Fans	1,650	kW,	1,650	1,650	0	kW,
24	Gas Turbine Auxiliaries	2,106	kW,	2,105	2,106	1	kW,
25	Steam Turbine Auxiliaries	1,053	kW,	1,053	1,053	0	kW,
26	Claus Plant Auxiliaries	211	kW,	211	211	0	kW,
27	Miscellaneous Balance-of-Plant	3,158	kW,	3,158	3,158	0	kW,
28	Transformer Losses	2,250	kW,	2,250	2,250	0	kW,
29	**Total**	120,567	kW,	121,632	120,567	-1,065	kW,
30	**Net Plant Performance**					0	
31	Auxiliary Load	120,567	kW,	121,632	120,567	-1,065	kW,
32	Net Plant Power	652,223	kW,	651,118	652,223	1,105	kW,
33	Net Plant Efficiency (HHV)	38.96%		38.89%	38.96%	0	
34	Net Plant Heat Rate (HHV)	8,759	Btu/kWhr	8,774	8,759	-15	Btu/kWhr
35	Coal Feed Flowrate	489,685	lb/hr	489,685	489,685	0	lb/hr
36	Thermal Input[1]	1,674,216	kW_{th}	1,674,216	1,674,216	0	kW_{th}
37	Oxygen Flowrate	416,180	lb/hr	416,677	416,180	-497	lb/hr
38	Condenser Duty	1,480	MMBtu/hr	1,480	1,480	0	MMBtu/hr

Figure 2.4.1. Results of Case 1.

	A	B	C	D	E	F	G
1							
2	MSCase2NPv2						
3	**Gross Plant Power Output**			**NETL**	**REI**	**DIFFERENCE**	
4	Gas Turbine Gross Power	464,020	kW,	464020	464,020	0	kWe
5	Sweet Gas Expander Gross Power	8,010	kW,	8010	8,010	0	kWe
6	Steam Turbine Gross Power	266,850	kW,	266860	266,850	10	kWe
7	**Total**	**738,880**	kW,	**738890**	**738,880**	**10**	kWe
8	**Auxiliary Load**						
9	Coal Handling	650	kW,	650	650	0	kWe
10	Coal Milling	1,320	kW,	1320	1,320	0	kWe
11	Coal Slurry Pumps	440	kW,	440	440	0	kWe
12	Slag Handling and Dewatering	290	kW,	290	290	0	kWe
13	Air Separation Unit Auxiliaries	2,000	kW,	2000	2,000	0	kWe
14	ASU Main Air Compressor	72,140	kW,	72760	72,140	620	kWe
15	Oxygen Compressor	11,030	kW,	11030	11,030	0	kWe
16	Nitrogen Compressor	28,373	kW,	28373	28,373	0	kWe
17	Sulfur Removal	3,057	kW,	3057	3,057	0	kWe
18	Tail Gas Recycle Compressor	1,030	kW,	1030	1,030	0	kWe
19	Boiler Feedwater Pumps	4,880	kW,	4880	4,880	0	kWe
20	Condensate Pumps	260	kW,	260	260	0	kWe
21	Flash Bottoms Pump	200	kW,	200	200	0	kWe
22	Circulating Water Pump	2,850	kW,	2850	2,850	0	kWe
23	Cooling Tower Fans	1,420	kW,	1420	1,420	0	kWe
24	Gas Turbine Auxiliaries	2,013	kW,	2013	2,013	0	kWe
25	Steam Turbine Auxiliaries	1,007	kW,	1007	1,007	0	kWe
26	Claus Plant Auxiliaries	201	kW,	201	201	0	kWe
27	Miscellaneous Balance-of-Plant	3,020	kW,	3020	3,020	0	kWe
28	Transformer Losses	2,160	kW,	2160	2,160	0	kWe
29	**Total**	138,341	kW,	138960	138,341	619	kWe
30	**Net Plant Performance**						
31	Auxiliary Load	138,341	kW,	138960	138,341	619	kWe
32	Net Plant Power	600,539	kW,	599930	600,539	-609	kWe
33	Net Plant Efficiency (HHV)	34.76%		34.72	34.76	0.02	PERCENT
34	Net Plant Heat Rate (HHV)	9,817	Btu/kWhr	9827	9,817	10	Btu/kWhr
35	Coal Feed Flowrate	505,381	lb/hr	505381	505,381	0	lb/hr
36	Thermal Input[1]	1,727,882	kW_{th}	1727883	1,727,882	1	kWth
37	Oxygen Flowrate	429,948	lb/hr	429948	429,948	0	lb/hr
38	Condenser Duty	1,280	MMBtu/hr	1280	1,280	0	MMBtu/hr

Figure 2.4.2. Results of Case 2

2.4.2. Example Calculations With NETL IGCC Flowsheet Using OTM ASU Model

In the following are provided example calculations performed using the OTM ASU model in the AspenPlus IGCC flowsheets obtained from NETL. As per our experience with implementing other models into the AspenPlus IGCC flowsheet, some modifications to the flowsheet were required to obtain a converged solution (e.g., disabling convergence loops).

Results
Several test cases have been implemented by REI with different combinations of REI models included in the AspenPlus IGCC flowsheets: only OTM, OTM and ROM, OTM and 2-stage gasifier, etc. Here we present results with the OTM model incorporated in the IGCC flowsheet.

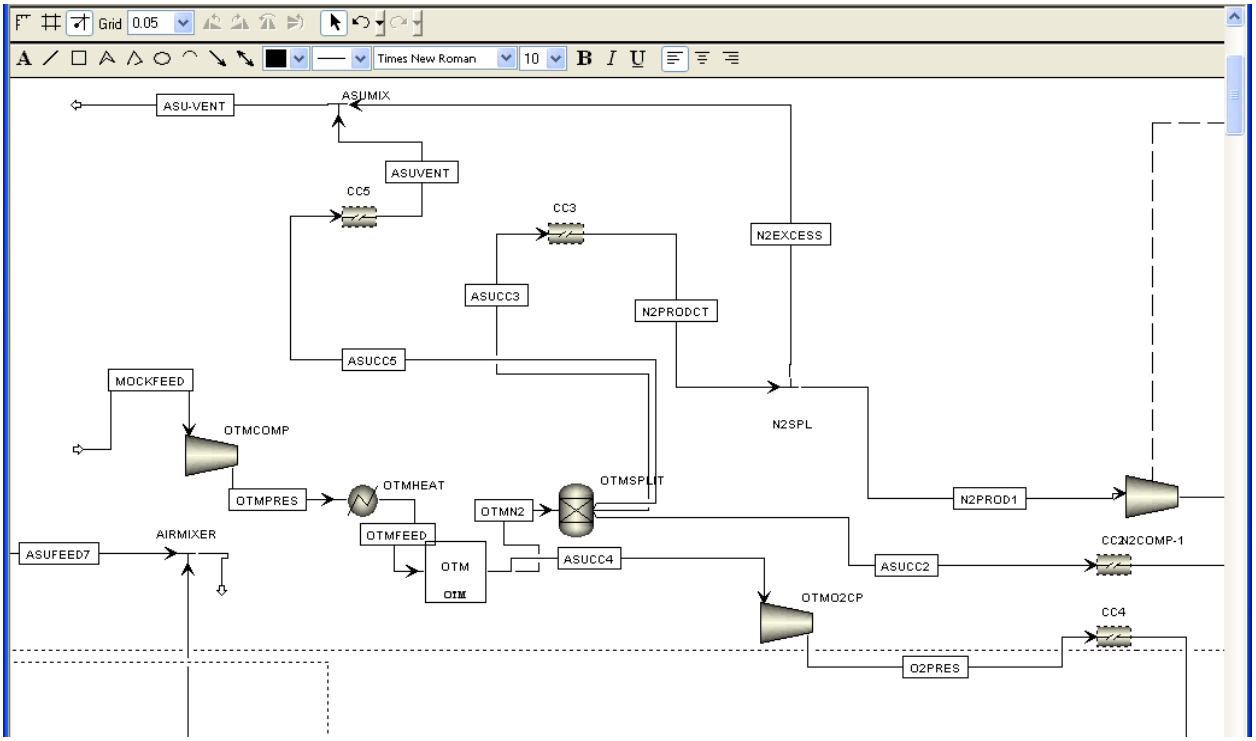

Figure 2.4.3. OTM model with COM-based CAPE-Open interace implemented in NETL AspenPlus IGCC flowsheet.

Figure 2.4.3 shows a portion of the AspenPlus IGCC flowsheet with the OTM model used in place of the ASU model which was originally used in the flowsheet. Several operations had to be performed in this flowsheet by REI to make the OTM model operational. These include:

- the OTM model can only use simple streams of type MIXED; hence stream class changers (CC1-CC5 in Figure 2.4.3) had to be used to eliminate empty SOLID and NC (non-conventional) sub-streams on entry to OTM and add them back after OTM exit;
- the air supply circuit to the ASU has been left in the flowsheet to keep other flowsheet components, like convergence loops, intact;

- the previous ASU model was cryogenic but the OTM model requires the air to be preheated and pressurized, which was accomplished by incorporating blocks OTMCOMP and OTMHEAT;
- the feed stream to the OTM had to be broken into two streams with the MOCKFEED stream now having a prescribed inlet flow rate and air composition for the OTM (obtained from the input to the original ASU) to avoid convergence errors;
- the OTM model has only two outputs: an oxygen (product) stream and a waste stream; extra components such as OTMSPLIT and OTMO2CP have been added to split the waste stream to work with existing streams in the flowsheet and to bring oxygen pressure to the same level present in the product stream of the old ASU model used;
- the OTM model has been incorporated into the flowsheet for illustrative purposes only; power requirements for all additional units added to make the modified flowsheet work (e.g., OTMCOMP) have been left unaccounted for, but could be included in the total energy balance if the flowsheet is (extensively) redesigned specifically for OTM model use; such modifications are out-of-scope with the current project. .

The IGCC flowsheet with the OTM model has been run, and its results are presented in Figure 2.4.4. Except for the ASU main air compressor power requirements, there is no siginficant change in IGCC plant performance; this power requirement change is due to shortcommings of the manner in which the OTM model has been used in the flowsheet.

				Initial	diff.
3	**Gross Plant Power Output**				
4	Gas Turbine Gross Power	463,940	kW_e	463940	0
5	Sweet Gas Expander Gross Power	8,340	kW_e	8340	0
6	Steam Turbine Gross Power	300,480	kW_e	300470	-10
7	**Total**	**772,760**	kW_e	772750	-10
8	**Auxiliary Load**				0
9	Coal Handling	630	kW_e	630	0
10	Coal Milling	1,280	kW_e	1280	0
11	Coal Slurry Pumps	420	kW_e	420	0
12	Slag Handling and Dewatering	280	kW_e	280	0
13	Air Separation Unit Auxiliaries	2,000	kW_e	2000	0
14	ASU Main Air Compressor	42,860	kW_e	59610	16,750
15	Oxygen Compressor	11,530	kW_e	11530	0
16	Nitrogen Compressor	22,801	kW_e	22803	2
17	Sulfur Removal	2,962	kW_e	2962	0
18	Tail Gas Recycle Compressor	1,070	kW_e	1070	0
19	Boiler Feedwater Pumps	4,880	kW_e	4880	0
20	Condensate Pumps	250	kW_e	250	0
21	Flash Bottoms Pump	200	kW_e	200	0
22	Circulating Water Pump	3,290	kW_e	3290	0
23	Cooling Tower Fans	1,650	kW_e	1650	0
24	Gas Turbine Auxiliaries	2,105	kW_e	2105	0
25	Steam Turbine Auxiliaries	1,053	kW_e	1053	0
26	Claus Plant Auxiliaries	211	kW_e	211	0
27	Miscellaneous Balance-of-Plant	3,158	kW_e	3158	0
28	Transformer Losses	2,250	kW_e	2250	0
29	**Total**	104,880	kW_e	121632	16,752
30	**Net Plant Performance**				0
31	Auxiliary Load	104,880	kW_e	121632	16,752
32	Net Plant Power	667,880	kW_e	651118	-16,762
33	Net Plant Efficiency (HHV)	39.89%		38.89%	-1%
34	Net Plant Heat Rate (HHV)	8,554	Btu/kWhr	8774	220
35	Coal Feed Flowrate	489,690	lb/hr	489685	-5
36	Thermal Input[1]	1,674,234	kW_{th}	1674216	-18
37	Oxygen Flowrate	416,708	lb/hr	416677	-31
38	Condenser Duty	1,480	MMBtu/hr	1480	0

Figure 2.4.4. Results of IGCC flowsheet with COM-based CAPE-Open OTM model used.

2.5 Automated Reduced Order Models

REI used data obtained from the REI One Stage Entrained Flow Gasifier Process Model to develop and test the ROM engine. The ROM engine works in two steps.

1. The ROM is created. That is, the neural network based ROM engine has to be trained. This stage is performed off-line from AspenPlus. A stand-alone ROM creation utility reads training data from a text file and creates a neural network, which is saved for future use. Note that REI has created four neural networks, based on four different solid fuel types (see discussion for Task 2.4 in Section 1.2.4).
2. The neural network created in step 1 is loaded for the ROM computation (evaluation) in AspenPlus. Given that data used for neural network training (both independent and dependent variables) is normalized to the interval [0,1], two more files containing minimum and maximum data values are required for ROM evaluation.

Because the ROM has been created based on REI gasifier data, this model implementation in IGCC flowsheet is similar to that of the gasifier models for which AspenPlus calculator blocks are used for the data transfer between the ROM and AspenPlus sub-streams. As with the gasifier models, the Intel FORTAN compiler is required for model operation. Also, mass balance warnings are produced by AspenPlus similar to those for gasifier model operation due to the use of the calculator blocks.

As shown in Figure 2.5.1, the only input parameter for the ROM is the coal type. If any input variables are out of range for the ROM then a fatal error is triggered.

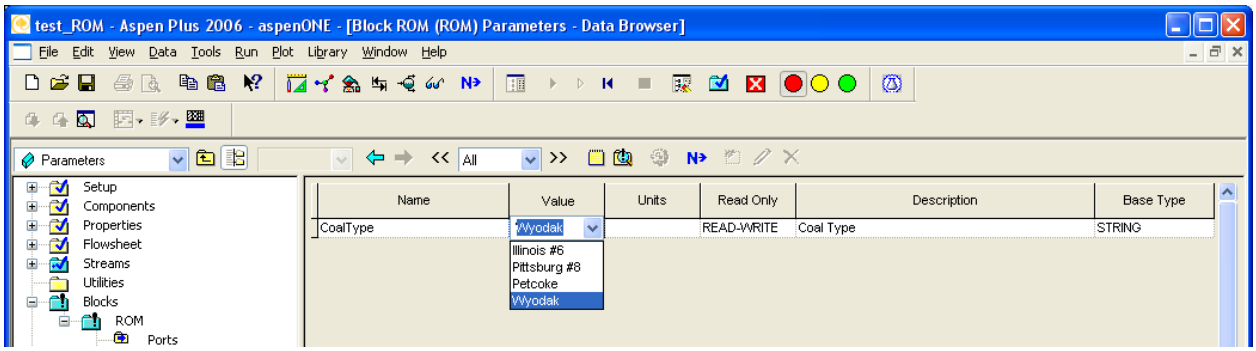

Figure 2.5.1. REI ROM input parameters with COM CAPE-Open interface.

After ROM execution, the output is placed in the output stream. REI has performed two calculations using ROM in the AspenPlus IGCC flowsheet: one uses the ROM in place of a gasifier and the second uses the OTM model in addition to the ROM. Results of flowsheet runs are shown in Figure 2.5.2 and Figure 2.5.3. As with all other model runs using the AspenPlus IGCC flowsheets, these are example calculations only.

Gross Plant Power Output			Initial	Diff.
Gas Turbine Gross Power	507,380	kW_e	463940	-43,440
Sweet Gas Expander Gross Power	8,310	kW_e	8340	30
Steam Turbine Gross Power	324,930	kW_e	300470	-24,460
Total	**840,620**	kW_e	772750	-67,870
Auxiliary Load				0
Coal Handling	670	kW_e	630	-40
Coal Milling	1,360	kW_e	1280	-80
Coal Slurry Pumps	450	kW_e	420	-30
Slag Handling and Dewatering	300	kW_e	280	-20
Air Separation Unit Auxiliaries	2,000	kW_e	2000	0
ASU Main Air Compressor	63,760	kW_e	59610	-4,150
Oxygen Compressor	12,250	kW_e	11530	-720
Nitrogen Compressor	29,631	kW_e	22803	-6,828
Sulfur Removal	3,146	kW_e	2962	-184
Tail Gas Recycle Compressor	900	kW_e	1070	170
Boiler Feedwater Pumps	5,660	kW_e	4880	-780
Condensate Pumps	270	kW_e	250	-20
Flash Bottoms Pump	200	kW_e	200	0
Circulating Water Pump	3,560	kW_e	3290	-270
Cooling Tower Fans	1,780	kW_e	1650	-130
Gas Turbine Auxiliaries	2,290	kW_e	2105	-185
Steam Turbine Auxiliaries	1,145	kW_e	1053	-92
Claus Plant Auxiliaries	229	kW_e	211	-18
Miscellaneous Balance-of-Plant	3,436	kW_e	3158	-278
Transformer Losses	2,450	kW_e	2250	-200
Total	135,487	kW_e	121632	-13,855
Net Plant Performance				0
Auxiliary Load	135,487	kW_e	121632	-13,855
Net Plant Power	705,133	kW_e	651118	-54,015
Net Plant Efficiency (HHV)	39.65%		38.89%	-0.76%
Net Plant Heat Rate (HHV)	8,605	Btu/kWhr	8774	169
Coal Feed Flowrate	520,107	lb/hr	489685	-30,422
Thermal Input[1]	1,778,229	kW_{th}	1674216	-104,013
Oxygen Flowrate	375,497	lb/hr	416677	41,180
Condenser Duty	1,600	MMBtu/hr	1480	-120

Figure 2.5.2. Results of calculations for replacing gasifier model with REI ROM in AspenPlus IGCC flowsheet.

Gross Plant Power Output			Initial	Diff.
Gas Turbine Gross Power	507,380	kW_e	463940	-43,440
Sweet Gas Expander Gross Power	8,310	kW_e	8340	30
Steam Turbine Gross Power	322,700	kW_e	300470	-22,230
Total	**838,390**	kW_e	772750	-65,640
Auxiliary Load				0
Coal Handling	670	kW_e	630	-40
Coal Milling	1,360	kW_e	1280	-80
Coal Slurry Pumps	450	kW_e	420	-30
Slag Handling and Dewatering	300	kW_e	280	-20
Air Separation Unit Auxiliaries	2,000	kW_e	2000	0
ASU Main Air Compressor	63,760	kW_e	59610	-4,150
Oxygen Compressor	12,250	kW_e	11530	-720
Nitrogen Compressor	31,377	kW_e	22803	-8,574
Sulfur Removal	3,146	kW_e	2962	-184
Tail Gas Recycle Compressor	900	kW_e	1070	170
Boiler Feedwater Pumps	5,660	kW_e	4880	-780
Condensate Pumps	270	kW_e	250	-20
Flash Bottoms Pump	200	kW_e	200	0
Circulating Water Pump	3,540	kW_e	3290	-250
Cooling Tower Fans	1,770	kW_e	1650	-120
Gas Turbine Auxiliaries	2,284	kW_e	2105	-179
Steam Turbine Auxiliaries	1,142	kW_e	1053	-89
Claus Plant Auxiliaries	228	kW_e	211	-17
Miscellaneous Balance-of-Plant	3,426	kW_e	3158	-268
Transformer Losses	2,450	kW_e	2250	-200
Total	137,184	kW_e	121632	-15,552
Net Plant Performance				0
Auxiliary Load	137,184	kW_e	121632	-15,552
Net Plant Power	701,206	kW_e	651118	-50,088
Net Plant Efficiency (HHV)	39.43%		38.89%	-0.54%
Net Plant Heat Rate (HHV)	8,653	Btu/kWhr	8774	121
Coal Feed Flowrate	520,107	lb/hr	489685	-30,422
Thermal Input[1]	1,778,229	kW_{th}	1674216	-104,013
Oxygen Flowrate	416,053	lb/hr	416677	624
Condenser Duty	1,590	MMBtu/hr	1480	-110

Figure 2.5.3 Results of calculations for replacing gasifier and ASU model with REI ROM and OTM models, respectively, in AspenPlus IGCC flowsheet.

2.6 Implement CAPE-Open compliant coupling between AspenPlus and selected GE GateCycle Models

As discussed in Chapter 1 (see Task 2.5), REI and Enginomix have implemented a COM-based CAPE-Open interface for the GE GateCycle 7FB model which allows using the 7FB model in AspenPlus/APECS flowsheet simulations.

Illustrated in Figure 2.6.1 are the model input and output parameters that can be accessed within AspenPlus. As previously discussed in Chapter 1, the 7FB model has an extensive list of inputs and outputs. Thus, by design, to keep the problem manageable most of the model parameters have been kept internal to the 7FB model and only the key model parameters are exposed to AspenPlus for use (i.e., input) by the user. Note that when the 7FB model is used within an AspenPlus IGCC flowsheet many of the model inputs (e.g., syngas flow rate and composition) are specified from existing streams within the flowsheet.

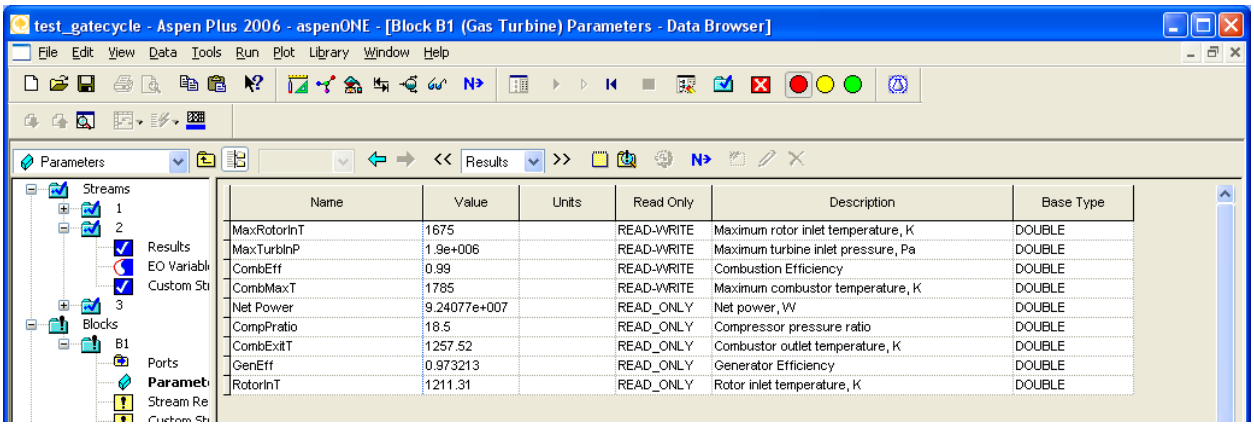

Figure 2.6.1. Parameters for GE GateCycle 7FB model displayed in AspenPlus.

Example calculations have been performed using the COM-Based CAPE-Open GateCycle 7FB model coupled to a simplified version of the AspenPlus IGCC flowsheet. Stream class changer blocks must be used to connect the model to the IGCC flowsheet to account for the different stream types used in the 7FB model and the IGCC flowsheets; the 7FB model uses conventional streams and the IGCC flowsheet allows for mixed class of streams. In addition, if species other than ones supported by the 7FB model (i.e., Ar, CO, CO2, H2, H2O, N2, O2, H2S, SO2, CH4) are present in the syngas they must be separated from the input stream and added back downstream of the 7FB model block.

One of the model output parameters is the net power of the turbine, which is accessible from AspenPlus, so that it can be included in a convergence loop and thus allowing the user to obtain the desired net power from the 7FB turbine by adjusting the incoming syngas and air flowrates.

Chapter 3. Conclusions

The modeling capability provided to NETL from this project by REI included VE-Suite based Virtual Engineering software and enhanced equipment models to support NETL's APECS framework for advanced power generation systems. Enhancements to the software framework facilitated a critical link between APECS and the virtual engineering capabilities provided by VE-Suite (e.g., equipment and process visualization, information assimilation). Model enhancements focused on improving predictions for the performance of entrained flow coal gasifiers – a key component to the advanced plant concepts – and important auxiliary equipment used in coal gasification systems. The models have been benchmarked against data in the literature, where available. COM-based CAPE-Open model interfaces have been employed where needed. The improved simulation capability has been demonstrated on selected test problems.

The project team included experts in gasification, CO2 capture issues, process simulation and representatives from technology developers and the electric utility industry. An Advisory Panel was formed to provide guidance to the project. To optimize the benefit to NETL, REI coordinated its efforts with NETL and NETL funded projects at Iowa State University (ISU), Carnegie Mellon University (CMU) and ANSYS/Fluent, Inc.

Specific accomplishments are summarized below.

- Provided to NETL (in coordination with ISU, NETL and ANSYS/Fluent) software to support VE-Suite communicating and interacting with AspenPlus/APECS. Specifically,
    - developed CASI, a C++ interfacing library for AspenPlus/APECS and
    - Modification to VE-Suite to support the VE-Suite-to-AspenPlus coupling.
- Provided to NETL the REI Entrained Flow Gasifier Process Models with a COM-based CAPE-Open interface. Improved sub-models for the entrained flow gasifier were developed and tested.
    - An enhanced sub-model for predicting the pressure dependence on the emissivity properties used in radiative heat transfer calculations in an entrained flow gasifier model has been described and tested. The sub-model provides a subtle, but important, improvement in the predictive capability of the model for addressing potential thermal damage of equipment surfaces that might occur within the gasifier (or other downstream equipment) due to operating at higher pressures than previous practice.
    - A sub-model that includes gasification reactant/product inhibition effects in the gasification rate for entrained flow gasifier models has been descried and tested. Calculations using the sub-model indicate that to increase carbon conversion, it is more effective to increase the operating temperature (e.g., stoichiometric ratio) rather than increasing the gasifier volume because of the inhibition by CO of gasification rates at high carbon conversion; the inhibition effects will complicate scale-up for higher pressure operation (e.g., CO2 capture ready plants); and the gasification rate due to moisture dominates the gasification rate due to CO2.
    - A sub-model to predict ash vaporization due to the high temperatures that exist in the gasifier. Calculations using the model provide insight on changes in gasifier

design and/or operation can impact the amount of vaporized ash in the syngas that could potentially deposit on surfaces in equipment downstream of the gasifier.

- Provided to NETL REI process models, with a COM-based CAPE-Open interface, for selected plant equipment.
- Provided to NETL detailed process models for a cryogenic ASU and an OTM ASU that were originally provided to REI for use in this project by Praxair, a project team member.
  - The Cryogenic ASU model was provided as a HYSYS model and thus re-implemented as a native AspenPlus model.
  - The OTM ASU model was provided to REI as an MS EXCEL model and thus was re-implemented using C++ and a COM-based CAPE-Open interface.
- Provided to NETL a standalone ROM generator based on FANN, a publicly available neural network library package. The ROM generator is "general purpose" and was demonstrated for datasets obtained from the REI Entrained Flow Gasifier model. The generated ROM includes a COM-based CAPE-Open interface.
- Provided to NETL a COM-based CAPE-Open coupling between GE GateCycle and APECS. The coupling was developed with assistance from Enginomix, a project team member. Example calculations have been performed for the 7FB gas turbine model that was developed under other DOE funding.
- Demonstration of the improved modeling capability using AspenPlus IGCC flowsheets for plant configurations with and without CO2 capture.

APECS represents an important step toward providing engineers and scientists with a fully integrated environment for performing power plant simulation and engineering. As such, NETL will benefit in several ways from the improved modeling capability developed in this project.

- The improved simulation capabilities incorporated into APECS will enable researchers and engineers to better understand the interactions of different equipment components, identify weaknesses and processes needing improvement and thereby allow more efficient, less expensive plants to be developed and brought on-line faster and in a more cost-effective manner.
- It provides DOE with a mechanism to enable and foster collaborations amongst a broad range of power plant researchers from universities, industry, or DOE, whether US or International based, to assist in the development and deployment of advanced power generation plants.
- Although this project focused on plant configurations for coal gasification, with little effort APECS can be extended to support other advanced power generation systems (e.g., USC, Oxy-combustion boiler development and CO_2 capture) for retrofits to existing plants or developing new plants.

List of Figures

List of Tables

References

Ahn,.D.H., Gibbs, B.M., Ko, K.H., Kim, J.J., "Gasification rate analysis of coal char with a pressurized drop furnace," Fuel Vol 81, pp. 539-546, 2001

Antoulas A.C., and Sorensen, DC, "Approximation of large-scale dynamical systems: an overview," Int. J. Appl. Math. Comput. Sci. 2001, Vol. 11, No. 5, pp. 1093-1121.

ARANZ, http://www.aranz.com/research/modelling/theory/rbffaq.html, 2008.

Bai Z, "Krylov subspace techniques for reduced-order modeling of large-scale dynamical systems," Applied Numerical Mathematics, Vol. 43, 2002, pp.9-44.

Barrett, W.M., Strunja-Yoshikawa, S., "Importing And Using Com-Based Co Compliant Unit Operations in USEPA Metal Finishing Pollution Prevention Tool", Proceedings of the 2007 AIChE Meeting, Salt Lake City, Utah, November 4-9, 2007.
See also: http://www.epa.gov/nrmrl/std/mtb/p2tools/cape.htm

Bender, E., "An Equation of state for predicting vapour-liquid equilibria of the system N2-Ar-O2", Cryogenics, pp. 11-18, January, 1973.

Bender, E., "Equations of State Exactly Representing The Phase Behavior Of Pure Substances," Proc. 5th Sym. Thermophys. Prop. 5, 227-235, 1970.

Benedetto, Pasini, La Marca, Falcitelli, Tognotti, "NOx emission prediction from 3D complete modelling to reactor network analysis", COMBUSTION SCIENCE AND TECHNOLOGY, vol. 153, 2000

Bezzo, F., Macchietto, S., and Pantelides, C.C., "A general methodology for hybrid multizonal/CFD models, part I., theoretical framework," Computers and Chemical Engineering, Vol. 28, 2004, pp.501-511.

Bockelie, M.J., Denison, M.K., Chen, Z., Linjewile, T., Senior, C.L., Sarofim, A.F., Holt, N., "CFD modeling for Entrained Flow Gasifiers,"*Proceedings of the Gasification Technologies Conference, 2002*, San Francisco, CA, Oct.28-30, 2002.

Bockelie, M.J., "IGCC and FutureGen", proceedings of a Combustion Short Course provided by REI to power plant engineers/managers and researchers from the Republic of Korea, Salt Lake City, Utah, June 26-27, 2007.

Bockelie, M., Swensen, D.A., Denison, M.K., Maguire, M., Yang, C., Chen, Z., Sadler, B., Senior, C.L., Sarofim, A.F. "A Computational Workbench Environment for Virtual Power Plant Simulation", Contract DE-FC26-00NT41047, Final Report, December, 2004.

Bockelie, M.J., Swensen, D.A., Yang, C., Denison, M.K., Senior, C.L., Sarofim, A.F., "A Software Framework For Modeling Advanced Power generation Systems" Proceedings of the

30th International Technical Conference on Coal Utilization & Fuel Systems, Clearwater, Florida, USA, April 16-21, 2005.

Bockelie, M., Swensen, D.A., Denison, M.K., "A Virtual Engineering Framework for Simulating Advanced Power Systems", DOE Cooperative Agreement No: DE-FC26-05NT42444, Progress Report, January 31, 2006a.

Bockelie, M., Swensen, D.A., Denison, M.K., "A Virtual Engineering Framework for Simulating Advanced Power Systems", DOE Cooperative Agreement No: DE-FC26-05NT42444, Progress Report, April 31, 2006b.

Bockelie, M.J., Denison, M.K., Swensen, D.A., Senior, C.L., Sarofim, A.F., "Modeling Entrained Flow Coal Gasifiers," Proceedings of the *31st International Technical Conference on Coal Utilization & Fuel Systems*, Clearwater, FL, May 21-25, 2006c.

Bockelie, M., Swensen, D.A., Denison, M.K., "A Virtual Engineering Framework for Simulating Advanced Power Systems", DOE Cooperative Agreement No: DE-FC26-05NT42444, Progress Report, July 31, 2006d.

Bockelie, M.J., Denison, M.K., Shim, H., Senior, C.L., Sarofim, A.F., "Issues in Modeling Entrained Flow Coal Gasifiers," Proceedings of the *23rd Annual International Pittsburgh Coal Conference*, Pittsburgh, PA, Sept. 25-28, 2006e.

Bockelie, M., Swensen, D.A., Denison, M.K., "A Virtual Engineering Framework for Simulating Advanced Power Systems", DOE Cooperative Agreement No: DE-FC26-05NT42444, Progress Report, October 31, 2006f.

Bockelie, M., Swensen, D.A., Denison, M.K., "A Virtual Engineering Framework for Simulating Advanced Power Systems", DOE Cooperative Agreement No: DE-FC26-05NT42444, Progress Report, January 31, 2007a.

Bockelie, M., Swensen, D.A., Denison, M.K., "A Virtual Engineering Framework for Simulating Advanced Power Systems", DOE Cooperative Agreement No: DE-FC26-05NT42444, Progress Report, April 31, 2007b.

Bockelie, M., Denison, M., Swensen, D., Senior, C., Sarofim, A., "Modeling IGCC Systems with APECS," Proceedings of the *32st International Technical Conference on Coal Utilization & Fuel Systems*, Clearwater, FL, May, 2007c.

Bockelie, M., Swensen, D.A., Denison, M.K., "A Virtual Engineering Framework for Simulating Advanced Power Systems", DOE Cooperative Agreement No: DE-FC26-05NT42444, Progress Report, July 31, 2007d.

Bockelie, M., Swensen, D.A., Denison, M.K., Borodai., S., "A Virtual Engineering Framework for Simulating Advanced Power Systems", DOE Cooperative Agreement No: DE-FC26-05NT42444, Progress Report, October 31, 2007e.

Bockelie, M., Swensen, D.A., Denison, M.K., Borodai., S., “A Virtual Engineering Framework for Simulating Advanced Power Systems”, DOE Cooperative Agreement No: DE-FC26-05NT42444, Progress Report, January 31, 2008a.

Bockelie, M., Swensen, D.A., Denison, M.K., Borodai., S., “A Virtual Engineering Framework for Simulating Advanced Power Systems”, DOE Cooperative Agreement No: DE-FC26-05NT42444, Progress Report, April 31, 2008b.

Bockelie, M.J., Denison, M.K., Swensen, D.A., Senior, C.L., Sarofim, A.F., "Detailed Modeling Entrained Flow Coal Gasifiers," Proceedings of the *33rd International Technical Conference on Coal Utilization & Fuel Systems*, Clearwater, FL, June 2-5, 2008c.

Bockelie, M., Swensen, D.A., Denison, M.K., Borodai., S., “A Virtual Engineering Framework for Simulating Advanced Power Systems”, DOE Cooperative Agreement No: DE-FC26-05NT42444, Progress Report, July 31, 2008d.

Bockelie, M.J., Denison, M.K., Swensen, D.A., Senior, C.L., Sarofim, A.F., "Modeling Entrained Flow Coal Gasifiers," Proceedings of the *25th Annual International Pittsburgh Coal Conference*, Pittsburgh, PA, Sept. 29-Oct. 2, 2008e.

Buhmann, M., *Radial Basis Functions*, Cambridge University Press, 2000.

Chatterjee, A., “An introduction to the proper orthogonal decomposition,” Current Science, Vol. 78, No. 7, 2000, pp. 808-817.

Chen, C. Miyoshi, T., Kamiya, H., Horio, M., and Kojima, T., “On the Scaling-up of a Two-Stage Air Blown Entrained Flow Coal Gasifier”, The Canadian Journal of Chemical Engineering, **77**, 745-750 (1999).

Chen, C., Horio, M., and Kojima, T., “Numerical Simulation of Entrained Flow Coal Gasifiers”, Chemical Engineering Science, **55,** 3861-3883 (2000).

Ciferno, J., “2006 Cost & Performance Comparison of Fossil Energy Power Plants,” Proceedings of the *31st International Technical Conference on Coal Utilization & Fuel Systems*, Clearwater, FL, May 21-25, 2006a.

Ciferno, J. and Klara, J., “2006 Cost & Performance Comparison of Fossil Energy Power Plants,” Proceedings of the *23rd Annual International Pittsburgh Coal Conference,* Pittsburgh, PA, Sept. 25-28, 2006b.

Cormen, T., Leiserson, C., Rivest, R. and Stein, C. *Introduction to Algorithms*, 2nd Ed., MIT Press and McGraw-Hill, Section 29.3: The simplex algorithm, pp.790–804, 2001.

Eddings, E.G., Sarofim, A.F., Lee, C.M., Davis, K.A. and Valentine, J.R., "Trends in Predicting and Controlling Emissions from Coal-Fired Boilers," Fuel Processing Technology, Vol. 71, pp.39-51, 2001.

Erbes, M.R., Perz, E. and Swensen, D.A., "CAPE-OPEN Unit Plugs for Advanced Power Plant Equipment Modeling," Proceedings of the *3rd Annual U.S. CAPE-OPEN Conference*, San Francisco, CA, November 15, 2006.

Ewan, B.C.R., Boysan, F., and Swithenbank, J., "Closing the Gap Between Finite Difference and Stirred Reactor Combustor Modelling Procedures," *Twentieth Symposium (International) on Combustion*, 1984.

Falcitelli M., Pasini S., Tognotti L., "An algorithm for extracting chemical reactor network models from CFD simulation of industrial combustion systems," Combustion Science and Technology, vol. 174, 2002

Felderhof, B.U. and Deutch, J.M., J. Chem. Phys. 64 (ll), p.4551, (1976).

Fermglia, M., Longo, G., Toma, L., "CAPE Open Modules for the Process Sustainability Prediction Framework – Description and Application", Proceedings of the 2007 AIChE Meeting, Salt Lake City, Utah, November 4-9, 2007.

Flagan, R. C., Fuel Processing Technology, **39**, 319-336, 1994.

Friedlander, "Smoke, Dust, and Haze", Oxford, New York, 2000.

Grosshandler, W.L., "RADCAL: A Narrow-Band Model for Radiation Calculations in a Combustion Environment," NIST Technical Note 1402, April 1993.

Gugercin, S. and Antoulas A.C., "Model reduction of large-scale systems by least squares," Linear Algebra and its Applications, Vol. 415, 2006, pp. 290-321.

Harris, D., Roberts, D., Henderson, D. "Gasification Behavior Of Australian Coals", Research Report 43, CSIRO Energy Technology, a report prepared for the Cooperative Research Centre For Coal In Sustainable Development, November 2003.

Haynes, B. S., Private Communication, 2000.

Hertz, J.A., "Introduction to the Theory of Neural Computation," Santa Fe Institute Studies in the Sciences of Complexity, 1991.

Holmes, P., Lumley, J.L., and Berkooz, G., *Turbulence, Coherent structures, Dynamical Systems and Symmetry*, Cambridge University Press, 1996.

Holt, N., "Gasification & IGCC – Design Issues and Opportunities", presented at the GCEP Advanced Coal Workshop hosted by BYU, Provo, Utah, March 15-16, 2005.

Kalmanovitch , D.P. And Frank, M., "An Effective Model of Viscosity of Ash Deposition Phenomena," in Proceedings of the Engineering Foundation Conference on Mineral Matter and Ash Deposition from Coal, ed., Bryers, R.W. And Vorres, K.S.,Feb. 22-26, 1988.

Keating, M.H., et al. *Mercury Study Report to Congress, Volume I: Executive Summary*, EPA-452/R-97-003, December 1997.

Kirby, M., *Geometric Data Analysis: An Empirical Approach to Dimensionality Reduction and the Study of Patterns*, Wiley, John & Sons, New York, 2000.

Klara, J.M., "Cost and Performance Baseline for Fossil Energy Plants, Volume 1: Bituminous Coal and Natural Gas to Electricity", Final Report, DOE/NETL-2007/1281, May, 2007.

Kohl, Arthur L., and Nielsen, Richard B., "Gas Purification." Fifth Edition, Gulf Publishing Company, Houston, Texas. 1997.

Korens, Nick, and Simbeck, Dale R., and Wilhelm, Donald J., "Process Screening Analysis of Alternative Gas Treating and Sulfur Removal for Gasification." Prepared for U.S.D.O.E./N.E.T.L. Task Order No. 739656-00100. December 2002.

Liang YC, Lee HP, Lim SP, et al., "Proper orthogonal decomposition and its applications - part I: theory," Journal of Sound and Vibration 252 (3): 527-544 May 2 2002.

Lee, C.M., "Modeling of the Vaporization and Subsequent Reaction of Selected Minerals During Pulverized Coal Combustion", MS Thesis, U of Utah ME Dept., August, 2000.

Lee, C., Davis, K., Heap, M., and Sarofim, A., "Modeling the Vaporization of Ash Constituents in a Coal-fired Boiler," 28th International Symposium On Combustion, Edinburgh, Scotland, 2000.

Liu, G. and Niksa, S. "Coal conversion submodels for design applications at elevated pressures. Part II. Char gasification," Progress in Energy and Combustion Science 30, pp. 679-717, 2004.

McDaniel, J.E. and Hornick, M.J., "Tampa Electric Polk Power Station Integrated Gasification Combined Cycle Project, Final Technical Report," Prepared by the Tampa Electric Company for the U.S. Department of Energy, Cooperative Agreement DE-FC-21-91MC27363, August, 2002.

Mühlen H-J, van Heek KH, Jüntgen H, "Kinetic studies of steam gasification of char in the presence of H2, CO2 and CO" Fuel, Vol 64, July, 944-949, 1985.

Nelder, J.A. and Mead, R., "A Simplex Method for Function Minimization", Computer Journal, vol. 7, pp. 308-313, 1965.

Niksa, S., and Liu, G.-S., "Detailed Reaction Mechanisms for Coal-Nitrogen Conversion in Pulverized Fuel Flames," *Proceedings of the Combustion Institute*, Volume 29, pp. 2259–2265, 2002.

Osawe, M., Sloan D., Fiveland, W., and Madsen, J., "Fast co-simulation of advanced power plants using neural network components model," 3rd Annual US CAPE-OPEN Conference, AIChE Annual Meeting, San Francisco, CA, USA, Nov. 12-17, 2006.

Padia, A., Sc.D. Thesis "The behavior of Ash in Pulverized Coal under Simulated Combustion Conditions", Massachusetts Institute of Technology, 1976.

Patterson, J. H., Hurst, H. J., Quintanar, A., Boyd, B. k., and Tran, H., "Evaluation of the Slag Flow and Characterization of Australian Coals in Slagging Gasifiers", Cooperative Research Centre for Black Coal Utilization, May 2001.

Pedersen, L.S., Glarborg, P., Dam-Johansen, K., Hepburn, P.W., and Hesselmann, G., "A Chemical Engineering Model for Predicting NO Emissions and Burnout from Pulverised Coal Flames," *Combust. Sci. and Tech.* 132: 251-314, 1998.

Prasad, R., Chen, J., Chen, H., Lane, J., White, J., Corpus, J., Shreiber, E., Spero, J., van Hassel, B.A., "Oxygen transport membranes for future IGCC power plants", *Proceedings of the Twentieth Annual International Pittsburg Coal Conference*, Pittsburgh, PA, USA, September 15-19, 2003.

Quann, R.J., Sc.D. Thesis in Chemical Engineering, Massachusetts Institute of Technology, 1982.

Quann, R., and Sarofim, A.F., "Vaporization of Refractory Oxides during Pulverized Coal Combustion", Nineteenth Symposium (International) on Combustion, pp. 1429-1440, The Combustion Institute, Pittsburgh, PA (1982).

QUICKPROP, http://www.cs.cmu.edu/afs/cs/project/ai-repository/ai/areas/neural/systems/qprop/0.html, 2008

Ratafia-Brown, Jay, and Manfredo, Lynn, and Hoffman, Jeffrey, and Ramezan, Massood, "Major Environmental Aspects of Gasification-Based Power Generation Technologies." Prepared for : U.S.D.O.E/N.E.T.L. Gasification Technologies Program. December 2002.

Roberts, D., Tinney, J., Harris, D., "Char Reactivity In Gas Mixtures: Competition And Inhibition", CSIRO Energy Technology Reference IR/797, a report prepared for the Cooperative Research Centre For Coal In Sustainable Development, September 2005.

Sarofim, A.F., Nsakala y. Nsakala, and Kobayashi, S., "Options for CO2 Capture: Near term technologies of interest oxy-fuel and IGCC", a tutorial presented at the *31st International Technical Conference on Coal Utilization & Fuel Systems*, Clearwater, FL, May 21-25, 2006.

Schneyer, G.P., Cook, J.L., Brownell, D.H.,Jr. and Blake, T.R., "Dynamic simulation of a single-stage entrained flow coal gasifier," EPRI final report, December, 1982.

Senior, C.L. et al., "Toxic Substances from Coal Combustion – A Comprehensive Assessment", Final Report Volume II, DOE Contract No. DE-AC22-95PC95101, July, 2001.

Shah, M., Raybold, T., Jamal, A., Drnevich, R., Bonaquist, D., Jones, R., "IGCC: CO2 Capture Ready?", Proceedings of the Gasification Technologies Conference 2006, San Francisco, CA, October 9-12, 2005.

Swensen, D.A. and Erbes, M.R., "Development of CAPE-OPEN Unit Operations for Advanced Power Systems Modeling," Proceedings of the *3rd Annual U.S. CAPE-OPEN Conference*, San Francisco, CA, November 15, 2006.

Swensen, D.A., Zitney, S.E., Bockelie, M.J., "Development of Cape-Open Unit Operations For Advanced Power Systems Modeling", Proceedings of the *2007 AIChE Meeting*, Salt Lake City, Utah, November 4-9, 2007.

Swithenbank, J., Poll, I., and Vincent, M.W., "Combustion Design Fundamentals," *Fourteenth Symposium (International) on Combustion*, 1972.

UofUtah, Proceedings of a workshop entitled "The Future of Coal In A Carbon-Constrained World", (see http://www.cleancoal.utah.edu/presentations.htm), May 23, 2008.

Urbain, G., Cambier, F., Deletter, M., and Anseau, M.R., Trans. J. Gr. Ceram. Soc., Vol. 80, p. 139, 1981.

van Hassel, B.A., "Oxygen transfer across composite oxygen transport membranes", Solid State Ionics, vol. 174, pp. 253-260, 2004.

van Heek, K. H. and Mühlen, H.-J. "Chemical kinetics of carbon and char gasification," in *Fundamental Issues in Control of Carbon Gasification Reactivity*, Lahaye, J. & Ehrburger, P. (eds.), The Netherlands: Kluwer Academic Publishers, 1991.

Visual Numerics, http://www.vni.com/books/dod/pdf/Cmath.pdf, 2008.

Satterfield, C.N., Mass Transfer in Heterogeneous Catalysis, Massachusetts Institute of Technology Press, (1970).

Stryjek, R. and Vera, J.H., PRSV: An Improved Peng-Robinson Equation of State for Pure Compounds and Mixtures, Can. J. Chem. Engng. 64, 323 (1986).

Szekely, J., Evans, J.W. and Sohn, H.Y., Gas Solid Reactions, Academic Press, 1976.

van Baten, J.M., "An Introduction to COCO", Proceedings of the 2007 AIChE Meeting, Salt Lake City, Utah, November 4-9, 2007.
See also: http://www.cocosimulator.org/

Ward, C.R., "Mineral Matter in the Springfield-Harrisburgh (No. 5) Coal Member of the Illinois Basin, Ill. State Geo. Survey., Circular 498, (1977).

Wall, T., "Combustion Processes for Carbon Capture", Plenary Lecture, Proceedings of the 31st International Symposium on Combustion, Universität Heidelberg, Heidelberg, Germany August 6-11, 2006.

Bibliography

Provided below are references that contain general background information on topics relevant to this report.

Coal gasification (general):

Gasification Technologies Council web site: http://www.gasification.org/
DOE NETL web site for coal gasification:
http://www.netl.doe.gov/technologies/coalpower/gasification/index.html

Coal gasification (reference texts for system descriptions and CFD modeling):
Higman, C., van der Burgt, M., *Gasification*, Elsevier, 2003.
Smoot, L.D. and Smith, P.J., *Coal Combustion and Gasification*, Plenum Press, NY, NY 1985.

Coal gasification (conference web sites with papers specific to topic):
Clearwater Coal Conference: http://www.coaltechnologies.com/
Gasification Technologies Council Conference: http://www.gasification.org/conferences
Pittsburgh Coal Conference: http://www.engr.pitt.edu/pcc/

Process Simulation Software:
AspenPlus - http://www.aspentech.com/products/aspen-plus.cfm
DOE NETL APECS
- http://www.netl.doe.gov/technologies/coalpower/advresearch/ces.html
- http://www.netl.doe.gov/onsite_research/Facilities/apecs.html
GE GateCycle - http://www.gepower.com/prod_serv/products/oc/en/opt_diagsw/gatecycle.htm

ISU VE-Suite software: http://www.vesuite.org/

ROM:
General tutorial on ROM by Prof. Chatterjee:
http://www.iisc.ernet.in/currsci/apr102000/tutorial2.pdf

Reference text on ROM by Prof. Kirby
Kirby, M., *Geometric Data Analysis: An Empirical Approach to Dimensionality Reduction and the Study of Patterns*, Wiley, John & Sons, New York, 2000.

CMU PowerPoint presentation on ROM: http://www.colan.org/News/Y07/398c.pdf

Acronyms and Abbreviations

ASU	Air Separation Unit
atm	Atmosphere
Btu	British Thermal Unit
CAPE-Open	Component Architecture for Process Engineering Open Standard
CCSD	Center for Coal Sustainable Development (Australia)
CFD	Computational Fluid Dynamics
CGE	Cold Gas Efficiency
CMU	Carnegie Mellon University
COCO	Cape-Open-to-CAPE-Open
COFE	CAPE-Open Flowsheet Environment
COM	Component Object Model
CORBA	Common Object Request Broker Architecture
CSIRO	Commonwealth Scientific and Industrial Research Organization
DOE	US Department of Energy
EPA	US Environmental Protection Agency
EPRI	Electric Power Research Institute
FutureGen	DOE FutureGen Program
GE	General Electric
GUI	Graphical User Interface
HHV	Higher Heating Value
IDL	Interface Definition Language
IGCC	Integrated coal Gasification Combined Cycle
ISU	Iowa State University
MEMS	Micro-electrical-mechanical Systems
MSE	Mean Square Error
MWe	Megawatt Electric
NETL	National Energy Technology Laboratory
NIST	National Institute of Standards and Technology
PFR	Plug Flow Reactor
POD	Proper Orthogonal Decomposition
PSR	Perfectly Stirred Reactor
RBF	Radial Basis Function
REI	Reaction Engineering International
REKS	Reaction Engineering Kinetics Solver
ROM	Reduced Order Model
SVN	Subversion open source versioning software
tpd	Tons per day
UI	User Interface
US	United States of America
USC	Ultra Super Critical
VE-Suite	Virtual Engineering Suite
1D	One-dimensional
3D	Three-dimensional